UNIVERSITEIT
STELLENBOSCH
UNIVERSITY

# The reliability based design of composite beams for the fire limit state

by

Etienne van der Klashorst

Thesis presented for the degree of Master of Science at the Department of Civil Engineering of the University of Stellenbosch

Promotors:
Prof. P.E. Dunaiski
and
J.V. Retief

March 8, 2007

# Declaration

I, the undersigned, hereby declare that the work contained in this dissertation is my own original work and that I have not previously or in part submitted it at any university for a degree.

E. van der Klashorst




Date

# Summary

In the past use was made of prescriptive design rules to provide for the fire limit state. Modern Design Codes provide the scope and the means to design for fire in a performance based manner. The Eurocode provides guidance on the actions on structures exposed to fire as well as methods to predict the structural behaviour of elements in fire.

Structural designers can now incorporate the use of parametric fire curves to describe compartment fires. These fire models are not an extension of the old nominal standard temperature time curves. Parametric curves are analytical models that are based on natural fire behaviour. The temperature in the fire compartment can be predicted in a scientific manner taking account of fire loads, ventilation conditions and compartment characteristics.

The combination of rational fire models and temperature dependant structural behaviour enables designers to predict whether elements will fail during a fire. This is an improvement on the empirical prescriptive fire resistance ratings, used to date.

Multi-storey steel framed structures, with composite floors, were identified as structures with high inherent fire resistance and robust behaviour. The composite beams in the floor structure were identified as critical elements when subjected to fire. The deterministic design and the reliability level of these elements were studied.

Deterministic fire design procedures are presented that can be used to design unprotected composite beams for the fire limit state. The reliability of the deterministic design procedures was evaluated through a First Order Reliability Method.

Parametric fire curves are suitable for reliability analysis due to the fact that they can be described by stochastic variables. The fire load was determined to be the dominant variable influencing the reliability level of the composite beams. The ventilation conditions of the fire compartment also has important implications for the temperature development of the composite beams.

The reliability analyses results show that reasonably sized composite beams can be used as unprotected elements in smaller fire compartments with moderate fire loads. It was found that a structural element's total probability of failure can be improved by the use of active fire fighting

measures. The benefit of active fire fighting measures can be quantified by considering their probability of failure.

By use of conservative assumptions and basic knowledge of fire engineering principles, rational design methods can provide safe and economical solutions for fire design of composite beams.

# Opsomming

In die verlede is daar gebruik gemaak van voorgeskrewe ontwerp reëls om voorsiening te maak vir die brand limietstaat. Moderne Ontwerp Kodes verskaf die vryheid en die hulpmiddels om op ‘n uitkoms gebaseerde grondslag vir die brand geval te ontwerp. Die Eurocode verskaf leiding aangaande die aksies op strukture wat aan brand blootgestel word. Metodes om die struktuur gedrag as gevolg van die brandlaste te voorspel, word ook verskaf.

Struktuur ontwerpers kan nou gebruik maak van parametriese brand kurwes om brande te beskryf. Parametriese modelle is nie ‘n ontwikkeling vanaf nominale brandmodelle nie. Parametriese modelle is analitiese modelle wat gebaseer is op natuurlike brangedrag. die temperatuur in die brandkompartement kan op wetenskaplike wyse bereken word deur brandlaste, ventilasie kondisies en kompartement eienskappe in ag te neem.

Die kombinasie van rasionele brandmodelle en temperatuur afhanklike strukturele gedra, stel ontwerpers in staat om the bereken of struktuur elemente sal faal tydens ‘n brand. Dit is ‘n verbetering op die empiries voorgeskrewe brand weerstands grade wat tot op hede in gebruik was.

Multi-verdieping staalraam geboue met saamgestelde vloer stelsels, is geïdentifiseer as strukture wat oor ‘n hoë graad van inherente brandweerstand beskik. Die saamgestelde balke in die vloer stelsel was op hul beurt geïdentifiseer is kritiese elemente wanneer die gebou blootgestel word aan ‘n brand. Die deterministiese ontwerp asook die betroubaarheidsvlak van sulke elemente is bestudeer.

Deterministiese brandontwerp metodes word uiteengesit wat kan gebruik word om onbeskermde balke vir die brand geval te ontwerp. Die betroubaarheid van die deterministiese ontwerp metodes is geëvalueer deur gebruik te maak van ‘n Eerste Orde Betroubaarheids Metode.

Parametriese brand kurwes verleen hulself aan betroubaarheidsanalise as gevolg van die feit dat hulle deur stogastiese veranderlikes beskryf kan word. Daar is vasgestel dat die brandlas die hoof veranderlike is, wat die betroubaarheidsvlak van saamgestelde balke beïnvloed. The ventilasie toestande in die brandkompartement hou ook noemenswaardige implikasies vir temperatuur ontwikkeling in.

Die resultate van die betroubaarheidsanalises wys dat saamgestelde balke van billike grootte as onbeskermde elemente gebruik kan word. Die voorafgaande stelling is onderhewig aan beperkings op kompartement grootte en die gemiddelde brandlaste. Daar is gevind dat struktuurelemente se totale waarskynlikheid van faling, verminder kan word deur die gebruik van aktiewe bradbeskermings metodes. Die voordele wat sulke metodes lewer kan gekwantifiseer word deur hul falings waarskynlikheid in ag te neem.

Deur konserwatiewe aannames en voldoende basiese kennis van brandingenieurswese beginsels kan rasionele ontwerp metodes veilige en ekonomiese oplossings lewer, vir die brand limietstaat.

# Acknowledgements

I would like acknowledge the contribution of the following people. Without each individual's support, encouragement and knowledge (in varying combinations of all three) this study would not have been completed.

- Professor P.E. Dunaiski, for his initial encouragement that set me on the path of further study. Also for his continued guidance and perspective throughout the trials and errors of this thesis.
- Professor J.V. Retief, who has the knack of always providing much needed insight and very helpful comment after every discussion.
- Heinrich Stander, my close friend and fellow student. Your encouragement through hardships, long nights and six years of shared study time will always be remembered. I also thank you for all the good times that were never too few and far between.
- Mariloö Madden, for your support throughout my studies. Your bright nature encouraged me endlessly. You have the ability to find the brightest side of every coin when I see them as identically dull.
- Professor M. Holický, for accommodating me at the Klokner Institute while I was studying in Prague. I also thank the rest of the staff and students at the Klokner Institute. You made my stay an experience to be remembered.
- Closer to home, I thank the staff in the office and the workshop and also my fellow students at the Civil Engineering department in Stellenbosch. You are the greatest people, always quick with a laugh and a bit of inspiration.
- Lastly I thank my father, Johan van der Klashorst, who will sadly not see the completion of this task. You were and still are a great inspiration. You were my greatest supporter and for that I thank you.

# Table of Contents

# List of Tables

# List of Figures

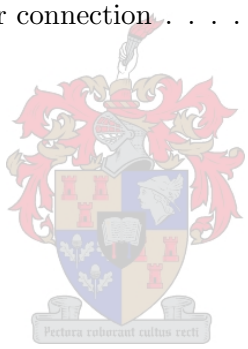

# List of symbols

| | |
|---|---|
| $(p_{f,fi})$ | The probability of the structural component failing during a fire |
| $\alpha$ | Sensitivity factors for random variables |
| $\alpha$ | The fraction of shear connection supplied |
| $\alpha_c$ | Coefficient of heat transfer by convection |
| $\beta$ | The reliability index |
| $\Delta\theta_{a,t}$ | The increase in temperature of various parts of a unprotected steel beam |
| $\Delta\theta_t$ | The increase of the ambient gas temperature during time interval $\Delta t$ |
| $\Delta_c$ | Creep deflection |
| $\Delta_e$ | The elastic part of the beam's deflection |
| $\Delta_i$ | Initial deflection of composite beam before composite action is attained |
| $\Delta_{sh}$ | Short term deflection due to short term imposed loads |
| $\Delta_s$ | Deflection due to the shrinkage of concrete |
| $\Delta_{tot}$ | Sum of all contributions to the deflection |
| $\Delta_{util}$ | $\Delta_{tot}/\Delta_{allow}$ |
| $\Delta t$ | Is the time interval |
| $\dot{h}_{net,c}$ | Net heat flux to surface area due to convection |
| $\dot{h}_{net,r}$ | Net heat flux to surface area due to radiation |
| $\dot{h}_{net}$ | The design value of the net heat flux |
| $\frac{A_i}{V_i}$ | The section factor of part $i$ of the steel profile |
| $\gamma_{m,fi}$ | The material factor for structural steel for the fire limit state, normally equal to unity |
| $\lambda$ | Thermal conductivity |
| $\lambda_b$ | The thermal conductivity of the enclosure boundary |
| $\lambda_p$ | The thermal conductivity of the fire protection material |
| $\mu_X$ | Mean of the random variable $X$ |
| $\phi_c$ | The material factor for concrete |
| $\Phi_E$ | The cumulative distribution function of the load effect |
| $\phi_E$ | Probability density function of the load effect |
| $\Phi_R$ | The cumulative distribution function of the resistance |

| | |
|---|---|
| $\phi_R$ | Probability density function of the resistance |
| $\phi_r$ | The material factor for reinforcement steel |
| $\phi_{sc}$ | The resistance factor for shear connectors |
| $\phi_s$ | The material factor for structural steel |
| $\Phi_U$ | The cumulative distribution function of the standardised normal distribution |
| $\psi_{1,1}$ | Load combination factor for the frequent value of a variable action for the accidental limit state |
| $\psi_{2,1}$ | Load combination factor for the quasi-permanent value of a variable action for the accidental limit state |
| $\rho$ | Density |
| $\rho_a$ | The density of steel |
| $\rho_b$ | The density of the fire enclosure boundary |
| $\rho_c$ | The density of the fire protection material |
| $\sigma_X$ | Standard deviation of the random variable $X$ |
| $\theta_{a,t}$ | The steel temperature at time $t$ |
| $\Theta_g$ | Gas temperature in the fire compartment |
| $\theta_t$ | The ambient gas temperature at time $t$ |
| $\varepsilon_f$ | The emissivity coefficient of the fire |
| $\varepsilon_f$ | The free shrinkage strain of concrete |
| $\varepsilon_m$ | The emissivity coefficient related to the surface material |
| $\zeta_E$ | The model uncertainty coefficient for the load effect |
| $\zeta_R$ | The model uncertainty coefficient for the resistance |
| $A_{cv}$ | The combined area of both longitudinal shear planes in a composite beam |
| $A_c$ | The area of concrete above the flange of the steel section between longitudinal shear planes |
| $A_c$ | The effective area of the concrete slab for the calculation of shrinkage deflection |
| $A_f$ | The surface area of the floor |
| $A_{p,i}$ | The area of the inner surface of the fire protection material per unit length of part $i$ of the steel section |
| $A_p$ | The concrete pull out area when calculating the shear resistance of a shear connector |
| $A_{rl}$ | The area of longitudinal reinforcement between longitudinal shear planes |
| $A_{rt}$ | The area of transverse reinforcement crossing both shear planes in a composite beam |
| $A_{sc}$ | The area of the shear connector |
| $A_s$ | The area of the steel profile |
| $A_t$ | The total area of the enclosure |
| $A_v$ | Area of vertical openings |
| $b_{eff}$ | The effective width of the concrete compression zone of a composite beam |
| $b_e$ | The width of the transformed concrete slab according to the modular ratio $n = \frac{E_s}{E_c}$ |

| | |
|---|---|
| $b_f$ | The width of the flange of the steel section |
| $c$ | Specific heat |
| $c_a$ | The temperature dependant specific heat of the steel |
| $c_b$ | The specific heat of the fire enclosure boundary |
| $c_p$ | The specific heat of the fire protection material |
| $C_r$ | The compressive force in the steel section |
| $C_r^{'}$ | The compressive force in the concrete slab |
| $d$ | Diameter of a shear stud |
| $d_p$ | The thickness of the fire protection material |
| $E$ | The load effect |
| $e$ | The moment arm for the corresponding compressive force $C_r$ |
| $e$ | The natural base number $\simeq 2.7182818284590$ |
| $e^{'}$ | The moment arm for the corresponding compressive force $C_r^{'}$ |
| $F$ | The compressive force due to bending of the composite beam |
| $f_{c,\theta i}$ | The compressive stress in slice $i$ of a heated concrete slab |
| $f_c$ | The characteristic compressive strength of concrete |
| $f_{yr}$ | The yield strength of reinforcement steel |
| $f_y$ | The yield strength of structural steel |
| $G_k$ | The characteristic permanent load |
| $h$ | The height of the fire compartment |
| $h$ | The height of the steel profile |
| $h_{cr}$ | The critical depth or depth of concrete that is subject to a strength reduction |
| $h_c$ | The effective depth of the concrete slab |
| $h_d$ | The depth of the profiled steel deck |
| $h_{eq}$ | The weighted average of compartment window heights |
| $h_s$ | Height of the shear stud after welding |
| $h_{u,n}$ | The thickness of slice $n$ when determining the reduced compressive force in a heated concrete slab |
| $h_u$ | The thickness of the concrete compression zone in a composite beam |
| $h_w$ | The height of the web of the steel profile |
| $I_e$ | The effective moment of inertia |
| $I_s$ | The moment of inertia of the steel section |
| $I_t$ | The transformed moment of inertia of the composite beam |
| $k_{c,\theta}$ | Reduction factor for the strength of the concrete, surrounding a shear stud connector |
| $k_{shadow}$ | The correction factor for the shadow effect |
| $k_{u,\theta}$ | Temperature reduction factor for the strength of steel, of a shear stud connector |

| | |
|---|---|
| $k_{y,\theta i}$ | The reduction factor of the yield strength of steel for part $i$ of the steel section |
| $l$ | The fire compartment length |
| $l$ | The length of the composite beam |
| $M_{cr}$ | The resistance moment of the composite beam |
| $M_u$ | The ultimate design moment |
| $N$ | The number of shear connectors supplied to transfer shear force in the composite beam |
| $n$ | The total number of concrete layers in compression including the top layer that is at a lower temperature than $250°C$ |
| $n_t$ | The modular ratio, $\frac{E}{E_{ct}}$ |
| $O$ | The opening factor |
| $p_{fi,55}$ | The probability of getting a fully engulfed fire compartment during the life of the structure |
| $P_{fi,Rd}$ | The design shear resistance of a shear connector for the fire limit state |
| $p_f$ | Probability of failure |
| $P_{Rd}$ | The design shear resistance of a shear stud connector at normal temperature |
| $q_{f,d}$ | The design fire load related to the compartment's floor area |
| $Q_{fk}$ | The characteristic fire load |
| $Q_k$ | The characteristic imposed load |
| $q_{rr}$ | The factored shear resistance of a shear connector used in ribbed slabs |
| $q_{rs}$ | The factored shear resistance of a shear connector used in a solid slab |
| $q_{t,d}$ | The design fire load related to the total area of the compartment |
| $s$ | The longitudinal stud spacing |
| $T$ | The tensile force caused by bending of the composite beam |
| $t$ | The effective thickness of the composite slab according to SANS 10162:2004 |
| $t$ | Time |
| $t_\alpha$ | The time constant needed to reach a RHR of 1 MW |
| $t_{lim}$ | The limiting time to maximum tempertaure in case of a fuel controlled fire |
| $t_{slab}$ | The total thickness of the composite slab |
| $t_w$ | The thickness of the web of the steel section |
| $V_r$ | The shear resistance of the composite beam |
| $V_u$ | The ultimate longitudinal shear force in the concrete slab along a composite beam |
| $w$ | The fire compartment width |
| $w$ | The width of the composite beam |
| $w_d$ | The average width of the flute of the steel decking |
| $x$ | The distance to the plastic neutral axis of the composite beam from the top of the steel section |
| $y$ | The distance to the centroid of the transformed section |
| $y_T$ | The position of the tensile force due to bending |
| $z$ | The distance to the centroid of the steel tension block |

# Definition of terms and acronyms

*Composite beam* – In this document composite beams are beams that are built from a steel section (I or H profile), a structural grade profiled steel sheet that serves the dual role of load bearing element and permanent shuttering and concrete cast on top of the profiled sheet. Composite action is achieved by use of headed shear studs that transfer the shear force between steel section and profiled concrete slab.

*FEM* – Finite Element Method

*Flashover of a compartment fire* – This is the rapid transition from the fire growth period to the stage where the fire is fully developed i.e. there is a total surface involvement.

*FLS* – Fire Limit State

*FORM* – First Order Reliability Method

*Fuel controlled fire* – After ignition the fire is fuel controlled because there is enough oxygen in the compartment. If there is enough oxygen available the fire might be fuel controlled at a later stage as well.

*LSE* – Limit State Equation

*PDF* – Probability density function

*PNA* – Plastic Neutral Axis

*RHR* – Rate of Heat Release

*SLS* – Serviceability Limit State

*Steel section* – The structural steel profile/joist of a composite beam.

*Temperature-time curve* – A curve relating temperature in a fire compartment, to time. Used to model a compartment fire.

*Through-welded shear studs* – When steel shear studs are welded to the top of the steel section and no holes are made in the profiled sheets beforehand. The studs are welded through the sheets.

*ULS* – Ultimate Limit State

*Ventilation controlled fire* – When there is not enough oxygen in the fire compartment to combust most of the fuel load. The energy release rate is then determined by the amount of oxygen that enters the compartment.

# Chapter 1

# Introduction

## 1.1 Description of the structural fire engineering problem

The design of structures for accidental situations, such as fires, is an important part of the design process. In the past prescriptive codes were used for the design of structures for fire. Use was made of standard temperature time curves to represent compartment fires. These curves are simple to use and conservative, but there is no rational basis by which to asses the reliability of a structure subjected to such a fire. Many of the Eurocodes are currently at the end of their development stage and supply guidance to design structures for the fire scenario. The Eurocodes give designers freedom to use calculation models that range from simplified to advanced.

Using more advanced fire engineering methods, the structural engineer can design structures on a performance based platform. Rational design methods, such as parametric fire curves, are analytical models that can be implemented to describe compartment fires and their effects in a more realistic and scientific way. Through rational design one can achieve an economic design and realise architectural performance, especially with regard to steel structures. From an academic point of view, designers will find satisfaction in the fact that design recommendations are based on scientific theory and a broad experimental data base.

The design of structures for the fire limit state confronts the engineer with a new set of considerations that are not all structural in nature. Failure at the accidental limit state may lead to extended damage of the structure and even progressive collapse. The design considerations for the fire limit state can not be neglected as they tie in with the robustness and redundancy of the structure.

The general design problem can be expressed as follows: a structure is subjected to a fire load which originates as result of an accidental compartment fire. The structure has a certain fire compartment geometry and use. The structure is made of certain materials and utilises a certain structural system. According to applicable building regulations, the structure must survive a fire for a specified time. The question arises: how will the structure react to the applied fire load as a function of time?

In the fire scenario a few aspects can be highlighted in order to simplify the problem and solve the design issue. Firstly, the designer must determine the fixed variables. These are aspects such as the function of the structure and in many cases the shape or geometry of the structure. The use of the structure will often dictate how the structure will look. For example, a modern office building could have larger fire compartments than a residential building because of the fact that many modern office spaces follow an open plan design. The spacing of columns and the sizes of windows are sometimes given as a fixed element by the architect, etc.

Secondly, the fire load in the building follows from the building occupation and can either be fixed or variable depending on the type of structure. Offices will in general have storage areas and work spaces. Industrial structures could have storage areas for highly combustible materials and therefore much higher fire loads than residential structures.

Thirdly, the structural materials could be specified by the architect or the designer and may or may not be flexible. The designer must decide on the use of composite structural elements, protected steel or even unprotected steel elements.

The structural fire engineer must consider the effect of certain structural and non-structural design decisions from the conceptual design stage. Because of the fact that so many factors influence the fire resistance time of a structure, well informed decisions must be made even when the conceptual design of a structure is done. This could result in structures that are more economical and even architecturally more pleasing.

At the stage where all fixed input has been determined, a decision must be made concerning the level of analysis for the fire design. The Eurocode differentiates between three levels of design. Use may be made of simplified calculation models, advanced calculation models or testing. Simplified models are based on conservative assumptions and are usually only applicable to single element design. Advanced calculation models could include whole structure analysis using Finite Element Method (FEM) applications. In this document the use of simplified calculation models will be discussed.

A further choice remains to be made. The design fire scenario must be identified and the design fire must be estimated. With the "design fire scenario" is meant that the designer must anticipate possible ignition sources, fuel sources and even the spread of the fire in a compartment. In this step the occupation and fire load of a compartment are considered. A choice regarding the design fire is made on the basis of the data gathered. Following this the effect of the fire on the structure must be determined, i.e. the thermal analysis and eventually the mechanical response of the structure.

Throughout the process it can be seen that the designer must balance the quality of the out-

put and the cost of the input. In the most simple case use could be made of design tables or nomograms, in order to find the fire resistance of structural elements. On the other extreme the designer could make use of advanced design tools such as Computational Fluid Dynamics (CFD), in order to estimate the behaviour of the design fire in a specified compartment and then with further use of the FE Method temperature and mechanical analysis could be performed. As the complexity level increases the accuracy of results increases and visa versa.

Lastly, a very important factor to consider is the issue of structural robustness. The fire limit state is an accidental limit state that could lead to failure of local structural elements. The designer must consider the effects of the local failure on total structural stability. An analysis of this type is clearly highly uncertain and could best be described in a probabilistic fashion. With this in mind it could be sensible to solve the fire engineering problem in a probabilistic way.

The flow chart shown in figure 1.1 on page 5 shows the process that can be followed to do fire design. The flow chart describes the process for simplified calculation models. For advanced calculation techniques the amount of input needed will increase but the principles stay the same. Testing of structures in fire is an advanced topic and is not covered here.

## 1.2 Risk, reliability and robustness

This document presents some of the concepts concerning the general fire design method. When considering structural fires one must implicitly take note of the robustness of the structure under consideration. It has been stated that the loss of single elements in a structure could lead to progressive collapse and this must be a main consideration when dealing with the accidental limit states. Structural robustness deals with systems reliability and is best described by probabilistic concepts. The determination of how robust a structure is, is difficult to determine in a fully probabilistic fashion. The principle of structural robustness however resides in concepts of risk and reliability that must be used to put an estimate on the structure's ability to be robust. Section 2.3 will define the terminology and concepts of robustness more clearly.

Steel framed structures with composite floors have been shown to be very robust structures in the fire scenario. These structures are highly redundant due to their ability to redistribute loads to unaffected areas of the structure. In this document the focus will always be on the use of composite beams in steel framed structures, when presenting the general concepts of fire design.

Composite floor structures have the ability to develop membrane behaviour when they undergo large displacements due to thermal expansion and loss of stiffness due to material degradation of the steel section, [32, 34]. This load carrying mechanism is not an attribute of composite beams but rather of the composite slabs that make up the floor of a fire compartment. Membrane behaviour is a two dimensional structural effect and is beyond the scope of this study in terms

of the reliability analysis of the building's components.

The design of structures utilising the ability of composite slabs to develop membrane behaviour is a new concept. The methods that were developed, are available to engineers and are at a "Level 1" stage, meaning that the designer can make use of tabulated data coupled with given structural configurations, [34]. The basic concepts of design implementing the membrane capacity of composite floor slabs will be shown in section 2.4. However, in the scope of conventional design composite beams will be analysed to analyse the reliability of a composite steel framed structure in a fire.

## 1.3 Purpose of the investigation

The design of structures for the fire limit state is a relatively new aspect that can be approached in a rational design manner. Structural fires are part of the accidental limit states and are tied in with the overall stability of structures. The purpose of the investigation presented here is as follows:

- To present general methodologies and input data that a structural fire engineer should consider when designing a steel structure with composite slabs for fire.
- To show the importance of fire safety and the role of structural engineering in improving reliability and reducing costs.
- Through structural engineering principles, to choose a representative structural element that can be used to show the process of the design for fire.
- To analyse a representative structural element's probability of failure for the ultimate, serviceability and fire limit states.
- To show that fire engineering principles can be used in conjunction with reliability procedures to improve structural performance, while not compromising safety.
- The outcomes of the reliability analysis can be used to make conclusions and provide recommendations with specific regard to composite steel framed buildings designed for fire.

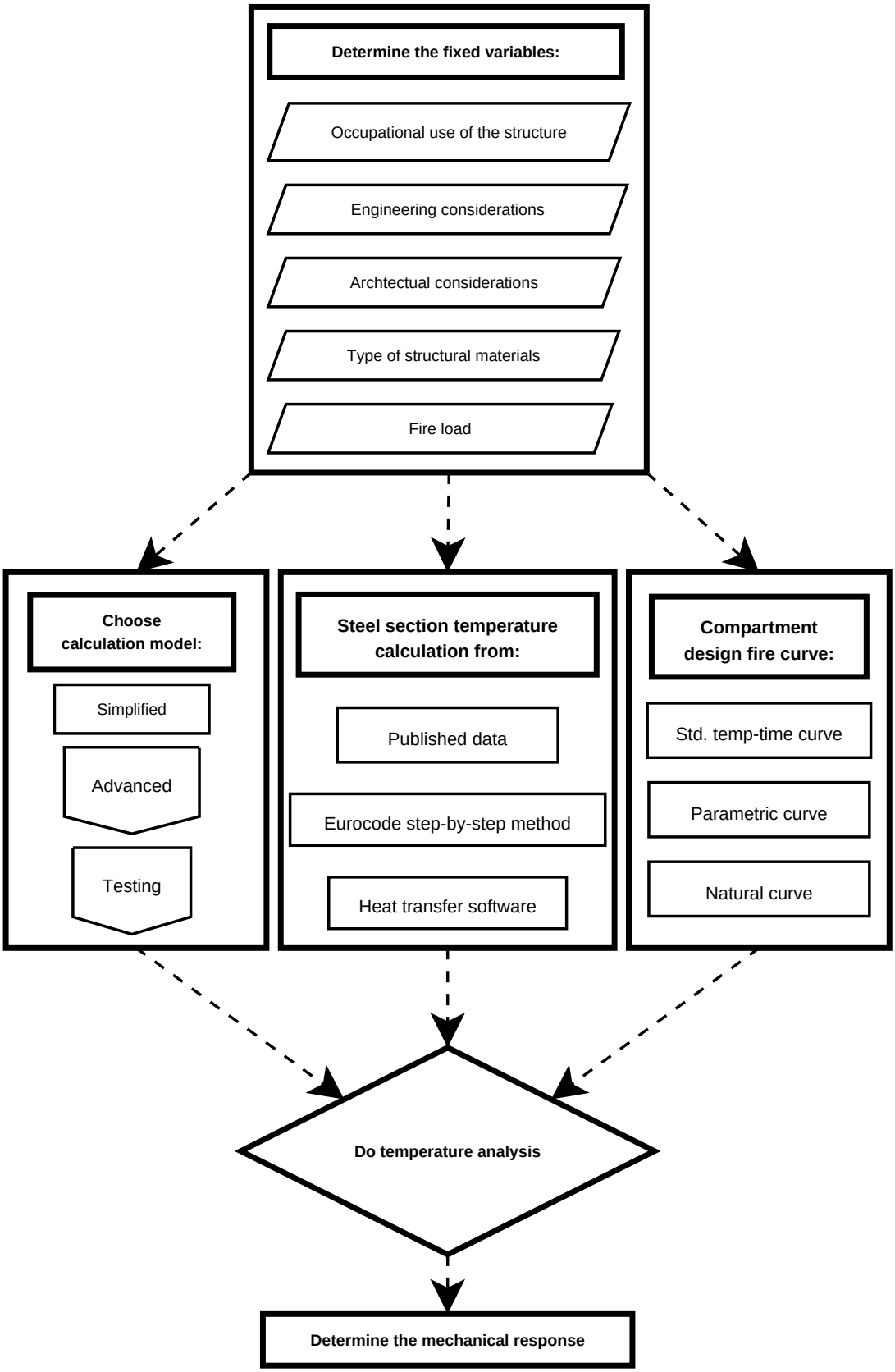


**Figure 1.1:** Flow chart of the process that can be followed in order to design structures for the fire limit state

# Chapter 2

# The global fire engineering concept

The global fire engineering concept is a general procedure that attempts to:

> "describe a performance based more realistic and credible approach to the analysis of structural safety in case of fire, which takes account of real fire characteristics and of active fire fighting measures", [13].

In general this procedure consists of the following steps:

- Taking stock of the structural characteristics relevant to fire development
- Quantifying the risk of a fire
- According to the quantified risk, establishing the fire load
- Determining the design temperature time curve resulting from the fire load
- Determining the behaviour of the structure as result of the fire
- Deducing the design resistance time from the structural response model
- Lastly the safety of the structure can be verified against the required fire resistance time

This new approach to fire safety moves away from the prescriptive approach of the past where elements of the structure were rated as having a certain fire resistance time. Emphasis is placed on human safety and active fire resistance measures. According to Schleich [13], when the safety of people is being addressed in an optimal way the structure itself will also benefit.

The global fire engineering concept is based on statistical data and probabilistic procedures. By using fundamental principles combined with newly developed methods, structural safety can be achieved in a performance based manner.

## 2.1 Historical background to structural fire engineering

It is a well known fact that fires of all kinds have large destructive potential. Fires can be very dangerous in terms of property damage and injury to people or even loss of human life. Structures have to possess a level of fire resistance in order to minimise the damage to property and in order to enable people to escape the structure before collapse of the structural elements. In the latter case for example, escaping a building could mean that the fire fighters have to assist or rescue an occupant. Building regulations will therefore specify the required fire resistance time, that a certain type of structure should possess, in order for fire fighters to have a chance to be effective.

Buchanan [14] states in his book titled: "Structural design for fire safety", that the earliest insurance companies promoted fire brigades and fire codes but they were more interested in the protection of property than human life. In modern times the protection of property is considered as being largely the affair of the owner or insurance company and is therefore not the main concern of more recent fire codes.

The fire resistance times specified by Building Regulations vary for the type of structure and its occupational use. Many aspects determine the required resistance times set by the authorities. The ISO-fire resistance requirements in Europe dictate that the minimum resistance periods for elements of the structure are a function of: the type of structure, the number of storeys, the height of the structure, the number of occupants per storey, the size of the compartment, the number of exit routes and whether a sprinkler system is installed or not, [13]. In general the required fire resistance time is between zero and one hundred and twenty minutes in steps of thirty minutes.



In the past, and to a large degree at present, the fire resistance of structural elements has been determined by single element furnace tests. It is now accepted that these tests provide very conservative results because of the fact that structural interaction cannot be taken into account, [27, 30]. Full scale testing such as was performed at the Building Research Establishment's (BRE) test facility at Cardington in the United Kingdom are normally prohibitively expensive, [27]. The results of such full-scale testing have, however, enabled researchers to draw very important conclusions concerning structural behaviour during fires, [34, 32, 33].

According to Cameron [16] fire tests have been carried out in some form since the late 18th century. The use of a temperature time curve that specifies a rate of temperature increase has been in use since an American standard proposed it in 1917. Standard temperature time curves such as the ISO 834 specification are a later development, but as was the case with the earliest temperature time curves they bear no relation to a "real" compartment fire.

A natural fire curve such as discussed in section 2.2.1 describes the development of a compartment fire more accurately as it consists of a heating phase and a cooling phase, like it would

naturally occur for fires that burn out. It is important that the designer must understand the basics of fire development and the differences between a natural fire curve and empirical curves such as the ISO 834 curve. The Eurocodes present the use of both the standard temperature-time curves and parametric temperature development curves, [3]. The parametric curves are a step towards the use of natural or real fire development models.

Over the years methods were proposed to equate an expected real fire to the standard fire test. In order to do this the concept of "equivalent fire severity" is used. In 1928 Ingberg proposed to compare the area under different temperature time curves to establish equivalency of fires, [14]. There is however no theoretical significance to this because heat transfer from a fire to a surface is mostly by radiation. According to the Eurocode parametric fire models the nett heat flux is calculated as the sum of the convective and radiative heat flux. The radiative heat flux is however calculated as a function of temperatures to the power of four where $\dot{h_{net,r}} = f(\varepsilon_m; \varepsilon_f; \theta_t^4; \theta_{a,t}^4)$ and therefore plays a more significant role in temperature development. The heat transfer during short, hot fires may be much greater than for long, cool fires even if the areas under the temperature time curves are identical.

More realistic concepts include the maximum temperature concept and the minimum load capacity concept. The equivalent fire severity is defined for the maximum temperature model, as the time to exposure of the standard fire that would result in the same maximum temperature as would occur in a complete burnout of the fire compartment. When applying the minimum load capacity concept, the equivalent fire severity is the time of exposure to the standard fire that would result in the same load bearing capacity as the minimum which would occur for a complete burnout of the fire compartment. Various empirical formulae were developed for equivalent fire exposure times, in general applicable to protected steelwork, see Buchanan [14].

In modern times various computer based tools have been developed to enable the designer to determine more accurate fire development models. Many different software applications are available, with their use ranging from the determination of the temperature time curve to the smoke movement in a structure and the response of humans to a fire scenario. Karlsson and Quintiere supply an extensive list of available software in their book titled: "Enclosure Fire Dynamics", [20].

Fires can never be totally prevented and therefore the designer must accept a certain level of risk when considering the design of a structure. Structural fire design attempts to minimise the risk to property and life.

## 2.2 General Principles

Following the schematic flow cart represented in figure 1.1 on page 5, the general principles of fire design can be divided into sections namely:

- Fire models
- Thermal response models and
- Mechanical response models

Structural fire engineering can be divided into two main design regimes. At the outset they seem similar and they are to a large degree overlapping. On the one hand a structural fire engineer can design the structural fire or on the other hand he may concern himself mainly with the structural design due to a given fire. It is important to make this distinction because the one aspect can influence the other and visa versa but often they must be seen as separate entities.

This can be explained by an example: A certain office building is to be constructed in a suburban "office park" setting. The architect proposes a modern design of steel and glass that would set the trend of this new development. The building has a large entry hall and open plan office space with composite floor beams spanning up to 9 m. The building will be equipped with a state of the art air conditioning system and in effect very little natural ventilation. Active fire fighting measures are limited to fire alarms that detect smoke. Fire extinguishers and safe escape routes are taken as a standard feature of all public buildings.

If a fire engineer were to be present from the conceptual design stage of this structure some of his inputs might have been directed to influencing the likelihood of getting a certain design fire, when a fire would occur. Some of the input could have concerned the size of the fire compartments, the size of window openings, the height of the ceiling and also the implementation of active fire fighting measures, such as sprinklers and more advanced fire alarms.

The structural fire engineer could on the other hand receive a brief that communicates the fact that the variables mentioned above are fixed. It is up to the engineer to find a cost effective and architecturally pleasing solution to the design problem. The solution must adhere to building regulations in terms of fire resistance time and it must be found according to a given design fire load.

This document is in general directed towards the second approach of dealing with a specified design fire. The following sections are however intended to introduce fire engineering principles that could influence the design process. Whether input variables are open to modification or fixed, it is important to understand their significance for fire design.

### 2.2.1 Fire models

It has already been stated that various temperature-time fire curves or models exist. The temperature time curve is needed because of the fact that fire development is a very random and unpredictable event. The development of the gas temperature increase and subsequent decrease are however the starting point for structural fire design. It therefore follows that the designer must choose a temperature time curve as basis for design. Milke [26] states that it is particularly challenging to define the design fire in terms of both heat flux and time duration. In the past these aspects were very vaguely defined but recent research has given the designer a foothold to solve the dilemma. As it will be shown here, it is very important to estimate a realistic design fire as it has an important effect on the fire resistance time of the structure.

In the past prescriptive codes dictated that structural and insulation elements must have a specified fire resistance according to a furnace test, which was conducted following the standard temperature time curve. For fire testing of components and materials see SABS 0177: Part II-1981, [12]. It has been stated that the standard temperature time curve has no realistic bearing on a actual compartment fire. The curves, such as the Eurocode curves that can be seen in figure 2.1, have no decay phase like all "natural" fires should have. The three nominal fire curves that are presented in figure 2.1 are given by the following expressions: the standard temperature time curve:

$$\Theta_g = 20 + 345(\log_{10}(8t + 1)) \tag{2.1}$$

the external fire curve:

$$\Theta_g = 660(1 - 0.687e^{-0.32t} - 0.313e^{-3.8t}) + 20 \tag{2.2}$$

and the hydrocarbon fire curve:

$$\Theta_g = 1080(1 - 0.325e^{-0.167t} - 0.675e^{-2.5t}) + 20 \tag{2.3}$$

where the gas temperature ($\Theta_g$) is in all cases calculated for the time in minutes ($t$).

In more recent developments it has been shown that natural fires can be modelled in a reasonably accurate manner by use of computer software programs and even parametric curves, like the ones found in the Eurocode, [3]. The Eurocode parametric curves are useful in the fact that they are described by a limited number of equations that can easily be implemented in a spreadsheet. The equations are physically correct but in a study presented by Schleich [13] it is shown that the calculated maximum temperature and measured temperatures show approximately 0.75 correlation. It must be understood therefore that the algebraic equations are limited in their scope and must be used appropriately.

In the paper presented by Lamont, Usmani and Gillie [25] titled: "Behaviour of a Small Composite Steel Frame Structure in a "Long Cool" and a "Short Hot" Fire, a misconception of the

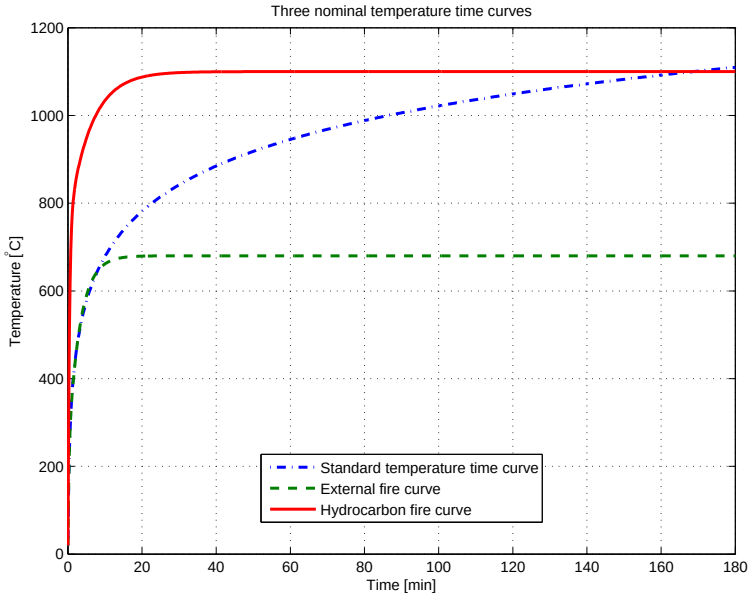


**Figure 2.1:** Eurocode 1991-1-2 Standard temperature time curves

past regarding equivalent fire exposure is revealed. As was stated previously, designers used to equate natural fires to the standard fire by means of equivalent exposure times. Using Pettersson's Swedish fire curves which were developed in 1976 (See Pettersson O., Magnusson S.E. and Thor J. "Fire Engineering Design of Steel Structures") and opening factors of 0.02 and 0.08 $m^{1/2}$, it was demonstrated that a short hot fire due to more ventilation causes more structural damage than the longer cooler fire. According to the equivalent fire exposure method the short hot fire equates to a standard fire of approximately 60 minutes, while the parametric fire with a longer duration is approximately equal to a 120 min standard exposure.

The reason given by Lamont et al. [25] for this discrepancy boils down to the fact that the rate of temperature development in a fire plays a critical role in the stress state of a structural member. The thermal gradient developed in a composite beam is much more significant to the thermal response than the duration of the fire and its effect on the material properties of the steel and concrete.

Lamont et al. [25] says the following:

> "Perhaps the most important conclusion from this analysis are the questions raised on the suitability of traditional thinking about structural fire resistance in terms of "time to failure" based on "standard exposure"... These contradictions highlight the inadequacies of the traditional approach and emphasises the need for greater understanding in this field so that fire resistance design is based on structural engineering limit state concepts involving quantitative estimation of performance for appropriately chosen design fire scenarios."

The parametric temperature time curves seen in figure 2.2 were produced according to the

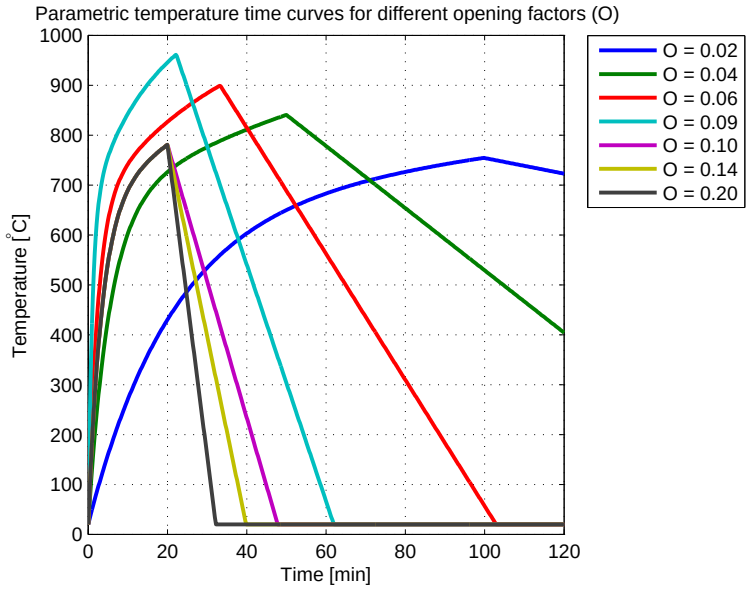


**Figure 2.2:** Eurocode 1991-1-2 Annex A Parametric temperature time curves. Opening factor $O = A_v\frac{\sqrt{h_{eq}}}{A_t}$ varies. Fire load = 600 MJ/m$^2$. $A_f = 100$ m$^2$, $A_t = 360$ m$^2$ and $t_{lim} = 20$ min

recommendations of Eurocode 1991-1-2 Annex A, [3]. The basic equations are as follows. For the heating phase of the fire:

$$\Theta_g = 20 + 1325(1 - 0.324e^{-0.2t^*} - 0.204e^{-1.7t^*} - 0.472e^{-19t^*}) \qquad [°C] \tag{2.4}$$

with:

$$t^* = t \cdot \Gamma \qquad [h] \tag{2.5}$$

$$\Gamma = \frac{(O/b)^2}{(0.04/1160)^2} \tag{2.6}$$

$$b = \sqrt{\rho c \lambda}; \qquad 100 \leq b \leq 2200 \qquad [J/m^2s^{1/2}K] \tag{2.7}$$

$$O = \frac{A_v\sqrt{h_{eq}}}{A_t}; \qquad 0.02 \leq O \leq 0.2 \qquad [m^{1/2}] \tag{2.8}$$

Where:

| | |
|---|---|
| $\rho$ | The density of the boundary of the enclosure [kg/m$^3$] |
| $c$ | The specific heat of the boundary of the enclosure [J/kgK] |
| $\lambda$ | The thermal conductivity of the boundary of the enclosure [W/mK] |
| $O$ | The opening factor |
| $A_v$ | The total area of vertical openings in the walls [m$^2$] |
| $h_{eq}$ | The weighted average of window heights [m] |
| $A_t$ | The total area of enclosure (Walls, ceiling, floor and openings) [m$^2$] |

The Eurocode clearly states the limits of the parametric temperature-time curves. They are only valid for compartment areas up to 500 $m^2$ of floor area. There must be no roof openings and the maximum compartment height is 4 m. The limits on the opening factor ($O$) and the coefficient $b$ are as given in equations (2.7) and (2.8).

When the Gamma factor ($\Gamma$) is equal to one, the heating phase of the fire approximates the standard temperature time curve. The method presented in the Eurocode is able to take into account different boundary layers of materials and also different boundary materials on walls, ceiling and floor.

To find the maximum temperature in the heating phase $t^*$ must be equal to $t^*_{max}$.

$$t^*_{max} = t_{max} \cdot \Gamma \qquad [h] \tag{2.9}$$

with:

$$t_{max} = \max\left[\left(0.2 \cdot 10^{-3} \cdot \frac{q_{t,d}}{O}\right); t_{lim}\right] \qquad [h] \tag{2.10}$$

$$q_{t,d} = q_{f,d} \cdot \frac{A_f}{A_t} \qquad 50 \leq q_{t,d} \leq 1000 \qquad [\mathrm{MJ/m^2}] \tag{2.11}$$

Where:

$q_{t,d}$ The design load of the fire load density related to $A_t$

$q_{f,d}$ The design load of the fire load density related to $A_f$ taken from Annex E of EN1991-1-2, [3]

The fire load defines the amount of energy that is available. The gas temperature that is reached however depends on how fast the temperature develops. This is called the Rate of Heat Release (RHR). The Rate of Heat Release is governed by the ventilation conditions of the fire compartment. Three phases of a fire can be identified: The growth phase, the stationary phase and the decreasing phase. For the growth phase of the fire, the design value for the RHR is given by the following equation:

$$RHR = \left(\frac{t}{t_\alpha}\right)^2 \qquad [\mathrm{MW}] \tag{2.12}$$

Where:

$t$ The time in seconds

$t_\alpha$ The time needed to reach a RHR of 1 MW

Guidance is given in Eurocode 1991-1-2 Annex E.4 on the value of $t_\alpha$, for various fire compartment occupations, [3]. The value of $t_{lim}$ in equation (2.10), can therefore be defined as: $t_{lim} = t/t_\alpha$ so that $RHR = 1$ MW. For a slow growth rate $t_{lim} = 25$ min and the corresponding limiting times for medium and fast growth rates are respectively 20 minutes and 15 minutes. As

the use of the time $t_{lim}$ suggests, a fire is only ventilation controlled once (2.10) returns values larger than the limiting time.

The Eurocode provides three different equations to describe the cooling phase of the fire depending on the time $t^*_{max}$:

$$\begin{aligned} \Theta_g &= \Theta_{max} - 625(t^* - t^*_{max} \cdot x) && ; \quad t^*_{max} \leq 0.5 \\ \Theta_g &= \Theta_{max} - 250(3 - t^*_{max})(t^* - t^*_{max} \cdot x) && ; \quad 0.5 < t^*_{max} < 2 \\ \Theta_g &= \Theta_{max} - 250(t^* - t^*_{max} \cdot x) && ; \quad t^*_{max} \geq 2 \end{aligned} \tag{2.13}$$

Where $t^*$ is as in equation (2.5), $t^*_{max} = (0.2 \cdot 10^{-3} \cdot q_{t,d}/O) \cdot \Gamma$ and the factor $x = 1$ if $t_{max} > t_{lim}$. If $t_{max} = t_{lim}$ the factor $x = t_{lim} \cdot \Gamma / t^*_{max}$.

When use is made of parametric fire curves or natural fire models, the design analysis must be performed for the total duration of the fire. When using simple calculation models this basically corresponds to finding the maximum temperature and the time when it occurs, of the structural element under consideration. Depending on boundary conditions, ventilation conditions and fuel load the maximum gas temperature in the compartment could be higher than the temperature shown by the standard fire. In most cases the use of parametric fire models produces much lower compartment temperatures than would be the case for the standard temperature time curve.

Figure 2.3 shows the temperature development of a steel profile according to a Eurocode parametric fire curve. The steel profile is divided into its three discrete parts namely, two flanges and the web. The opening factor for the compartment is 0,02. The standard temperature time curve is plotted on the graph as well. It can clearly be seen that a much lower mean steel temperature is reached when using the parametric temperature model. From the graph it can also be noted that it would be a fair approximation to take the steel section's temperature as constant throughout the section, at time of maximum temperature.

A further step may be taken towards finding a more accurate fire model by using fire development tools that were created in order to understand this phenomena better. Many of these tools are available free of charge on the internet. On such software package is CFast [19], which is available from `http://cfast.nist.gov`. CFast is a two-zone fire model used to calculate the evolving distribution of smoke, fire gases and temperature throughout compartments of a building during a fire. The modelling equations used in CFast take the mathematical form of an initial value problem for a system of ordinary differential equations (ODEs). These equations are derived using the conservation of mass, the conservation of energy, the ideal gas law and relations for density and internal energy.

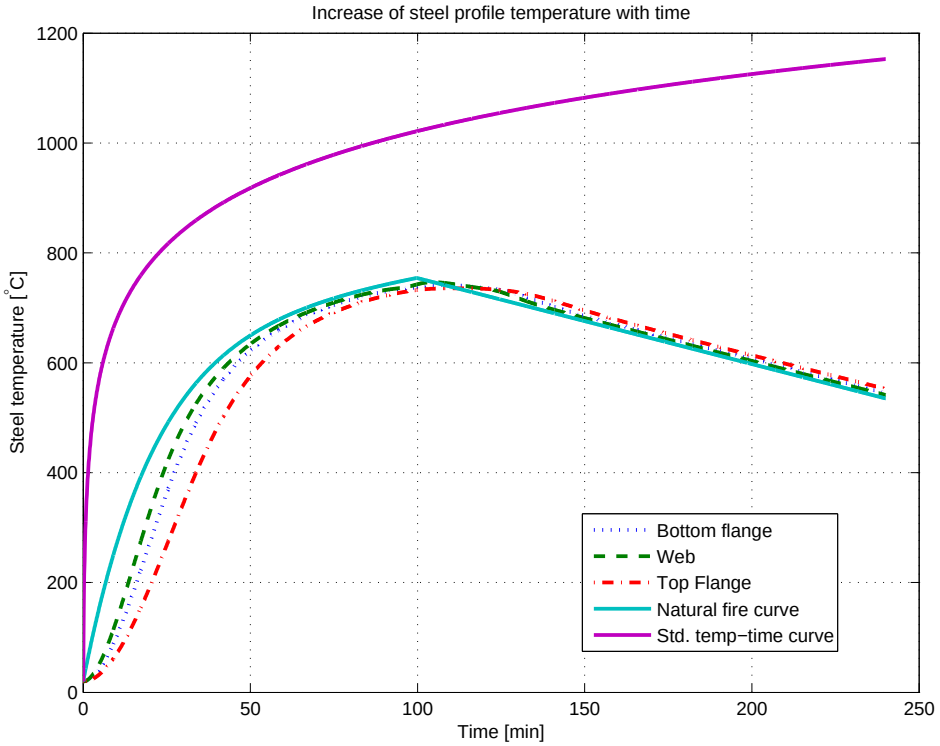


**Figure 2.3:** The increase of temperature for a I 406x140x46 steel profile that is part of a composite beam. Opening factor: $O = 0.02$, The fire is ventilation controlled

### 2.2.2 Thermal response models

The term "thermal response model" relates to what effect a given fire has on a structural element, or ideally the structure as a whole. It has been stated that the standard temperature time curve was originally developed to standardise the furnace tests that are still performed on structural elements. The fact of the matter is that such testing is prohibitively expensive. Due to this, much effort has been invested in the development and the calibration of mathematical models that can accurately predict the temperature of structural elements and further predict the response of the element to the increase in its temperature. The mechanical response due to fire will be discussed in section 2.2.3.

The development of accurate thermal response models is a difficult and time consuming process. When employing such a model to predict the temperature in various parts of structures, it would be difficult to validate the results if the structural setup were to deviate far from "standard" configurations. The Eurocodes provide scope for using advanced calculation models but they clearly state that the method should provide realistic analyses and should be based on fundamental physical behaviour. The advanced calculation methods should include separate calculation models for the thermal response and the mechanical response, [7, 6]. The research done in the past, such as shown in the PIT-report [29], is evidence that computational methods can be used to solve the engineering problem but also that care must be taken in their use.

Due to the inherent difficulty of predicting fire compartment temperatures and then translating this to the structure's temperature, many simplifications are made. Some of these simplifications include: considering thermal response as a 2D effect, disregarding the position of the fire in relation to the element under consideration, simplifications regarding the geometry of the structure, etc. Research has shown that the thermal gradients that develop in elements have a much greater effect on the structural response than the mean temperature in a element. See Usmani et al. [30] and also Lamont et al. [25].

The determination of thermal gradients throughout a whole structural compartment is a complicated issue. The fire growth rate, position of the fire, ventilation effects and material properties make this task only suitable for advanced Computational Fluid Dynamics and Finite Element solutions. Hand calculation or even computer aided analytical methods are normally not suitable to solve this problem.

This brings the designer back to single element behaviour. By making assumptions such as calculating steel section temperatures using the lumped mass of the section and not considering a thermal gradient along the section, one can approximate the steel section's temperature response. Methods have been developed in order to estimate realistic temperature distributions in steel sections. The method proposed in the Eurocode [7, 6] is a step-by-step calculation technique that is simple to do using a computer and it can be used for any design fire curve. Buchanan also describes methods for the calculation of temperatures in steel and composite sections, [14]. In this study the Eurocode method for determining the temperature distribution in a composite beam will be used, [6]. Calculation of section temperature can be done for protected and unprotected sections. The report by Kirby [21] describes the Eurocode method for calculating steel temperatures.



The calculation of the temperature at a given time in a composite beam consisting of a profiled composite slab and a protected or unprotected steel section is a bit more advanced. It is clear that such a section will have a large thermal gradient through its depth. This gradient has structural implications that will be discussed in section 2.2.3. Buchanan [14] states that if a composite beam has the steel section exposed, the step-by-step method proposed in Eurocodes [6, 7] may be used. If a part of the steel section is buried in concrete, the effect of the thermal gradient becomes severe and the only accurate way to calculate section temperatures is to use a heat transfer computer program.

The rate of temperature rise in a steel section depends on the massivity factor of the steel section. This factor is better known as the section factor. The definition of the section factor is: Section factor $= \frac{A_p}{V}$, or the perimeter area divided by the volume of the section. The section factor is important because the rate of heat input is directly proportional to the exposed steel area. It makes sense then that two sections with the same cross sectional area but different exposed surfaces will have different rates of temperature rise. A small compact section will be

less affected by the fire than a deep section with a thin web and flanges.

To calculate temperatures of elements the thermal properties of the materials they are made of must be known. The thermal properties of most construction materials are well known. Eurocode 1992-1-2 and 1993-1-2 give detailed thermal characteristics for concrete and steel respectively. Many documents have been published that give thermal properties of insulation materials and almost all handbooks on the subject of structural fire engineering and compartment fires will supply some information, see references [14, 20, 13, 18].

Table 2.1 shows the thermal properties of some insulating/fire protection materials. The values shown are taken from references [13] and [14]. It should be noted that most of the values given are only approximate because of the fact that they vary with temperature. Although the properties vary with temperature they can be used for design purposes as given, i.e. the characteristics at normal temperature. Normally one would use a constant value for the thermal properties of protection materials but one would use the temperature dependant properties for structural materials. Figure 2.4 shows the variation of the specific heat of structural steel with temperature. The specific heat of a substance can be defined as the energy required to raise the temperature of a unit mass of the substance by 1 degree. The spike in the plot is due to a magnetic phase transition in the steel, [13].

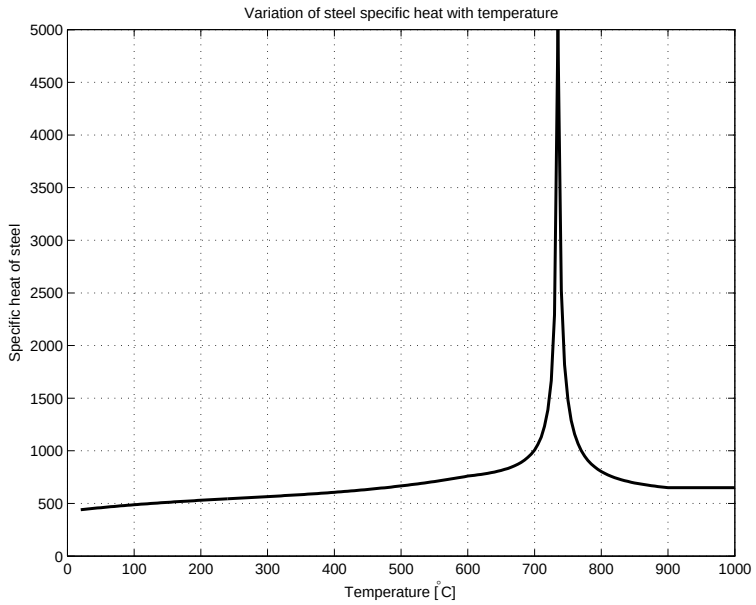


**Figure 2.4:** The specific heat of steel versus the steel temperature showing the pronounced spike at 735°C. (Reproduced according to Eurocode 1993-1-2 [7] specifications)

Gross [18] gives the temperature dependant properties of the materials listed in table 2.1. The protection systems used in modern construction are under constant development and therefore in many cases the new materials would differ significantly from one source to the next. It would be good practice to design according to proprietary thermal properties.

**Table 2.1:** Thermal properties of some typical passive fire protection materials

| Material | Density $\rho$ [kg/m$^3$] | Thermal conductivity $\lambda$ [W/mK] | Specific heat $c$ [J/kgK] |
|---|---|---|---|
| Sprayed mineral fibre | 300 | 0.12 | 1200 |
| Gypsum board | 800 | 0.2 | 1700 |
| Mineral wool | 150 | 0.2 | 1200 |
| Fibre calcium silicate board | 600 | 0.15 | 1200 |
| Vermiculite-cement spray | 350 | 0.12 | 1200 |

Figure 2.5 shows the reduction factor for steel yield strength plotted against temperature. The figure is included to highlight the importance of calculating correct steel section temperature. From the figure it can be seen that there is a sudden drop in steel strength at approximately 400°C and that steel retains only 47% of its strength at 600°C. An error in the calculation of steel temperature could have a considerable effect on fire resistance time. The engineer must always design for safety but an over conservative design would be uneconomical.

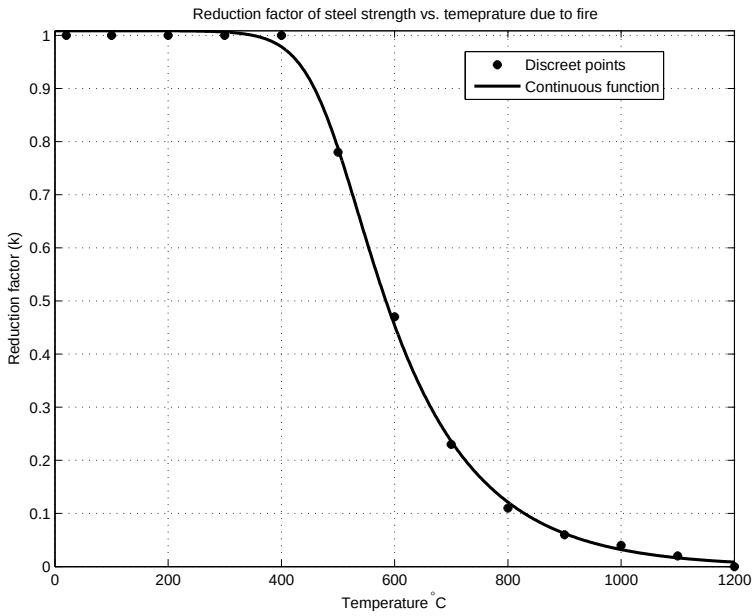


**Figure 2.5:** Reduction factor for steel yield strength against temperature. Discrete data from Eurocode 1993-1-2 [7]. Continuous function according to Cajot et al. [35]

To conclude it can be simply stated that the calculation of the distribution of heat in a structural element, due to a assumed fire development model, is a complex but also an important part of the fire design problem. Care must be taken in order to predict temperature profiles in

elements and structures in order to obtain safe solutions. The level of complexity of design is up to the engineer. The value of complex computer aided methods should be weighed against the cost of performing the analysis. The temperature response model is but one step in the fire design procedure. Needless to say, accurate fire models may lead to more accurate temperature response models that may eventually produce better structural response models.

### 2.2.3 Structural response to thermal actions

The mechanical response of a structural element is highly dependant on the element's boundary conditions. It is well known that steel beams in standard fire tests exhibit runaway type failures at much lower temperatures than seen in real fires. The runaway failure of steel beams are due to the very rapid loss of stiffness at elevated temperatures. The Broadgate accidental fire and the Cardington full scale fire tests showed that this does not actually occur in real structures. The work documented in the main report of the PIT-project by Usmani et al. [29], was one of the first major efforts to understand the behaviour of the Cardington fire tests by using computational models. This report explains the robust behaviour of unprotected composite frames in fire. One of the main conclusions of both the full scale testing and the computational models was that the boundary conditions play a significant role in the behaviour of structural elements. A brief review of the Cardington full scale tests and other accidental fires such as the Broadgate fire can be seen in section 2.5 of this report.

The paper by Rotter et al. discusses the response of a structural element under fire within a highly redundant structure, [28]. These structural interactions can be demonstrated by rather simple structural examples. Important interactions that must be taken into account are the role of expansion, loss of material strength, the effects of relative stiffness of the adjacent structure, development of large deflections, buckling and the effects of thermal gradients.

In the paper by Usmani et al. [30], the emphasis is again placed on the fact that whole structure behaviour governs the resistance of structures in fire. To quote from reference [30]:

> "Furthermore, it is the thermally induced forces and displacements, and not material degradation that govern the structural response in fire. Degradation (such as yielding and buckling) can even be helpful in developing the large displacement load carrying modes safely."

The large load carrying mode that is referred to is the membrane action that composite slabs develop in high temperature scenarios. The large deflections in the slabs produce this alternative load carrying mode that significantly contributes to the robustness of the structure. The methods that were developed by the British Building Research Establishment (BRE) to design for this beneficial behaviour will be discussed in section 2.4.

It can be said that the elements of a building structure that are most affected by fire are the

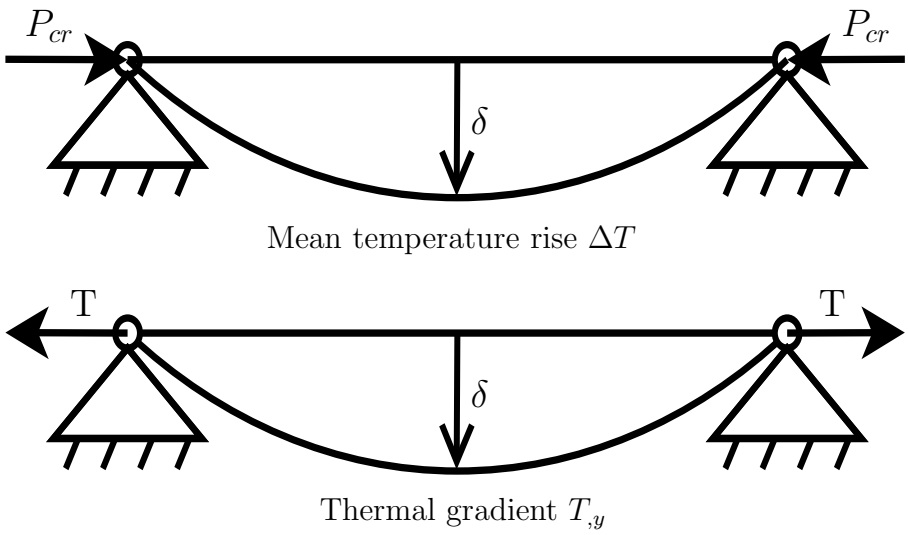


**Figure 2.6:** Diagram of the effect of temperature rise and thermal gradients on pinned beams

columns. Normally, in order to restrict damage to the elevation where the fire occurs, it would be necessary to protect the columns of the structure and therefore they will not be included in this discussion. The beams and slabs of the structure are also highly affected by fire and must therefore be protected according to traditional design trends. If they could be left unprotected large financial benefits might be evident for steel framed structures. The possibility of leaving beams and slabs unprotected increases the need to understand the behaviour of these elements. Consider the following effects on a steel beam in a fire.

#### 2.2.3.1 Thermal expansion

In a fire a beam will expand during heating and contract during cooling. This will obviously have an effect on the surrounding structure. The floor slabs of a structure are much more massive than the beams and when they expand they can exert enormous forces on the surrounding structure. The important factor to consider is the restraint that the surrounding structure provides. Rotter et al. [28] states that for a fully restrained steel element of grade 350 steel, compressive yield will take place at a temperature increase of only 142 °C. In this calculation the effects of material degradation was not taken into account.

To understand structural behaviour in restrained structures, consider the key relationship:

$$\varepsilon_{total} = \varepsilon_{thermal} + \varepsilon_{mechanical} \tag{2.14}$$

In a fire the deformation of the structure depends on the total strain. However, the stress state of the structure only depends on the mechanical strains. This is important to consider because where thermal strains are not restrained they will develop no forces in a structure. In most cases real structures will have a mix of mechanical strains due to the external load and mechanical strains due to restrained thermal expansion, [28].

In the PIT Project research report: "TM3" [24], the effects of thermal restraint on simple beam elements are explained. In the report it is shown that if there is a uniform temperature rise in a steel section with no thermal gradient, the behaviour consists of a clear pre- and post-buckling scenario. In the pre-buckling stage the thermal expansion is absorbed by straining of the material and very little displacement is produced. Before buckling of the beam thermal strain equals mechanical strain. Once buckling of the beam occurs all thermal strains produce deflection.

In general then, it can be said that large transverse deflections may develop in a structure if there is little rotational restraint but lateral restraint is provided. For a diagram of this see figure 2.6. These large deflections do not produce extensive plastification of the material and hence less destruction of the stiffness properties of the malarial. By contrast, in highly rotationally restrained structures deflections may be small but very high mechanical strains develop that cause plastification.

Due to the thermal expansion in a restrained structure the magnitude of the restraining force can be calculated on the presumption that the thermal strain equals the negative of the mechanical strain ($\varepsilon_{thermal} = -\varepsilon_{mechanical}$) i.e. the expansion is cancelled out by the restraining force $P$. The thermal thrust takes place at a critical buckling temperature seen in equation (2.16). The equation is taken from reference [30].

$$\begin{aligned} P &= EA\varepsilon_m \\ &= -EA\varepsilon_T \\ &= -EA\alpha\Delta T \end{aligned} \tag{2.15}$$

For a slender beam the restraining force $P$ can be set equal to the Euler buckling load:

$$\begin{aligned} EA\alpha\Delta T &= \frac{\pi^2 EI}{l^2} \\ \Delta T_{cr} &= \frac{\pi^2}{\alpha} \cdot \left(\frac{r}{l}\right)^2 \end{aligned} \tag{2.16}$$

Where $E$ is the elastic modulus of steel, $A$ is the area of the section, $\alpha$ is the thermal expansion coefficient of steel and $\Delta T$ is the change in temperature.

The critical temperature that causes buckling may be as low as $100 - 200°C$. Even if one considers that rigid rotational restraint will almost never be achieved, buckling and post buckling phenomena will be seen at very moderate fire temperatures.

This phenomena was physically observed during the Cardington full scale fire tests. In the restrained beam test or test 1 of the series, local buckling of the test beam occurred just inside the furnace wall on both sides of the beam. The local buckling was again observed in test 3 which was a corner compartment test and in test 5 that took place in a large fire compartment,

[34].

The fact that thermal buckling takes place at relatively low temperatures, even in cases where the beams were designed as simply supported, is beneficial to the structure as a whole. When the buckling mechanism develops, damage due to thermal expansion is restricted to the fire compartment. In steel framed structures where composite floors are used, the concrete slabs restrain the steel beam's thermal expansion. Due to the thermal gradient and this restraint against expansion, the concrete slab is deflected downward. It is this interaction that develops large membrane forces, [28].

#### 2.2.3.2 Thermal gradients

Thermal gradients have a significant effect on structural behaviour. Concrete elements like the floor slabs of composite beams exhibit very slow rates of heat transfer. The exposed surfaces of the elements will be at fire compartment temperature on the one side and normal ambient temperature on the other. This produces high thermal gradients. Inner surfaces will therefore expand much more than outer surfaces and produce thermal bowing. Note that the beam or floor plate will curve towards the fire. In terms of concrete floor slabs above fire compartments the slab will still be in compression due to the thermal bowing. The slab that forms the floor of such a compartment will however develop a tension in the concrete which is not desirable. Usmani et al. [30] says that in the early stages of a fire the effects of thermal bowing is much more important when considering composite beams where the steel section's and concrete slab's temperature differs considerably.



Again, consider a beam that is laterally restrained and pinned. A thermal gradient will result in a curvature in the beam which in turn results in the beam wanting to shorten. Because of the end restraint, a thermally induced tension will develop in the beam, see figure 2.6. The tension force is of course transmitted to the supports as end reactions. It has been said that a pure thermal expansion will introduce a compressive reaction force. Contrary to this it can be seen that a pure thermal gradient will introduce a tensile reaction. In a beam that is laterally and rotationally restrained a constant moment will develop across the length of the beam. If the surrounding structure is sufficiently stiff, the beam will remain straight and develop large thermally induced stresses.

Real structures will have some rotational restraint even when designed as simply supported. Depending on the amount of translational restraint, rotational restraint, mean temperature rise in the section and the magnitude of the thermal gradient, a structure will respond in a complex manner according to the basic principles outlined above.

To summarise refer to Usmani et al. [29]. This report is a convincing document concerning the development of computational models that predict the response of structures to fire. The

document lists several important "thermo-mechanical" phenomena that designers must consider. They are:

- Restrained thermal expansion that lead to thermal buckling in both beams and slabs
- Thermal bowing that lead to large hogging moments if beam ends are continuous and tensions if beam ends are pinned
- High axial forces induce $P - \delta$ moments and large deflections due to large thermal strains
- Material degradation
- The possible alternative load carrying mechanisms that develop in concrete slabs

### 2.2.4 Software to aid the design for fire

Karlsson and Quintiere [20] provide an extensive list of computer program resources on the internet concerning enclosure fires. Many of the applications listed concern the movement of people in burning structures, fire detection and suppression and even an algorithm for breaking window glass. The two fire development models that will briefly be discussed here are the zone models CFAST (Version 6) and OZone (V2.2). Although zone models are the less sophisticated numerical fire model, they have their own field of application and thus are essential tools in fire safety engineering applications.

The main hypothesis of zone models is that the compartments are divided into zones (in the vertical plane) in which the temperature distribution is uniform at any time. In real fires these zones can often be distinctly identified when the compartment is inspected after the fire. A hot layer filled with smoke can be found at the top of the compartment. The smoke will discolour the walls of a compartment and afterwards the two layers that developed during the fire can be identified. The development of the hot and the cold zone is a dynamic process and ever changing but the process can be modelled by use of differential equations and assumed boundary conditions.

CFAST or Consolidated model of Fire growth And Smoke Transport, is a two zone fire model that is said to be most extensively used to model fire and smoke spread in buildings, [19]. The graphical user interface can easily be used to model many interconnected rooms. The developers state that the program is not intended to be used with complex compartment geometries. For these complex applications computational fluid dynamics (CFD) models are appropriate. The technical report on CFAST shows the limitations of such a zone model and also gives the mathematical derivation of the problem.

OZone is another zone fire model. OZone combines the use of one zone and two zone models in its algorithm. The algorithm switches from the one zone model to the two zone model when some predefined criteria are encountered. The user interface that OZone provides is very user

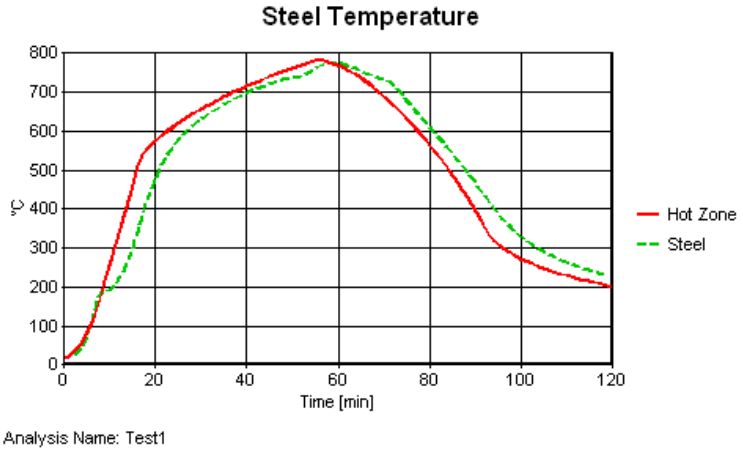


**Figure 2.7:** I 406x140x46 steel section's temperature compared to the hot zone temperature, calculated using OZone V2.2, [15]. The fire is ventilation controlled with a calculated fire load density of 410 MJ/m$^2$.

friendly. Many inputs can be specified by the user. They include: non-square/rectangular compartment geometry, definition of compartment boundaries with up to four different layers, the use of forced smoke extractors, time or temperature dependant ventilation conditions (such as for breaking window glass) and the calculation and resistance of steel elements in the compartment. As in the case of CFAST the reader is advised to consult the technical documentation of OZone [15] before using the program.

Figure 2.7 is a plot of a I 406x140x46 steel section's temperature compared to the gas temperature of the fire compartment. Ozone was used to produce the graph. The fact that OZone incorporates a method to calculate the temperature of many steel sections makes this program especially useful for the designer of steel structures. The heating of the steel profile is calculated using the Eurocode 1993-1-2 methods. The gas temperature that is used as input, is either the upper zone temperature or a fictive local temperature obtained by Hasemi's method or the maximum of these two temperatures. The Ozone guide [15] supplies a description of the Hasemi method.

The fire resistance of tension, compression and beam elements are calculated by OZone on the basis of Eurocode 1993-1-2, [7].

## 2.3 Structural robustness

The robustness of structures is a topic that has come under the spotlight in recent times. The concept of structural robustness must however be properly defined. Engineers have an intuitive concept of what structural robustness means. Some of the words used by civil engineers to describe robustness are: stability, ductility, reserve strength capacity, redundancy or even as being the opposite of fragile, see reference [38] for an exposition of the interpretation of robustness in

various fields of science.

In the IABSE journal: "Structural Engineering International 2/2006", Professor Michael Faber[þ] says as introduction to various papers presented on structural robustness:

> "Typically modern structural design codes require that the consequence of damages to structures should not be disproportional to the causes of the damages. However, despite the importance of robustness for structural design, such requirements are not substantiated in more detail..."

It is further said that robustness is a property that can not only be associated with the structure itself but it is a product of several indicators, some of them being: risk, redundancy, variability of loads and resistances and even emergency preparedness and evacuation plans. In short, structural robustness deals with risk and the handling of risk. Risk can in many cases only be quantitatively measured in terms of probability as it inherently deals with uncertainty.

For robustness to make sense a system must be identified, certain performance criteria must be set and hazards must be identified, only then can a robustness analysis be performed, [38]. In the broad scope, the robustness analysis may be deterministic but for structural application this analysis must be done on a probabilistic basis.

In terms of traditional design for certain limit states the effect of accidental scenarios is not explicitly taken into account. The reason for this is that the probability of occurrence of such events is low. Val et al. [40] gives a figure of $(10^{-7} - 10^{-5})$ per housing unit per year. The fact of the matter is that when such an event takes place and the structure is not robust, the cumulative effects of the event can be severe.

In terms of risk and consequence, it is clear that different types of structures need different levels of robustness. For example, a public structure where many people gather must clearly be more robust than a private house for the simple reason that in case of a structural failure the consequence of a progressive collapse will be much more severe.

In this context it is clear that a reliability analysis must be performed on a damaged or undamaged structure using probabilistic methods and stochastic variables. A common way to test the robustness of a structure is by removing a key element from the structure (like an explosion or fire would do) and then calculating the probability of the failure of the system i.e. progressive collapse.

As this document deals with structural fires the problem will be approached by finding the probability of failure or the reliability ($\beta$-index) of the key element. This section will define robustness in terms of composite steel framed structures.

[þ] President of the Joint Committee on Structural Safety (JCSS)

Framed structures consisting of columns and beams supporting floor slabs represent one of the most common structural systems. These systems are very effective in compartmentalising fires and in redistributing the loads to other elements in the structure not affected by the fire. Such a structure would be termed "redundant" due to the existence of alternate load paths.

The mechanical structural response is however in many cases not the only failure that could lead to progressive collapse of the structure. Designers should also take the effects of other failures into account. A failure to compartmentalise the fire could lead to fire spread throughout the structure, which in turn could lead to a progressive collapse. Val et al. [40] defines probability of progressive collapse as:

$$P(F) = P(F|DA_i)P(D|A_i)P(A_i) \tag{2.17}$$

$P(F)$ is the probability of failure due to an accidental event, $P(A_i)$ is the probability of event $A_i$ occurring, $P(D|A_i)$ is the probability of local damage given $A_i$ and finally $P(F|DA_i)$ is the probability of progressive collapse given the occurrence of the local damage $D$ due to $A_i$.

According to this basic equation the probability of progressive collapse can be decreased by doing one or all of three things:

- Reduce the likelihood of the event $A_i$ happening
- Reduce the probability of local damage due event $A_i$
- Reduce the likelihood of progressive collapse due to a local failure

When considering structural fires, the probability of the fire occurring ($P(A_i)$) can be reduced by many means, but this will not be discussed in this document. The last two factors that can be reduced deal directly with the structure but they depend on the event $A_i$. To design for all possible events is not practicable. To solve this, Val et al. [40] proposes to define the robustness of the structure as an internal property of the structure itself and reduces equation (2.17) to:

$$P(F) = P(F|D)P(D) \tag{2.18}$$

According to this equation the probability of failure is equal to the probability of failure given that local damage occurred times the probability of the local damage happening. Starossek [39] defines robustness as an insensitivity to local failure and also implies with this that the robustness of a structure is an internal property independent of the event that causes the failure.

Starossek [39] supplies three reasons why modern design codes do not handle the potential for progressive collapse sufficiently and highlights the difficulties involved in addressing these problems:

- The codes are reliability based but only consider local failure and do not have scope to handle the potential global failures

- Low probability and unforeseeable events are not taken into account
- The probabilistic concepts implemented require a target failure probability to be specified and society does not seem able to reach consensus about what this should be.

Improvements of current design methods can be made by implementing reduction factors on the resistance side of design equations or by doing fully probabilistic analysis for any given design situation. In the former case this would involve detailed study of all possible structures to determine what these factors should be. In the latter case non linear static or dynamic analysis of structures would have to be coupled with probabilistic methods that would give rise to complex and computationally demanding processes.

In view of the fact that methods to design robust structures are needed and keeping the limitations that exist in mind, engineers need to apply judgement when thinking of the robustness of structures. Tools like reliability analysis and event tree analysis can be applied to get insight into the robustness of a certain structure. Be it as it may, it is important that robustness consideration is a part of every design process.

## 2.4 The Building Research Establishment's method for the design of composite slabs

This section will briefly describe the new fire design method that was developed in the United Kingdom for steel framed structures with composite floors. The membrane action developed in composite slabs is an alternative load path present in structures that make use of a floor configuration similar to that of the Cardington frame. The alternative load path makes the structure redundant and therefore robust or collapse resistant. The Building Research Establishment (BRE) method can therefore be seen as a step towards consideration of robustness in design, as described in the previous section.

According to Bailey [31], when using this method one can leave 40% to 50% of steel beams unprotected. Bailey [32] supplies the background to the design method. General tabulated data and application rules can be found in the document by Newman et al. [34].

The large scale fire tests that were conducted in a number of countries have shown that the fire performance of real buildings is much better than expected. This increased fire resistance is due to structural interaction of the elements in the structure. The changes in the geometry of a composite floor can be beneficial to its load carrying capacity (in contrast to columns). The composite floor develops membrane behaviour and new fire design methods attempt to make use of this alternative load path.

The recommendations provided by the Newman et al. [34], are limited to non-sway steel framed

buildings with composite floors and beams that are simply supported. The structure must be in the fire risk categories of up to 60 min. The recommendations do not apply to slim-floor construction or pre-cast construction.

The method is based on the fact that the floors of the structure under consideration are divided into floor design zones. The floor design zones must adhere to certain rules. The basic rules are that each zone should be rectangular with edge beams on all boundaries, internal beams spanning in one direction only and there should be no columns inside the design zone. The boundary beams around the zone would normally be protected. The economy of using this method comes from the fact that all beams inside a design zone can be left unprotected.

Membrane action is due to in plane forces within the depth of the floor slab. During a fire the serviceability limit state does not need to be satisfied. Therefore, large deflections can develop provided that the fire compartment maintains integrity and that overall structural collapse does not occur. If concrete slabs are horizontally restrained around their perimeter the reinforcement can develop full tensile stresses at large slab displacements. This behaviour is commonly called tensile membrane action. Membrane action does not however depend on horizontal restraint, given that the slab is two way spanning. An analogy can be drawn to a bicycle wheel, where the tensile "net" in the centre of the slab forms a compression ring on the slab perimeter. This compression ring can be termed compressive membrane action, [31].

According to what is stated above, certain requirements must be met for membrane action to develop during fire. For a slab panel membrane action can develop if the perimeter beams are designed not to form plastic hinges, i.e. vertical stability is ensured around the slab edge. Diagonal yield lines can then form in the slab panel, which leads to membrane action. For this reason perimeter beams of floor design zones must be protected. Bailey states that the individual slab panels are all designed as if they are horizontally unrestrained. This is a conservative approach but can be justified in the following way: A slab panel in the centre of a structure is arguably horizontally restrained due to the continuity of the reinforcement over the supports. This can not be said for slab panels at the edge of structures. The internal panels develop large hogging moments over supports during fire. This moment and the forces in the floor slab will in general lead to fracture of reinforcement over the edge beams. Therefore all slab panels are conservatively designed as being horizontally unrestrained.

The "Level 1" guidance given in [34] consists of design tables and is therefore empirical. Using the design tables implies that the internal beams have been designed according to British Design Codes. The information supplied in the design tables themselves consists of what type of reinforcement mesh to use and what the distributed load is that must be added to the boundary beams as a function of the dimensions of fire zone. The reason for the additional load on the boundary beams is the fact that the membrane behaviour of the slab transfers a proportion of the load that the internal beams would normally carry, directly to the edge beams that are

parallel to the internal beams.

An important factor to take into account when designing edge beams is that the beams have to be anchored to the floor slab by looping reinforcement mesh over shear studs. With "edge beams" is meant structural edge beams and not floor design zone edge beams, although they would implicitly be on the edge of the floor zones as well. Although the slabs are conservatively designed as being horizontally unrestrained care must be taken to ensure as much horizontal restraint and reinforcement ductility as possible.

In order to restrict the fire damage to the fire compartment, it is recommended that columns be fire protected over the full height of the column, including connections. If this is not done local squashing of the columns will transfer structural damage to other floors. This recommendation is mainly in view of repairing the building after the fire.

The BRE method is conservative in a number of ways. Some of them include: the continuity of the slab that is ignored, the contribution of the steel deck that is ignored and the catenary action that the unprotected steel beams will develop that is also ignored. Bailey [31] states that more research work is required to define the extent of the conservatism.

As the research continues, future results may include analytical equations that can be used instead of the design tables. Currently the derivation of the design table information is rather complex and unsuitable for everyday design work.

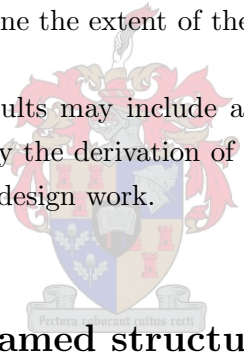

## 2.5 Multi-storey steel framed structures for the fire scenario

This section will briefly describe the Cardington fire tests and Broadgate fire. Some conclusions for general design of multi-storey steel framed structures can be drawn from this and will be implemented in this document, when presenting the design of composite beams in general and for the ultimate limit state.

A series of tests were carried out at the Building Research Establishment's Cardington laboratory from 1995 to 1996. In literature the tests are commonly referred to as the Cardington full scale fire tests. A fire that can be seen as influential in promotion of the full scale fire tests is the Broadgate accidental fire. The Broadgate fire occurred in 1990 in a partially completed 14-storey office block. At the time of the fire passive protection was incomplete and active fire protection was not working yet. The floor system was designed as composite, [34].

The Cardington building was designed and constructed as a typical multi-storey office building. The following information was gathered from the publication authored as "A European Joint Research Programme", [27].

- The design complied with Eurocodes 1993 and 1994.
- In plan the building covered an area of 21 m×45 m, with an overall height of 33 m. Along the length of the building there were five equally spaced bays and along the width there were three bays with the middle bay 9 m wide.
- In the centre of the building was a 9 m×2.5 m lift core. Two 4 m×4.5 m stairwells were placed at either end of the building.
- The structure was designed as a braced frame with the bracing members situated in the lift and stairwell cores.
- The beams were designed as simply supported and acted compositely with the floor slab by means of 95×19 mm diameter shear studs.
- The composite floor consisted of 0.9 mm steel decking (PMF CF70), which was continuous over a minimum of two spans. Grade 35 lightweight concrete ($\rho = 1900$ kg/m$^2$) was used with A142 anti crack mesh consisting of 6 mm diameter wires at 200 mm centres. The overall minimum depth of the slab was 130 mm.

The main conclusion drawn from both the fire testing and the accidental fire as well as numerical modelling of such structures, is that composite steel framed buildings behave differently than predicted by single element testing. Runaway failure and progressive collapse do not occur.

The Cardington structure can be considered as the model structure on which the BRE method for composite slabs is based. Section 2.4 outlined the approach that one would follow to make use of membrane action in design. This is however an advanced method and an analytical limit state equation cannot be explicitly derived. The application of reliability analysis of membrane behaviour is therefore beyond the scope of this document. In order to consider the robustness of a structure, as defined in section 2.3 of this document, one must calculate the reliability index of critical elements of the structure under consideration. Due to the fact that the columns in a structure resembling the Cardington frame would be protected, the composite beams found in the floor structure will be considered.

From what was seen in the Cardington tests and the subsequent modelling of the structure in fire, the following model was used for the composite beams that were studied:

The composite beams have relatively long spans and are designed as simply supported. Due to local buckling taking place even in structures designed as simply supported, no added benefit would be derived from continuous beams. From the recommendations for membrane action stating that the edge beams of floor plate zones must be protected, both unprotected and protected composite beams were studied. The floor plates are profiled composite slabs that span transversely to secondary composite beams.

Chapter 3 will show the general deterministic design of composite beams for the ultimate and serviceability limit states. Chapter 4 will then proceed to show the assumptions made and the methods used in order to find the reliability of a composite beam.

# Chapter 3

# Deterministic design of composite beams

## 3.1 Introduction

The deterministic design of composite beams can be divided into three main sections headed under the design for the ultimate, serviceability and fire limit states. The main assumptions regarding the design are discussed in order to supply the necessary background for the limit state equations used in the next chapter, regarding the reliability based design of the composite beams.

The composite beams discussed in the following sections are simply supported beams. In the case of fire design, the beams are heated from below. This distinction is made due to the fact that a composite beam heated from the top will behave completely differently from a beam heated from the bottom. The behaviour of beams heated from below are governed by the loss of strength of the steel section as its temperature rises. In the case of the composite beam that supports the fire compartment's floor, the steel beam will be effectively shielded from the heat source by the concrete slab.

## 3.2 Ultimate limit state

A composite beam must be designed for three stages at the ultimate limit state. The construction stage before placing of the concrete. The construction stage after the wet concrete has been placed and finally the design of the beam after composite action is attained. The following sections will outline the main assumptions made when designing composite beams for these three stages.

Composite beams have various failure modes that need to be checked for the ultimate limit state. During the construction stages before the beam attains composite action the steel joist

must be checked for bending and shear failure. After composite action develops, additional failure modes must be inspected. They are failure of the shear connection and failure in longitudinal shear through the concrete slab.

For vertical shear, only the contribution of the web area of steel section may be taken into account, see SANS 10162-1:2004 §17.3.2 [1]. To find the flexural capacity of the beam no concrete in tension should be taken into account.

Note that one must make a fundamental choice when designing composite beams. This choice concerns whether the beams in question are propped during construction or whether they are left un-propped. This design assumption will directly affect the deflection of the beam, which of course is a serviceability aspect. The calculations for the ultimate limit state will however also differ. In section 3.3 the deflection of simply supported composite beams will be discussed.

### 3.2.1 Construction stage

At the construction stage, before the concrete has been placed on the profiled steel sheeting, the load effect must be calculated by taking the following loads into account: the permanent load from the steel beam and steel decking and the live load due to construction workers and equipment. At this stage of construction, it might be necessary to provide lateral support for the steel beam in order to obtain a satisfactory slenderness ratio.

One of the main advantages during construction when using the profiled sheets and welded steel studs, is that the in-plane stiffness of the sheeting will laterally brace the compression flange of the steel section while the load of wet concrete is placed on the steel beam at the second construction stage.

At the second stage of the construction the added load of the wet concrete and an increased construction live load must be taken into account. The steel beam is still the only load bearing element as the composite action of the beam has not been achieved as yet. At this stage the profiled steel sheeting is attached to the compression flange of the steel section. The South African National Standard SANS 10162-1:2005 [1] allows the calculation of the moment capacity of the steel section by taking the resistance of the beam as the plastic moment resistance of the section.

Note that plastic analysis may be used to design composite beams. If plastic analysis is performed the requirements of clause 8.6 of SANS 10162-1:2005 [1] must be met. This clause amongst other things specifies that the width to thickness ratios of the element must meet the requirements for class 1 sections and that the element must be laterally restrained.

### 3.2.2 Composite beam

For composite action the load effect is determined by taking the following loads into account:

- Permanent loads: Concrete, steel section, steel decking, raised floor/screet, services and the ceiling
- Imposed loads: Partitions and normal imposed load due to human traffic, furnishings etc.

The composite beam will have a design effective width dependant on the beam's location. For interior beams the effective width can be determined according to SANS 10162-1:2004 [1] as the lesser of 0.25 times the composite beam's span or the average distance between parallel supports. For edge beams the effective width can be calculated as the lesser of 0.1 times the composite beam span plus the width of the top flange of the steel profile or half the clear distance between parallel supports.

An important factor that the designer must take into account is the amount of shear connection that will be supplied. In order to increase the economy of the design a reduced number of shear connectors can be installed so that 100% of the shear force is not transmitted between the concrete slab and steel section. The South African Steel Construction Handbook [11], states that a large reduction in the number of shear connectors can be achieved with only a small reduction in the flexural capacity of the composite beam, see figure A.1 in appendix A.

The number of shear connection installed will however have an influence on the fire resistance of the composite beam. If a small number of shear connectors are installed the capacity of the beam at the fire limit state may be dominated by this failure mode. It is important that both bending and shear connector failure be tested for fire. Refer to section 3.4.3 and also equation (3.33) on page 47. For initial design it might be prudent to design a partial shear connection because of the fact that full shear connection is more expensive and normally not much more beneficial.

The moment capacity of a composite beam can be calculated using the laws of static equilibrium of the composite section. The tension force in the steel section is:

$$T_r = \phi_s A_s f_y \tag{3.1}$$

and the compression force in the concrete is:

$$C_r^{'} = 0.68 \cdot \phi_c \cdot b_{eff} \cdot \alpha \cdot t \cdot f_{cu} \tag{3.2}$$

When partial shear connection is used the plastic neutral axis will always lie within the steel section due to the fact that the shear connection can not transmit the full tensile force developed. The fact that the full plastic tensile capacity is developed in the steel section has the effect that only a small portion of the possible concrete compressive block is used to achieve

equilibrium. However, by reducing the effective depth of the compression block, one can easily calculate the position of the plastic neutral axis, as one knows it is located in the steel section.

In the case where partial shear connection is used, a part of the steel section will generally also be in compression. In equation (3.2) the factor $\alpha$ is the fraction of shear connection supplied: $\alpha \leq 1$. Due to equilibrium the tensile force in the steel section is equal to the sum of the compressive forces in the steel section and concrete slab:

$$T_r = C_r + C_r^{'} \tag{3.3}$$

We also know that the tensile force in the steel section is equal to a tensile force in the whole area of the section ($A_s$) minus the compressive force in a unknown area of the steel section. Thus:

$$T_r = \phi_s A_s f_y - C_r \tag{3.4}$$

By equating equations (3.3) and (3.4) the compressive force in the steel can be found:

$$C_r = \frac{\phi_s A_s f_y - C_r^{'}}{2} \tag{3.5}$$

The area of the steel section in compression can be found by simply dividing the force $C_r$ by the steel yield strength:

$$A_{sc} = \frac{C_r}{\phi_s f_y} \tag{3.6}$$

The plastic neutral axis will either be in the top flange of the steel section or in the web. For simplicity, the equations shown here assume that the plastic neutral axis lies within the flange. The distance from the top of the steel profile to the plastic neutral axis is therefore the area in compression, divided by the width of the steel section's flange:

$$x = \frac{A_{sc}}{b_f} \tag{3.7}$$

In order to calculate the moment in the beam, the distance to the centroid of the steel tension block can be calculated. $z$ is the distance from the bottom of the steel beam:

$$z = \frac{[A_s(\frac{h}{2}) - A_{sc}(h - \frac{x}{2})]}{A_s - A_{sc}} \tag{3.8}$$

The distance from the plastic neutral axis to the centroid of the concrete zone in compression ($e^{'}$) and the distance from the plastic neutral axis to the centroid of the steel compression zone ($e$), can then be calculated as:

$$e^{'} = h - z + t_{slab} - \frac{\alpha \cdot t}{2} \tag{3.9}$$

$$e = h - z - \frac{x}{2} \tag{3.10}$$

Finally, the resistance moment of the composite beam can be calculated by taking moments around the position of the tensile force in the section:

$$M_{cr} = C_r e + C_r^{'} e^{'} \tag{3.11}$$

For an illustration of the dimensions and areas used in the calculations, refer to figure 3.1.

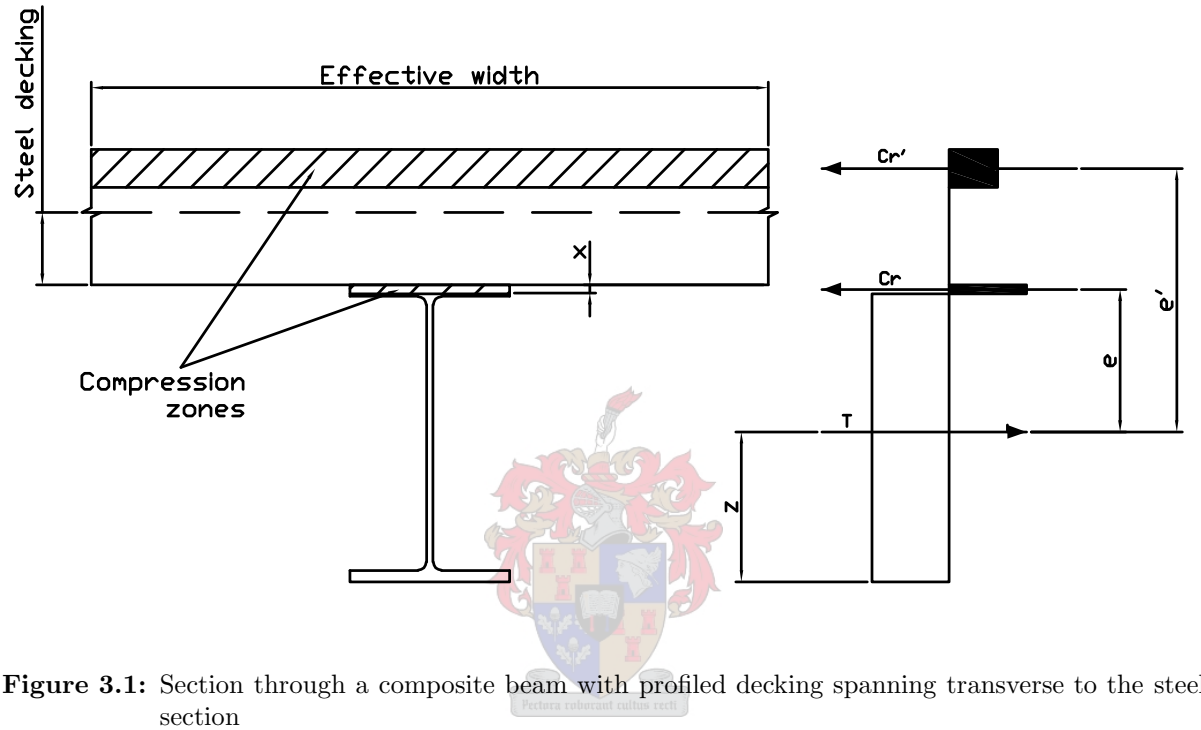


**Figure 3.1:** Section through a composite beam with profiled decking spanning transverse to the steel section

The resistance of the composite beam against vertical shear must be checked. The composite beam is designed using plastic analysis and therefore according to the South African Standard §13.4.1.2, [1]:

$$V_r = 0.55 \cdot \phi_s \cdot t_w \cdot h_w \cdot f_y \tag{3.12}$$

### 3.2.3 The design shear resistance of headed stud shear connectors

The factored shear resistance of end welded studs can be obtained using the equations presented in the SANS 10162-1:2004 Design Code, [1]. The design shear resistance of such studs will vary according to their placement. The following is taken from SANS 10162-1:2005 [1] §17.7.2.2: in ribbed slabs with ribs parallel to the beam when the ratio of the average width of the flute of the steel decking to the depth of the profiled steel deck ($w_d/h_d$) is greater or equal to 1.5, the factored shear resistance is equal to the shear resistance of a shear connector used in a solid slab. For the expression of $q_{rs}$ see equation (3.14). When $w_d/h_d < 1.5$, then $q_{rr}$ is given by the

following equation:

$$q_{rr} = \phi_{sc}\left(0.77 \cdot \frac{w_d}{h_d} \cdot d \cdot h_s (f_{cu})^{0.8} + 10.5 \cdot s \cdot d(f_{cu})^{0.2}\right) \leq q_{rs} \tag{3.13}$$

$$q_{rs} = 0.45 \cdot \phi_{sc} A_{sc} \sqrt{f_{cu} E_c} \leq \phi_{sc} A_{sc} f_u \qquad \text{[N]} \tag{3.14}$$

In ribbed slabs with the ribs perpendicular to the beam and $h_d = 75\ mm$:

$$q_{rr} = 0.31 \cdot \phi_{sc} \cdot \rho \cdot A_p \sqrt{f_{cu}} \leq q_{rs} \tag{3.15}$$

Where:

| | |
|---|---|
| $q_{rr}$ | The average width of the flute of the steel decking |
| $q_{rr}$ | The shear resistance of a headed stud in a ribbed slab |
| $q_{rs}$ | The shear resistance of a headed stud in a solid slab |
| $h_d$ | The depth of the profiled steel deck |
| $\rho$ | Factor equal to 1 for normal density concrete and 0.85 for semi-low density concrete |
| $A_p$ | The concrete pull out area |
| $w_d$ | The average width of the flute of the steel decking |
| $h_d$ | The depth of the profiled steel deck |

For calculated values of the design shear resistance of headed studs, refer to table 9.3 of the Southern African Steel Construction Handbook (Limit States Design) [11]. In this document use will always be made of 19 mm studs, "Bond-dek" profiled sheeting and grade 25 MPa concrete. For single studs in ribbed slabs with the ribs perpendicular to the steel section, $q_{rr} = 82.3$ kN. When studs are used in pairs at 90 mm centres with the ribs of the slab perpendicular to the beam, the design resistance per stud is: $q_{rr} = 58.4$ kN.

### 3.2.4 Longitudinal shear in composite slabs

The force that the shear connectors must transmit between the steel section and concrete slab, is a force along the length of the beam and therefore a longitudinal force. The longitudinal shear referred to in this section is the force within the concrete slab. The shear force between the steel section and the slab gives rise to a compressive force in the concrete slab and the longitudinal reinforcement. There exist a number of different longitudinal shear planes through the concrete slab, see figure 3.2. The total longitudinal compressive force ($q_{rr}$) minus the compressive forces between the shear planes, equals the shear force that must be resisted on the shear planes. The force on these shear planes can be seen in equation (3.16).

For this calculation the transverse cross sectional area of the concrete, adjacent to the beam, is designated as $A_c$, i.e. the area of concrete above the flange of the steel section between the

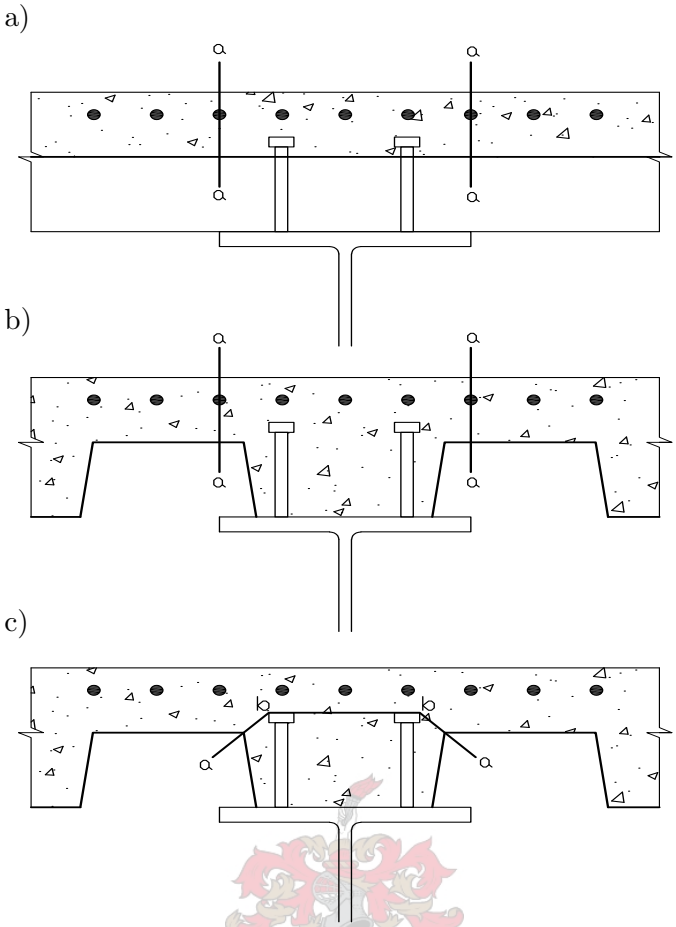


**Figure 3.2:** Section through a composite beam with profiled decking showing possible longitudinal shear planes

shear planes, when taking a transverse section through the beam. A concrete compressive force of $0.68\phi_c A_c f_{cu}$ and a longitudinal reinforcing steel force of $\phi_r A_{rl} f_{yr}$ develop.

$$V_u = \sum q_r - 0.68\phi_c A_c f_{cu} - \phi_r A_{rl} f_{yr} \tag{3.16}$$

$V_u$ is the combined shear force on the two longitudinal shear planes and $A_{rl}$ is the area of longitudinal reinforcement within the area $A_c$. The length of each shear plane is the distance along the beam between points of maximum and minimum bending moment. In a simply supported beam, with a uniformly distributed load, this is of course equal to half the actual length of the beam.

The factored resistance of the concrete shear planes is given as the lesser of the following two expressions according to SANS 10162 §17.9.10, [1]:

$$V_r = 0.8\phi_r A_{rt} f_{yr} + 2.67\phi_c A_{cv} \tag{3.17a}$$

or

$$V_r = 0.4\phi_c f_{cu} A_{cv} \tag{3.17b}$$

$A_{rt}$ is the area of transverse reinforcement crossing both shear planes. $A_{cv}$ is the combined area of both longitudinal shear planes. The area of longitudinal reinforcement can conservatively be neglected. Minimum transverse reinforcement is specified according to SANS 10162 [1] §17.5.4 as $A_{rt} > 0.002 \cdot \frac{A_{cv}}{2}$ for slabs with ribs parallel to the beam span and $A_{rt} > 0.001 \cdot \frac{A_{cv}}{2}$ for slabs with ribs perpendicular to the beam span. The reinforcement can be uniformly distributed.

Note that in a steel framed structure, using profiled steel sheeting to create composite floors, the fire resistance rating of the floor slab is usually specified using standard mesh reinforcement. In such a case the transverse and longitudinal reinforcement will be the same. Also consider that the primary beams will normally be designed as composite as well. In this case the profiled sheet spans in the same direction as the primary beam and therefore a few things will change, namely: the resistance of the shear connectors, the definition of the longitudinal shear planes and possibly the position of the critical sections through the beam.

## 3.3 Serviceability limit state

This section will outline the calculations that must be done to compute the deflections of a composite beam. Various components of the deflection must be considered. The total deflection to a large degree depends on the method of construction. As will be shown, the use of unpropped construction versus propped construction can influence the final deflection. If the beam is not propped during construction the initial deflection of the steel beam is greater because the concrete part of the composite beam can not contribute to the resistance of the section. It is possible to make use of pre-cambered beams in order to reduce initial deflections to acceptable limits. This method of construction enables one to use much longer spans, while still satisfying the serviceability limit state.

### 3.3.1 Deflection of composite beams

The case for beams left unpropped during construction will be considered first. One of the main benefits of the composite floor structure considered, is that speed of construction can be achieved. By propping the steel beams during construction this advantage of the structural system is taken away.

To calculate deflections, according to SANS 10162-1:2004 §17.3.1 [1], the following demands must be met:

- Calculation of deflections shall include the effects of creep and shrinkage of concrete
- The increased flexibility resulting from interfacial slip and partial shear connection shall be taken into account

- The aforementioned effects shall be established by tests or analysis, where practicable
- The effect that full or partial continuity in steel beams and concrete slabs might have must be considered in order to reduce the calculated deflections

The effective moment of inertia is defined in order to make accommodation for partial shear connection and interfacial slip effects:

$$I_e = I_s + 0.85(\alpha^{0.25})(I_t - I_s) \tag{3.18}$$

$I_s$ is the moment of inertia of the steel section, $I_t$ is the transformed moment of inertia of the composite beam and $\alpha$ is the fraction of full shear connection. The transformed moment of inertia is calculated by transforming the composite section to an equivalent steel section, using the modular ratio $n = \frac{E_s}{E_c} = \frac{200}{26}$ and is calculated as:

$$I_t = \frac{b_e t^3}{12} + b_e t \cdot \left(h + t_{slab} - y - \frac{t}{2}\right)^2 + I_s + A_s \left(y - \frac{h}{2}\right)^2 \tag{3.19}$$

In equation (3.19) $y$ is the distance to the centroid of the transformed section, from the bottom of the steel section:

$$y = \frac{A_s \cdot \frac{h}{2} + b_e t \cdot (h + (t_{slab} - t) + \frac{t}{2})}{A_s + b_e t} \tag{3.20}$$

Deflections due to shrinkage develop in composite beams as follows: as the concrete decreases in volume while it cures, tensile strains develop in the concrete. The concrete slab is connected via shear studs to the flange of the steel section. The concrete in tension causes a compressive force in the steel section. The tension force in the steel and the compressive force in the concrete, generate a positive (sag) moment in the composite beam, which causes a downward deflection. Note that the shrinkage deflection is directly proportional to the assumed free shrinkage strain. For the shrinkage of concrete the following model can be used:

$$\Delta_s = \frac{\varepsilon_f A_c L^2 y}{8 n_t I_t} \tag{3.21}$$

Where:

| | |
|---|---|
| $\varepsilon_f$ | The free shrinkage strain of concrete |
| $A_c$ | The effective area of the concrete slab |
| $E_{ct}$ | The effective modulus of concrete in tension |
| $L$ | The span of the beam |
| $n_t$ | The modular ratio, $\frac{E}{E_{ct}}$ |
| $y$ | The distance from the centroid of effective area of the concrete slab, to the elastic neural axis |
| $I_t$ | The transformed moment of inertia, but based on the modular ratio $n_t$ |

From Annex G §G.5 of SANS 10162-1:2004 [1], the effective modulus of concrete in tension can

be calculated as:

$$E_{ct} = 8300 - 4800(\sigma_{ct}); \qquad 0.3 \leq \sigma_{ct} \leq 1.2 \tag{3.22}$$

$\sigma_{ct} = 1.2$ corresponds to the maximum tensile stress that the concrete can develop due to shrinkage, without cracking taking place. §G.5 of SANS 10162-1:2005 [1] states that the shrinkage deflection is not sensitive to the modular ratio, due to the fact that both the effective moment of inertia and the distance to the centroid ($y$) vary with it. It must be realised that for a maximum tensile stress of 1.2 MPa due to shrinkage the transformed modular ratio $n_t$, is in the order of 80. Research has shown that changing the modular ratio from 20 to 80, for beams of usual proportions, decreases the shrinkage deflection in the order of 30%. Thus when using the elastic modulus for concrete in compression, (not $E_{ct}$ as in equation (3.21)), to calculate the modular ratio that is used in equation (3.21), it would be appropriate to reduce the shrinkage deflection by 30%. The reduction of 30% can be considered as an upper bound and it might be more appropriate to consider the research by Ferguson as is referred to in Annex G.5 of SANS 10162-1:2005 [1]. This research shows that a transformed modular ratio of 60 is considered as more appropriate, with a decrease in the shrinkage deflection of only about 15%.

According to Annex G.4 of SANS 10162-1:2005 [1] an appropriate value for the free shrinkage strain ($\varepsilon_f$), if no other data is available, is 800$\mu$ (This value is very conservative). According to prEN 1992-1-1:2003 [5] §3.1.4 the appropriate value of the free shrinkage strain can be assumed as approximately 400$\mu$. The free shrinkage strain is dependant on the water/cement ratio of the mix, percent fines in the mix, relative humidity, the characteristic value of the concrete compressive strength and the ratio of the concrete cross sectional area to the perimeter of the exposed part. Using the method given by SABS-0100-1 Annex C [10], the free shrinkage strain is calculated as approximately $\varepsilon_f = 380\mu$. In all further calculations presented in this document, a free shrinkage strain of $\varepsilon_f = 400\mu$, will be assumed.

For the simply supported non composite beam, loaded under self weight and not propped, the deflection calculation is as seen in equation (3.23). Note that the initial deflection is part of the beam's elastic deflection. The elastic deflection will be termed $\Delta_e$. In the case of an unpropped beam the elastic deflection is comprised of two parts. There is an initial deflection calculated using the steel section's moment of inertia, but also a deflection due to services and the long term part of the imposed load. The services are installed after the beam attains composite action and this part of the elastic deflection must be calculated using the composite beam's effective moment of inertia. In the case where the beam is propped the elastic deflection will take place in one step when the props are removed. For the propped case the elastic deflection will therefore be calculated using only the composite beam's effective moment of inertia.

$$\Delta_i = \frac{5}{384} \cdot \frac{W_{(beam,deck,concrete)} \cdot L^3}{EI} \tag{3.23}$$

$$\Delta_e = \frac{5}{384} \cdot \frac{(W_{live,long} + W_{services})\, L^3}{EI_e} \tag{3.24}$$

**Table 3.1:** Deflections of composite beams with various steel sections using a limiting deflection of $\Delta_{allow} = L/300$ and free shrinkage strain $\varepsilon_f = 400\mu$. The beams are not propped.

| Beam desig. | $I$ | $I_e$ | $I_t$ | $\Delta_i$ | $\Delta_{sh}$ [a] | $\Delta_c$ | $\Delta_s$ [b] | $\Delta_{tot}$ | $\Delta_{util}$ |
|---|---|---|---|---|---|---|---|---|---|
| | $10^6$ [mm$^4$] | $10^6$ [mm$^4$] | $10^6$ [mm$^4$] | [mm] | | | | | [%] |
| I305x165x46 | 99.30 | 333.26 | 412.05 | 40.91 | 6.73 | 2.26 | 9.79 | 59.69 | 1.99 |
| I356x171x45 | 121.00 | 389.68 | 480.15 | 33.53 | 5.75 | 1.93 | 8.91 | 50.13 | 1.67 |
| I356x171x57 | 161.00 | 488.00 | 598.12 | 25.54 | 4.60 | 1.56 | 8.64 | 40.33 | 1.34 |
| I406x140x39 | 124.00 | 403.07 | 497.03 | 32.50 | 5.56 | 1.86 | 8.29 | 48.20 | 1.61 |
| I406x178x54 | 187.00 | 551.62 | 674.40 | 21.92 | 4.07 | 1.37 | 7.95 | 35.31 | 1.18 |
| I406x178x67 | 243.00 | 678.05 | 824.54 | 17.12 | 3.31 | 1.13 | 7.69 | 29.24 | 0.97 |
| I457x191x67 | 294.00 | 792.09 | 959.81 | 14.15 | 2.83 | 0.97 | 7.07 | 25.02 | 0.83 |
| I457x191x82 | 371.00 | 952.75 | 1148.65 | 11.40 | 2.35 | 0.82 | 6.84 | 21.41 | 0.71 |
| I457x191x98 | 458.00 | 1120.20 | 1343.19 | 9.39 | 2.00 | 0.70 | 6.60 | 18.70 | 0.62 |
| I533x210x92 | 553.00 | 1320.10 | 1578.41 | 7.73 | 1.70 | 0.59 | 5.94 | 15.96 | 0.53 |
| I533x210x109 | 668.00 | 1527.89 | 1817.45 | 6.52 | 1.47 | 0.52 | 5.74 | 14.24 | 0.47 |

[a] Short term deflection
[b] Shrinkage deflection

For the composite beam loaded under short term imposed loads the deflection is calculated also using equation (3.23) but the effective moment of inertia is used for the beam.

$$\Delta_{sh} = \frac{5}{384} \cdot \frac{W_{(live,short)} \cdot L^3}{EI_e} \tag{3.25}$$

It is stated in [1] that one can make accommodation for creep effects by increasing the elastic deflections caused by self weight and long term imposed loads by 15%.

$$\Delta_c = 0.15 \cdot \frac{5}{384} \cdot \left( \frac{(W_{permanent} + W_{live,long})L^3}{EI_e} \right) \tag{3.26}$$

Table 3.1 shows some calculated deflections for a range of steel sections. It is clear that in many cases the calculated deflection of a composite beam is excessive and must be reduced. The total deflection can be reduced in a few ways but mainly by reducing the dominant initial deflection. Another factor that can be taken into account is the rotational resistance of beam to column connections. The beam's deflection was calculated for a simply supported structure. In reality the connections will always transmit moments to the columns. It is a difficult task to establish the stiffness of such connections without the aid of FEM analysis etc. Be it as it may the stiffness of connections and the continuity of the concrete slab, will reduce the deflection of the composite beam.

The initial deflection can be countered in two ways. Firstly the beam can be propped until composite action is achieved and secondly, the beams can be pre-cambered in order to compensate for the initial deflection. If the beams are propped during construction, the initial deflection of the beam must be calculated at the time when the props are removed. Use will therefore be

**Table 3.2:** Comparison of deflections for propped and un-propped beams using a limiting deflection of $\Delta_{allow} = L/300$ and free shrinkage strain $\varepsilon_f = 400\mu$.

| Beam desig. | Propped construction | | | | | | Unpropped construction | | | | | |
|---|---|---|---|---|---|---|---|---|---|---|---|---|
| | $\Delta_i$ | $\Delta_{sh}$ [a] | $\Delta_c$ | $\Delta_s$ [b] | $\Delta_{tot}$ | $\Delta_{util}$ | $\Delta_i$ | $\Delta_{sh}$ | $\Delta_c$ | $\Delta_s$ | $\Delta_{tot}$ | $\Delta_{util}$ |
| | [mm] | | | | | [-] | [mm] | | | | | [-] |
| I305x165x46 | 22.30 | 6.73 | 3.35 | 9.79 | 42.17 | 1.41 | 40.91 | 6.73 | 2.26 | 9.79 | 59.69 | 1.99 |
| I356x171x45 | 19.06 | 5.75 | 2.86 | 8.91 | 36.59 | 1.22 | 33.53 | 5.75 | 1.93 | 8.91 | 50.13 | 1.67 |
| I356x171x57 | 15.33 | 4.60 | 2.30 | 8.64 | 30.87 | 1.03 | 25.54 | 4.60 | 1.56 | 8.64 | 40.33 | 1.34 |
| I406x140x39 | 18.36 | 5.56 | 2.75 | 8.29 | 34.96 | 1.17 | 32.50 | 5.56 | 1.86 | 8.29 | 48.20 | 1.61 |
| I406x178x54 | 13.54 | 4.07 | 2.03 | 7.95 | 27.58 | 0.92 | 21.92 | 4.07 | 1.37 | 7.95 | 35.31 | 1.18 |
| I406x178x67 | 11.10 | 3.31 | 1.67 | 7.69 | 23.76 | 0.79 | 17.12 | 3.31 | 1.13 | 7.69 | 29.24 | 0.97 |
| I457x191x67 | 9.51 | 2.83 | 1.43 | 7.07 | 20.83 | 0.69 | 14.15 | 2.83 | 0.97 | 7.07 | 25.02 | 0.83 |
| I457x191x82 | 7.97 | 2.35 | 1.20 | 6.84 | 18.37 | 0.61 | 11.40 | 2.35 | 0.82 | 6.84 | 21.41 | 0.71 |
| I457x191x98 | 6.85 | 2.00 | 1.03 | 6.60 | 16.48 | 0.55 | 9.39 | 2.00 | 0.70 | 6.60 | 18.70 | 0.62 |
| I533x210x92 | 5.79 | 1.70 | 0.87 | 5.94 | 14.30 | 0.48 | 7.73 | 1.70 | 0.59 | 5.94 | 15.96 | 0.53 |
| I533x210x109 | 5.05 | 1.47 | 0.76 | 5.74 | 13.02 | 0.43 | 6.52 | 1.47 | 0.52 | 5.74 | 14.24 | 0.47 |

[a] Short term deflection
[b] Shrinkage deflection

made of the effective moment of inertia in order to calculate the initial elastic deflection.

Both methods (propping and pre-camber) have clear disadvantages from a cost point of view. In the first case the extended construction time and added labour will increase cost. In the second case added labour is needed to pre-camber the steel sections. Construction time will stay the same as for the case where the beams are left unpropped if the pre-cambering process is done off-site. Another factor to consider is the skill involved in achieving correct pre-camber on all beams within the structure. It is of course possible to redesign the beams in order to satisfy the serviceability limit state explicitly. This will require much larger steel sections that will also lead to higher construction costs.

Table 3.2 show a comparison of deflections for beams that are propped and unpropped. It can be seen that although the deflections are reduced, the benefit is not as much as can be achieved by pre-camber of the sections when the beams are pre-cambered to eliminate the initial deflection. If deflections must be reduced it would make more sense to pre-camber sections.

## 3.4 Fire limit state

In the following sections a basic design scenario is considered: for a composite beam an I-profile steel section is used and composite action is achieved by use of headed shear stud connectors. The number of connectors were determined by the design for the ultimate limit state, at normal temperatures. The stud connectors have a diameter of 19 mm and a overall length of 113 mm. The steel joist is connected to a ribbed concrete slab with a minimum thickness of 130 mm.

The minimum bound on the slab thickness is due to the required concrete cover over the shear studs. Refer to figure 3.3 for a drawing of a section through a typical composite beam and slab.

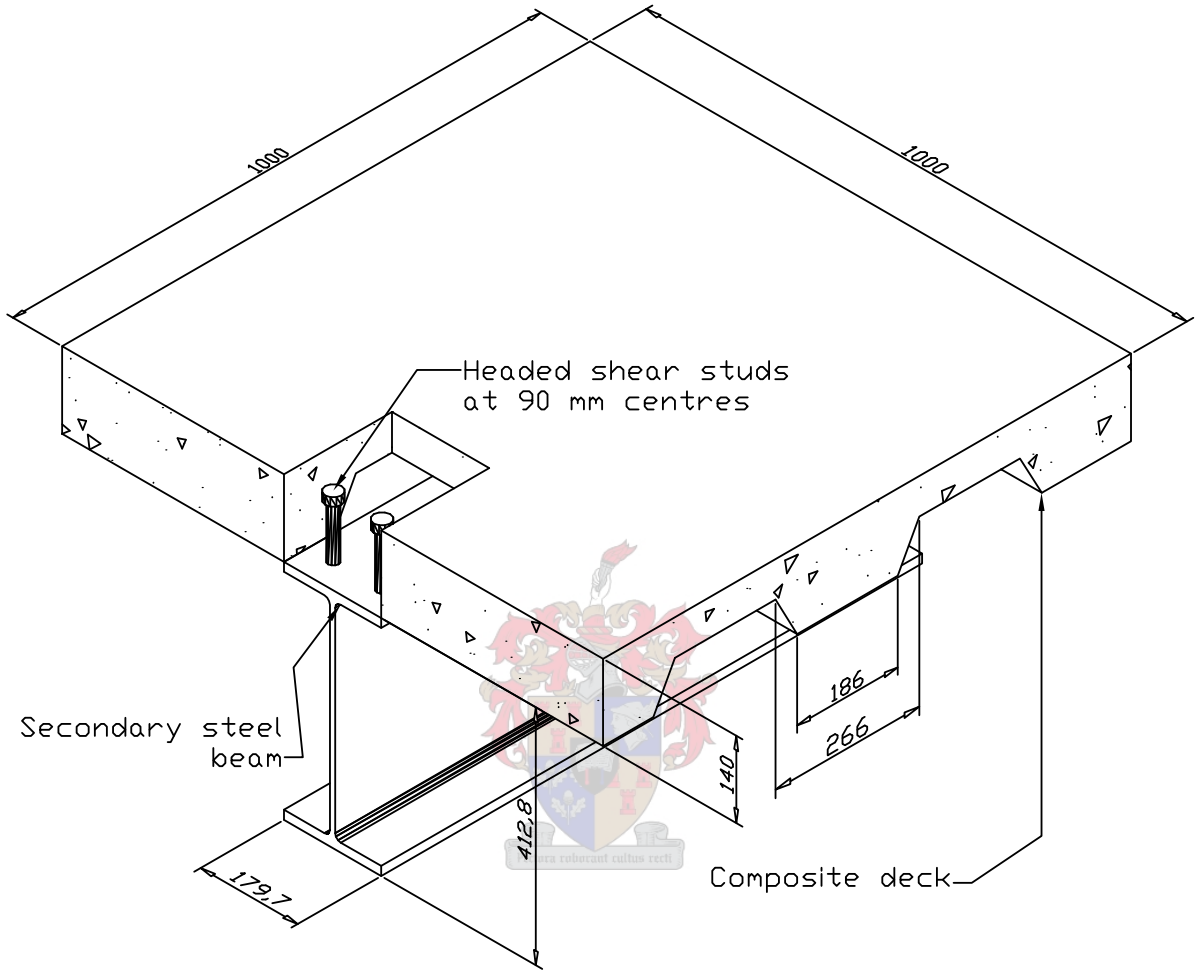


**Figure 3.3:** Section of unit length and unit width through a secondary composite beam

A clear distinction is made between the composite beam and the composite slab. The composite slab is a one way spanning element (due to the corrugated sheeting), that spans between supporting composite beams. Therefore the composite slab also acts as the compressive part of the composite beams under consideration. This document is concerned with the design for fire of the composite beams.

For the fire resistance rating of the composite slab consider that it is designed using a "Bond-dek" corrugated steel sheet with a height of 75 mm. "Bond-dek" is a product that is available in South Africa and is designed according to the British standard. In the South African Steel Construction Handbook [11] it is stated that "Bond-Dek" slabs, reinforced with welded steel

mesh of 8 mm thickness at 200 mm centres, can give up to 120 minutes fire resistance.

### 3.4.1 The procedure to design composite beams for the fire limit state

Following the methods set out in the literature review in chapter 2 and the procedure set out in this section, one can design composite beams with unprotected or protected, hot rolled steel sections and composite concrete slabs. This procedure is based on the Eurocode recommendations, see [3, 7, 4, 6]. A specific method is given in Annex C of prEN 1994-1-2 [6] for the design of composite beams under fire. This procedure is summarised by the following steps:

- Firstly the load effect must be determined according to rules for the combination of actions given by Eurocode 1990 for the Basis of Structural Design, [2]. These rules are given in Eurocode 1990 § 6.4.3.3 and also in § 4.3 Eurocode 1991-1-2, [3].
- The resistance of the composite beam may be calculated for the time, temperature or mechanical resistance domains. Annex C of prEN 1994-1-2 [6] calculates the moment resistance of a composite beam.
- In normal circumstances the required resistance of a structural component will be specified in the time domain by a relevant legislative document, such as building regulations or even a specification given by the owner.
- It is important to note that the simplified procedures applied to calculate resistances for the fire limit state, are in general only the application of reduction factors in order to give reduced mechanical resistances. In the text that follows this becomes apparent. In the literature review it was stated that structural interaction between building elements is very important when considering the behaviour of structures in the fire scenario. The simplified method presented here does not take structural interaction into account.

### 3.4.2 Bending failure – Loss of steel strength only

The ultimate load can be determined as follows:

$$\begin{aligned} E &= G_k + (\psi_{1,1} \text{ or } \psi_{2,1}) \cdot Q_{k,1} \\ &= (G_b + G_f + G_s) + 0.3 \cdot (Q_{k,1}) \qquad [\text{kN/m}^2] \end{aligned} \tag{3.27}$$

$G_b$ is the self weight of the steel beam, $G_f$ is the self weight of the floor and $G_s$ the weight of services, all in units of kN/m$^2$. The $\psi$-factors are combination factors for the accidental limit state. According to table A1.1 of EN 1990 [2], $\psi_{1,1} = 0.5$ and $\psi_{2,1} = 0.3$. The value may be set by the national annex and as can be seen in equation (3.27) the value of 0.3 was used in this study. According to the calibration study performed by Holický and Schleich, see chapter two and three of reference [13], the recommended value for the $\psi$-factor is 0.3.

The design moment that must be resisted for a simply supported beam is then:

$$M_u = \frac{E(w)(l)^2}{8} \qquad [\text{kN} \cdot \text{m}] \tag{3.28}$$

The resistance moment is calculated according to Eurocode 1994-1-2 Annex C, [6]. By this method, the tensile force in the steel joist must be determined first. This force in the steel is dependant on the temperature distribution in the steel profile. In the method in Annex C of [6] the steel profile (in this case an I-section) is divided into its three main parts and it is assumed that no heat transfer takes place between these parts. The tensile force and its location in the steel profile are calculated using the following general expressions:

$$T = \frac{[(k_{y,\theta 1})(f_y)(b_1 e_1) + (k_{y,\theta 2})(f_y)(h_w e_w) + (k_{y,\theta 3})(f_y)(b_2 e_2)]}{\gamma_{m,fi}} \tag{3.29}$$

$$y_T = \frac{\left[(k_{y,\theta 1})(f_y)(b_1)(\frac{e_1}{2})^2) + (k_{y,\theta 2})(f_y)(h_w e_w)(e_1 + \frac{h_w}{2}) + (k_{y,\theta 3})(f_y)(b_2 e_2)(h - \frac{e_2}{2})\right]}{T(\gamma_{m,fi})} \tag{3.30}$$

Where:

| | |
|---|---|
| $k_{y,\theta i}$ | The reduction factor for the steel yield strength $f_y$ |
| $b_1$ | The width of the bottom flange |
| $b_2$ | The width of the top flange |
| $e_1$ | The thickness of the bottom flange |
| $e_2$ | The thickness of the top flange |
| $e_w$ | The thickness of the web |
| $h_w$ | The height of the web |

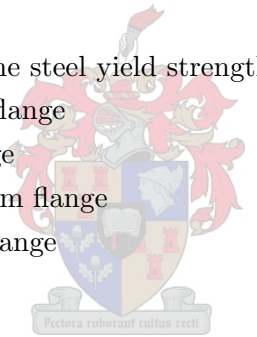

Note that the material factor $\gamma_{m,fi}$ is taken as 1 for the accidental limit states.

The Eurocode also makes the provision that if the steel section used has a depth of less than 500 mm, the temperature of the web may be taken as equal to that of the lower flange. Further, the section factor $\left(\frac{A_i}{V_i}\right)$ may be modified to reduce the temperature of the upper flange only if 85 % of the flange is in contact with the concrete slab or the voids are filled when use is made of profiled sheeting. The voids created by the profiled sheeting will normally not be filled, unless the beam under consideration is the edge beam of a fire compartment. It would therefore be safe to assume that the steel section is at uniform temperature.

For design, equations (3.29) and (3.30) simplifies to the following:

$$T = \frac{k_{y,\theta}(f_y)(A_s)}{\gamma_{m,fi}} \tag{3.31}$$

$$y_T = \frac{h}{2} \tag{3.32}$$

Annex C §C.1(2) of Eurocode 4 Part 1-2 [6] places the constraint seen in equation (3.33) on the tensile force. This takes into account the fact that partial shear connection was used in the design for the ultimate limit state.

$$T \leq N \cdot P_{fi,Rd} \tag{3.33}$$

When the tensile force in the steel section has been obtained, the thickness of the compression zone in the concrete slab can be determined from:

$$h_u = \frac{T}{\left(\frac{0.68(b_{eff})(f_c)}{\gamma_{m,fi}}\right)} \tag{3.34}$$

The thickness $h_u$ in equation (3.33) is however limited by §C.1(6) of Eurocode 4 Part 1-2 [6]. The compression zone must be smaller than the thickness of the concrete above the steel sheeting ($h_u \leq h_1$) where $h_1 = (t_{slab} - t_{sheet})$. This limitation is due to the fact that a composite slab with profiled steel sheeting is used. This limitation shows that a part of the steel section might be in compression and this must be taken into account.

When the calculations are implemented numerically, the fact that the steel section is assumed to be at a uniform temperature simplifies the procedure significantly. When the steel section might also be in compression, and it is assumed that the steel section is at three different temperatures for flanges and web, a different reduction factor must be applied to the part in compression. This is straightforward in the case when the plastic neutral axis lies within the steel section's flange. When one deals with deep steel sections, the plastic neutral axis might even be in the section's web. The strength of the material in the compression zone must be reduced by using two reduction factors for strength, if this is the case. Due to the uncertain temperature distribution the calculation of the reduction in steel strength can be inaccurate.

By assuming uniform temperature, the first error is made. For fires of longer duration, where the whole compartment heats up more slowly and uniformly, i.e. the steel section as well, the assumption of uniform temperature might be reasonable. In the case of fuel controlled fires with high energy release rates, large thermal gradients develop. In such a case a more uneven temperature distribution is expected in the steel section. The extent of the non-uniform temperature distribution is difficult to determine analytically. When the temperature development is uncertain, it might be wise to use advanced computer models to calculate the temperature distribution throughout the whole section (steel beam and slab).

### 3.4.3 Shear connector failure

In equation (3.33) $N$ is the number of shear connectors actually supplied in one critical length of the beam's span and $P_{fi,Rd}$ is the design shear resistance of a shear connector in the fire situation. The design shear resistance of a shear connector can then be calculated according to §4.3.4.2.5 of Eurocode 1994-1-2, [6]. The design shear resistance in case of fire must be taken as the lesser of:

$$\begin{aligned} P_{fi,Rd} &= 0.8 k_{u,\theta} P_{Rd} \\ P_{fi,Rd} &= k_{c,\theta} P_{Rd} \end{aligned} \tag{3.35}$$

In these equations $k_{u,\theta}$ and $k_{c,\theta}$ are the strength reduction factors for the steel studs and the concrete surrounding the studs, respectively. In order to find the applicable reduction factors, the temperature of the stud connectors may be taken as 80% of the temperature of the top flange. The temperature of the surrounding concrete may be taken as 40% of the top flange temperature. The value of the design shear resistance $P_{Rd}$ is taken as the values given in section 3.2.3.

### 3.4.4 Bending failure – Loss of concrete strength

In the same way as the steel section is subject to a reduction in material strength at elevated temperatures, the concrete slab will also lose strength at elevated temperatures. However, it is stated in prEN 1994-1-2 §4.3.4.2.2 [6] that a uniform temperature distribution may be assumed across the effective width of the beam and the temperatures over the thickness of the slab may be obtained from Table B.5 of the same document. Note that the method used to derive Table B.5 of Eurocode 1994-1-2 is applicable for the standard temperature time curve only. An important point to note is that for concrete temperatures below 250 °C it may be assumed that no strength reduction of concrete is considered.

The temperature distribution through a concrete element is much more difficult to calculate analytically, than for a steel section. The use of a profiled slab complicates matters. The concrete compressive block will not undergo strength reduction for most fires considered. The following dynamic develops: the steel section loses strength rapidly, due to the low thermal conductivity of concrete, only the bottom most parts of the slab loses strength. Due to the fact that static equilibrium must be preserved, the compression block at the top of the slab reduces in thickness, as the steel section keeps decreasing in strength. The effect is that the compression block moves ever further away from the heat affected part of the slab.

The loss of concrete strength could occur in slow burning ventilation controlled fires, where very slim slabs are supported by large steel sections or more likely, in slabs that are supported by protected steel sections. The maximum temperature for parametric fires, is normally reached at the early stages of the fire. If an economical design is achieved, the steel section will most

likely fail before loss of concrete strength takes place.

To calculate whether loss of concrete strength occurs, the heat profile in the concrete slab must be determined. Due to the limitation on the thickness $h_u$ in equation (3.33), two situations may occur: firstly, the critical depth may be less than the heat affected depth in the concrete slab:

$$(h_c - h_u) \geq h_{cr} \tag{3.36}$$

Secondly, the critical depth may be more than the heat affected depth in the concrete slab

$$(h_c - h_u) < h_{cr} \tag{3.37}$$

Where $h_c$ is the effective depth or thickness of the concrete slab, $h_u$ is the depth of the concrete compression zone and $h_{cr}$ is a depth determined according to Table B.5 of prEN 1994-1-2 [6] or by other means, such as heat transfer software. $h_{cr}$ can be seen as the depth of the concrete that is subject to a strength reduction, due to temperatures above 250 °C. The depth $h_{cr}$ is measured from the bottom of the concrete slab, or in case of a composite slab with steel sheeting, from the bottom of the effective thickness. The effective thickness ($h_{eff}$) can be determined from the Eurocode 1994-1-2 § B.4 [6] and is based on the cross sectional properties of the composite slab. In the case when a "Bond-dek" profiled steel sheet is used, with a 140 mm thick slab, the effective thickness is as follows:

$$\begin{aligned} h_c &= h_1 + 0.5h_2 \\ &= 65 + 0.5(75) \\ &= 102.5 \qquad \text{[mm]} \end{aligned} \tag{3.38}$$

The critical thickness $h_{cr}$ is dependant on the time of fire exposure. Table B.5 of Eurocode 1994-1-2 [6] state that after a fire duration of 30 minutes, 30 mm of the concrete slab is subject to a strength reduction. This depth increases to 50 mm after the slab has been exposed to fire for 60 minutes. It is stated in the Eurocode that table B.5 is a conservative approximation. If natural or parametric fire curves are used the temperature distribution in the concrete slab must be determined by other means.

If a part of the concrete slab is subject to a strength reduction, the following method may be used to determine the force in the concrete and hence the tensile force in the steel profile:

$$T = F = \frac{\left[(h_c - h_{cr})(b_{eff})(f_c) + \sum_{i-2}^{n-1}(0.01b_{eff})(f_{c,\theta i}) + (h_{u,n}b_{eff})(f_{c,\theta n})\right]}{\gamma_{m,fi}} \tag{3.39}$$

Where:

$$h_u = (h_c - h_{cr}) + 0.01(n-2) + h_{u,n} \qquad \text{[m]} \tag{3.40}$$

$n$ is the total number of concrete layers in compression, including the top layer that is at a

lower temperature than 250°C. In the first term of equation (3.40), $(h_c - h_{cr})$ is the part of the slab not subject to a strength reduction. The second and third terms divide the heat affected part into $n-2$ slices of 10 mm thick and slice $n$, with an arbitrary thickness. To determine the force in the concrete ($F$) is a iterative procedure. The procedure can be implemented by calculating the compressive force in the concrete using the original compression block depth ($h_u$), but applying concrete strength reduction factors to certain layers of concrete. A new compression block depth is calculated using the reduced compressive force and the procedure is repeated until it converges.

### 3.4.5 Longitudinal shear failure

Analogous to the calculation for normal temperatures, the total design longitudinal shear is determined by taking account of the force that develops in concrete shear planes, over the critical length of the beam. In the same way as with shear connector failure, reduction factors can be applied to the force that the shear connectors can resist. As the steel section weakens, as the fire progresses, the ultimate longitudinal shear will also become less. If the concrete does not undergo strength reduction the longitudinal shear resistance will be sufficient for fire, given that it was checked for normal temperature design. Depending on the heat profile in the concrete slab, the reinforcement might also undergo a strength reduction. If this happens it might be necessary to find a more accurate heat profile through the concrete slab to find the temperature of the reinforcement.



### 3.4.6 Example – Thermal response and mechanical response

This section will show calculations for the design of a secondary composite beam i.e. the profiled steel sheeting spans transversely to the steel section, see figure 3.3. The secondary beams are connected via fin plate connections to the primary beams and hence are simply supported. The secondary beam under consideration is an internal compartment beam, meaning it does not support edge walls. The voids between the sheeting and the steel section are not filled to stop fire spread. The beam supports a uniformly distributed load. The beam is 9 m long and the secondary beams are spaced 3 m centre to centre. The gridline spacing is chosen on the basis of the load bearing capacity of the "Bond-Dek" sheeting, see the Southern African Steel construction Handbook, [11].

Following the process described in the literature review and the preceding sections, the beam must firstly be designed for the ultimate and serviceability limit states. The values for the resistance in bending (for all stages of construction), longitudinal shear and deflection, for a rage of steel sections, can be found in table A.2 in appendix A on page 117. From the table it can be seen that the deflection of the beam limits the design in all cases considered. The I406x178x67 is the smallest section that can be used, which satisfies both the ultimate and serviceability limit states. The utilisation factor for the deflection ($\Delta_{tot}/\Delta_{lim}$) is just under

one. A lighter section could be used by taking possible rotational restraint into account which reduces the deflection of the beam. For purposes of an example the I406x178x67 section is used. A calculation intended to serve as example, can also be found in appendix A.

The opening factor is calculated by assuming that the windows are open at the time of the fire and that the rest of the glass will break in the early stages of the fire. One could get a more accurate fire model by using the software OZone or its like. In these calculations the Eurocode parametric curves will be used. The Eurocode curves do not make provision for a changing opening factor. Eurocode 1991-1-2 Annex A §4 [3] state that the thermal properties of the boundary may be taken at ambient temperature at the start of the fire.

Table 3.3 on page 52 shows all the data that must be gathered in order to do a fire design in general and specifically in order to use a parametric fire curve.

#### 3.4.6.1 Temperature development

To calculate the temperature development of the composite beam the Eurocode step-by-step procedure is used, [6, 7]. The temperature development calculation in the compartment and the composite beam was implemented numerically. The Matlab M-files and an explanation of the implementation can be found in appendix B.

The equations for the implementation of the Eurocode step-by step method for unprotected sections are as follows:

$$\Delta\theta_{a,t} = k_{shadow} \cdot \left(\frac{1}{c_a \rho_a}\right)\left(\frac{A_i}{V_i}\right) \dot{h_{net}} \Delta t \tag{3.41}$$

$$\dot{h_{net}} = \dot{h_{net,c}} + \dot{h_{net,r}} \tag{3.42}$$

$$\dot{h_{net,c}} = \alpha_c \left(\theta_t - \theta_{a,t}\right) \tag{3.43}$$

$$\dot{h_{net,r}} = \varepsilon_m \varepsilon_f (5.67 \times 10^{-8}) \left[(\theta_t + 273)^4 - (\theta_{a,t} + 273)^4\right] \tag{3.44}$$

$$k_{shadow} = 0.9 \cdot \left(\frac{e_1 + e_2 + \frac{1}{2}b_1 + \sqrt{h_w^2 + \frac{1}{4}(b_1 - b_2)^2}}{h_w + b_1 + \frac{1}{2}b2 + e_1 + e_2 - e_w}\right) \tag{3.45}$$

The values for the dimensions needed to calculate the factor for the shadow effect are the same as given for equations (3.29) and (3.30) on page 46.

The equations for the implementation of the Eurocode step-by step method for protected sec-

**Table 3.3:** Data needed to do a fire design

| Part | Property | Value | Unit |
|---|---|---|---|
| Requirement | Resistance time | 60 | [min.] |
| Loading | Construction 1 live | 0.5 | [kN/m$^2$] |
| | Construction 2 live | 1.0 | [kN/m$^2$] |
| | Composite beam live | 2.5 | [kN/m$^2$] |
| | Raised floor | 0.4 | [kN/m$^2$] |
| | Services | 0.25 | [kN/m$^2$] |
| | Ceiling | 0.15 | [kN/m$^2$] |
| | Partitions | 1.0 | [kN/m$^2$] |
| | Profiled steel sheeting | 0.117 | [kN/m$^2$] |
| | Concrete slab | 2.6 | [kN/m$^2$] |
| Composite beam | Length | 9 | [m] |
| | Effective width | 2.25 | [m] |
| | Steel section size | I406x178x67 | [-] |
| | Slab thickness | 0.140 | [m] |
| Fire compartment | Fire load | 511[a] | [MJ/m$^2$] |
| | Length | 4-30 | [m] |
| | Breadth | 9 | [m] |
| | Height | 3.6 | [m] |
| Opening factor | $A_v$ | $0.3 \cdot A_f$ | [m$^2$] |
| | $A_t$ | 367.2 | [m$^2$] |
| | $h_{eq}$ | 1.5 | [m] |
| Boundary materials | Type[b] | Brick | [-] |
| | Thermal conductivity | 1.2 | [W/mK] |
| | Specific heat | 1200 | [J/kgK] |
| | Density | 2000 | [kg/m$^3$] |
| Fire protection materials | Type | Gypsum board | [−] |
| | Thickness | 0.005 | [m] |
| | Thermal conductivity | 0.2 | [W/mK] |
| | Specific heat | 1700 | [J/kgK] |
| | Density | 800 | [kg/m$^3$] |

[a] The characteristic value for office areas given in Eurocode 1991-1-2 Annex E [3]

[b] Eurocode 1991-1-2 [3] makes accommodation for different boundary materials on floors, walls etc. but for simplicity the thermal properties of brick will be used for all surfaces

tions are as follows:

$$\Delta\theta_{a,t} = \left[\left(\frac{\frac{\lambda_p}{d_p}}{c_a\rho_a}\right)\left(\frac{A_{p,i}}{V_i}\right)\left(\frac{1}{1+\frac{w}{3}}\right)(\theta_t - \theta_{a,t})\Delta t)\right] - \left(e^{w/10} - 1\right)\Delta\theta_t \qquad (3.46)$$

$$w = \left(\frac{c_p \rho_p}{c_a \rho_a}\right) d_p \left(\frac{A_{p,i}}{V_i}\right) \tag{3.47}$$

For a description of all symbols, refer to the list of symbols of this document or the Eurocode 1994-1-2, [6]. From the equations above, it can be seen that the temperature must be calculated for time steps of $\Delta t$. The Eurocode states that for unprotected steel sections the time step must not be taken as more than 5 seconds. For protected sections the value of $\Delta t$ should not be more than 30 seconds.

Figure 3.4 shows the temperature development for a composite beam with a I406x178x67 steel section. The figures show the temperature development for the unprotected and protected section according to the standard temperature time curve and the parametric curve.

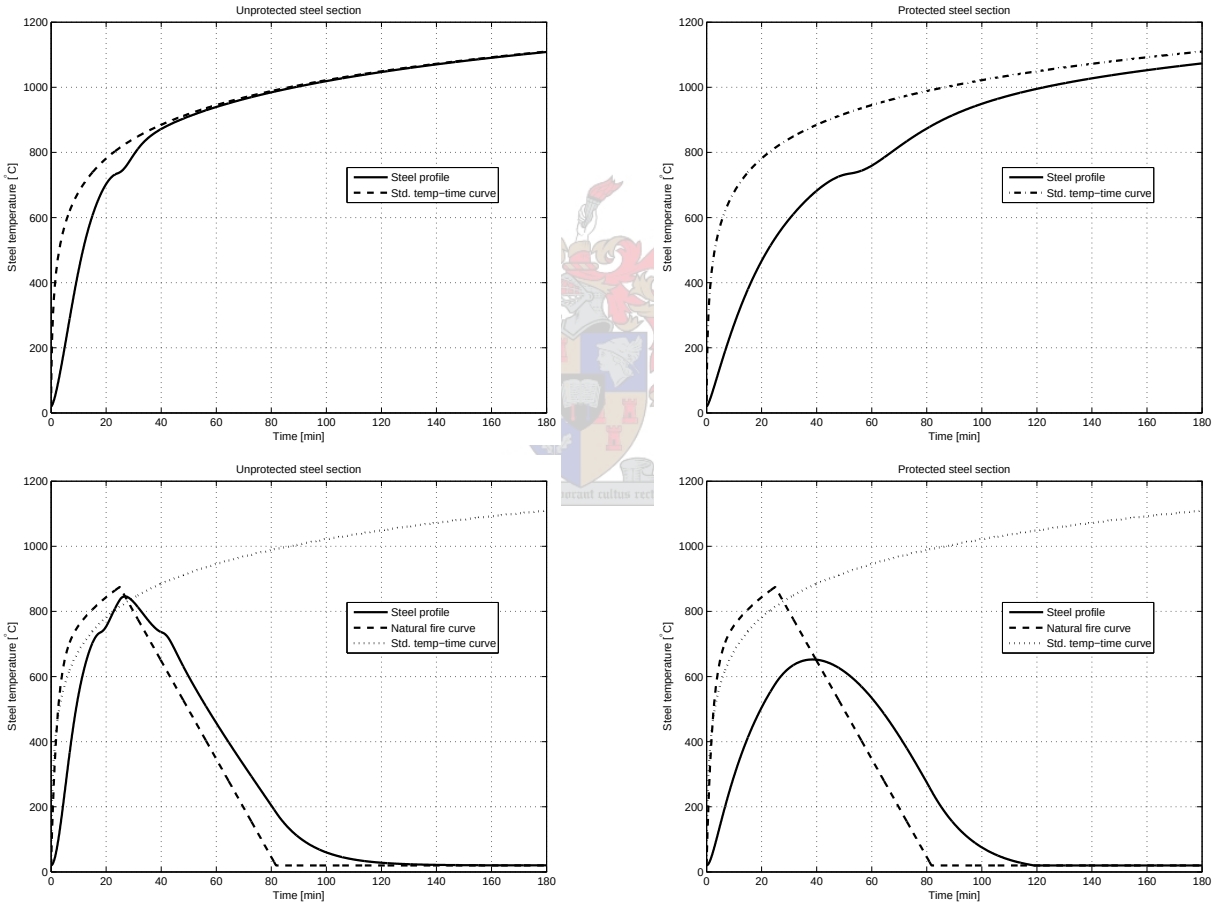


**Figure 3.4:** Development of steel temperature for different fire models. Clockwise from top-left: Std. temp-time curve – no fire protection, Std. temp-time curve – fire protected, Parametric curve – fire protected – $O = 0.0723$, Parametric curve – no fire protection – $O = 0.0723$.

In order to relate the floor area to the risk of fire activation one should make use of the design fire load ($q_{f,d}$). The Eurocode proposes that the design fire load density should be calculated as seen in equation (3.48) see Eurocode 1991-1-2 Annex E [3].

**Table 3.4:** Characteristic fire load densities fitting the Gumbel type I distribution, values in $[MJ/m^2]$

| | Mean | Std. deviation | 80% fractile | 90% fractile | 95% fractile |
|---|---|---|---|---|---|
| Dwelling | 780 | 234 | 948 | 1085 | 1217 |
| Hospital | 230 | 69 | 280 | 320 | 359 |
| Hotel room | 310 | 93 | 377 | 431 | 484 |
| Library | 1500 | 450 | 1824 | 2087 | 2340 |
| Office | 420 | 126 | 511 | 584 | 655 |
| School | 285 | 86 | 347 | 397 | 445 |
| Shopping centre | 600 | 180 | 730 | 835 | 936 |
| Cinema | 300 | 90 | 365 | 417 | 468 |
| Public space | 100 | 30 | 122 | 139 | 156 |

When calculating the design fire load in this manner, use is made of a semi-probabilistic approach that improves the structural reliability by considering non-structural factors like the use of sprinkler systems and fire detectors. In this section the fire resistance of the composite beam will be shown disregarding the added benefit of active fire protection measures.

$$q_{f,d} = q_{f,k} \cdot m \cdot \delta_{q1} \cdot \delta_{q2} \cdot \delta_n \qquad [\mathrm{MJ/m^2}] \tag{3.48}$$

Where: $m$ is the combustion factor, $\delta_{q1}$ and $\delta_{q2}$ are fire activation risk factors taking into account the size of the fire compartment and its occupancy. In the same way $\delta_n$ is a factor taking into account various active fire fighting measures. $q_{f,k}$ is the characteristic fire load density per unit floor area.

Table 3.4 presents a summary of characteristic fire load densities. The table is an extended version of the values supplied in Eurocode 1991-1-2 table E4 [3] and was extracted from Schleich et al. [13]. Kumar and Rao [22, 23] also present data on fire load densities for residential and office buildings.

From figure 3.4 on page 53 it can be seen that lower temperatures are expected in the steel profile when designing with the use of a parametric fire curve. The maximum temperature in the case where the beam is unprotected decreases from 940°C when using the standard temperature time curve to 846°C for the parametric curve. Also note that in this case the fire was ventilation controlled. This can be seen from the curves for parametric fires from the fact that the time to maximum temperature is greater than the time $t_{lim}$ specified for the fire growth rate.

When using parametric fire curves lower steel temperatures will almost always be reached. It can be seen from the curves presented in figure 3.4 that this was the case even when the rate of temperature increase is greater than specified by the standard temperature time curve. There is however a risk of wrong calculations due to unconservative assumptions regarding ventilation conditions and material properties. It would therefore be wise to do some sensitivity study in

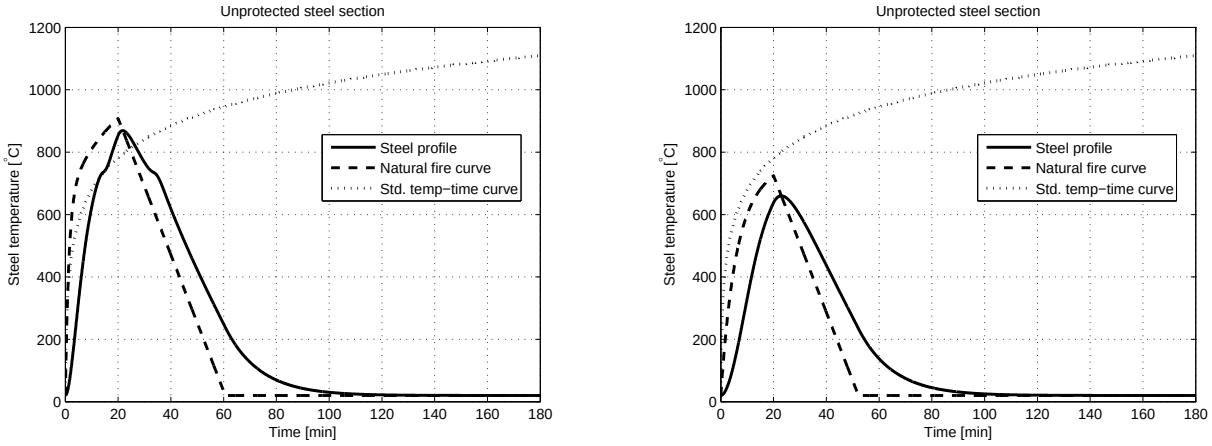


**Figure 3.5:** Effect of ventilation conditions on steel temperature. From left: Steel temperature development of I406x178x67 for an opening factor of $O = 0.0902$ and $O = 0.0903$. Note the change in temperature due to the slight change in opening factor.

order to find the range of expected temperatures.

Another factor that must be pointed out is that the calculated compartment and corresponding steel section temperatures differ significantly at the transition from fuel controlled to ventilation controlled fires. This can be seen from figure 3.5. The transition from the fuel controlled fire to the ventilation controlled fire is forced by changing the opening factor from $O = 0.0902$ to $O = 0.0903$. According to the model there is a corresponding temperature change of 209°C. This change is due to the implementation of a limiting opening factor ($O_{lim} = 0.1 \cdot 10^{-3} \cdot \frac{q_{t,d}}{t_{lim}}$) whenever the fire is fuel controlled. In the design scenario it would therefore be wise to check whether the maximum compartment temperature is sensitive to the discontinuity at the transition zone. If this is the case, a conservative approach might be followed by assuming that the fire could be ventilation controlled.

#### 3.4.6.2 Structural response

The composite beam with the I406x178x67 steel section undergoes temperature development as was seen in the previous section. The next step is to calculate the structural response of the beam due to the increased temperature of the materials.

Figure 3.6 on page 57 shows the structural response of the composite beam when the steel section is protected and not protected, for the standard temperature time curve. Figure 3.7 on page 58 show the beam's response due to a parametric fire curve. The graphs are plotted on a normalised scale in order to present the change in bending moment capacity and steel section temperature on the same graph. The heading for each graph shows the maximum steel temperature and bending moment. These values can be used with the graphs to deduce the failure moment (i.e. $M_r = M_u$) and the failure temperature. The failure temperature for the

specified beam is approximately 760°C. The time to failure is given in table 3.5.

**Table 3.5:** Time to failure of composite beams with I406x178x67 steel sections

| Temperature curve | Protection | Time to failure [min.] |
|---|---|---|
| Standard temp-time | Unprotected | 27 |
| | 5 $mm$ Gypsum board | 63 |
| Parametric | Unprotected | 21 |
| | 5 $mm$ Gypsum board | No failure |

From the plots in figures 3.6 and 3.7 it can be seen that the governing failure mode is the flexural resistance of the composite beam. For the protected beam subjected to the parametric fire, the force transmitted by the shear connection governs the design. The tensile capacity of the steel section is less than the capacity of the shear connection at time of failure. In the case where failure does not occur, the moment resistance is based on the shear connection capacity. The lines for bending failure and shear failure therefore coincide, as seen in figure 3.7.

In the numerical implementation of the fire design method the fire resistance of the beam is calculated at a number of time values. In order to find the failure/resistance time for a given situation, a polynomial is fitted to the data. The polynomial can be seen in the graphs as the red line going through the data points of minimum moment capacity. The horizontal line in the graphs is the ultimate/design moment ($M_u$) that stays constant.

Some of the conclusions that can be drawn from the calculations are:

- The steel section of the beam must be fire protected in order to achieve a the desired fire resistance rating even if the parametric temperature time curve is used.
- If the standard temperature time curve is used, the beam will not achieve a 60 minutes fire rating unless the beam is fire protected.
- In this specific case the design fire load with a characteristic value of 511 MJ/m$^2$ shows a higher temperature development rate than the standard temperature time curve.
- The next step would be to consider a reduced fire load due to the provision of active fire fighting measures. This will have a significant effect on the fire resistance of the beam.
- If it is architecturally permissable or even if it could be achieved by mechanical means, the designer could alter the ventilation conditions of the fire compartment. This could also lead to a parametric fire curve which is more forgiving in terms of the maximum temperatures reached.

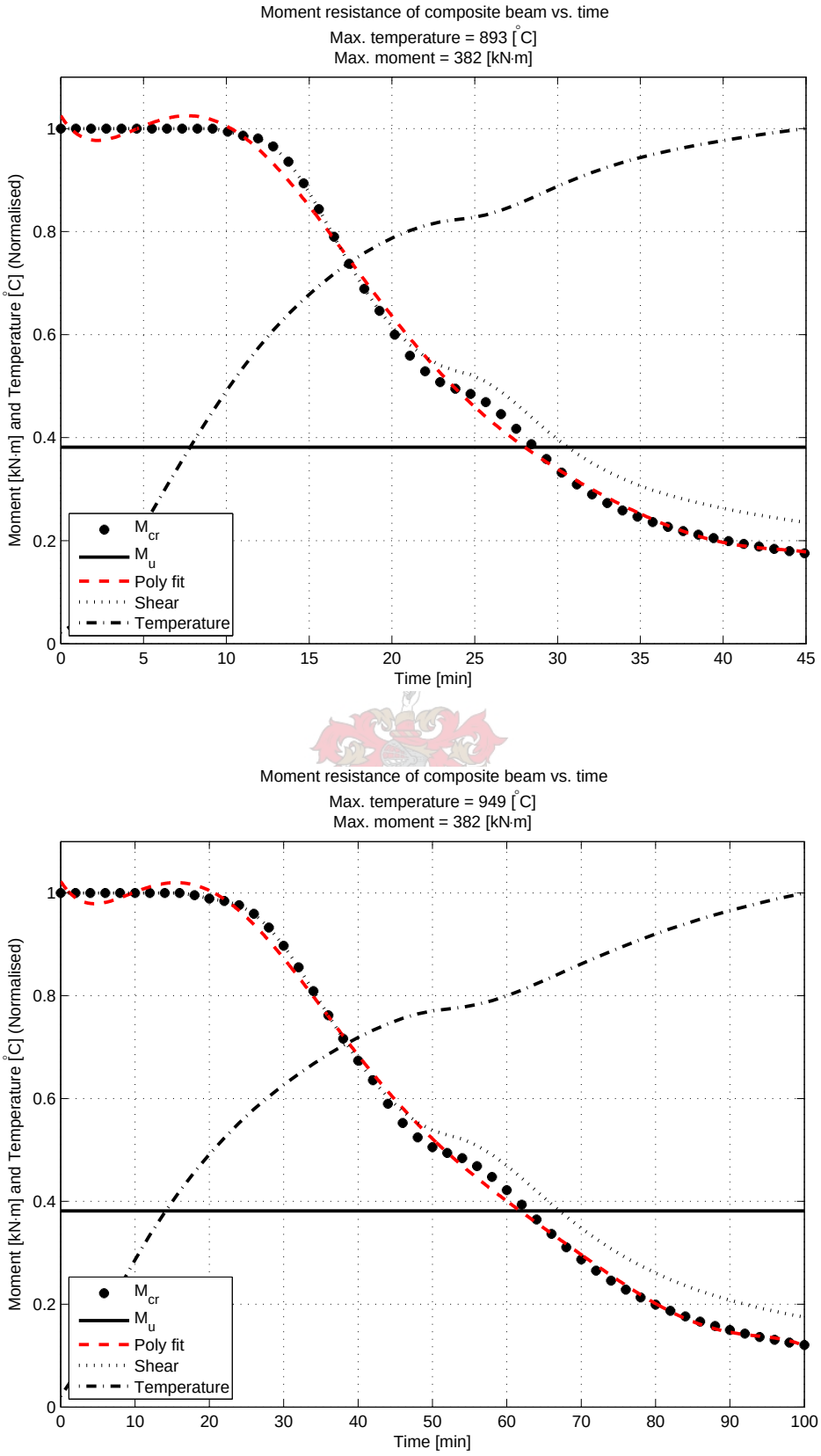


**Figure 3.6:** Loss of moment capacity of a composite beam due to standard temperature-time fire model. Top: no fire protection, Bottom: fire protected

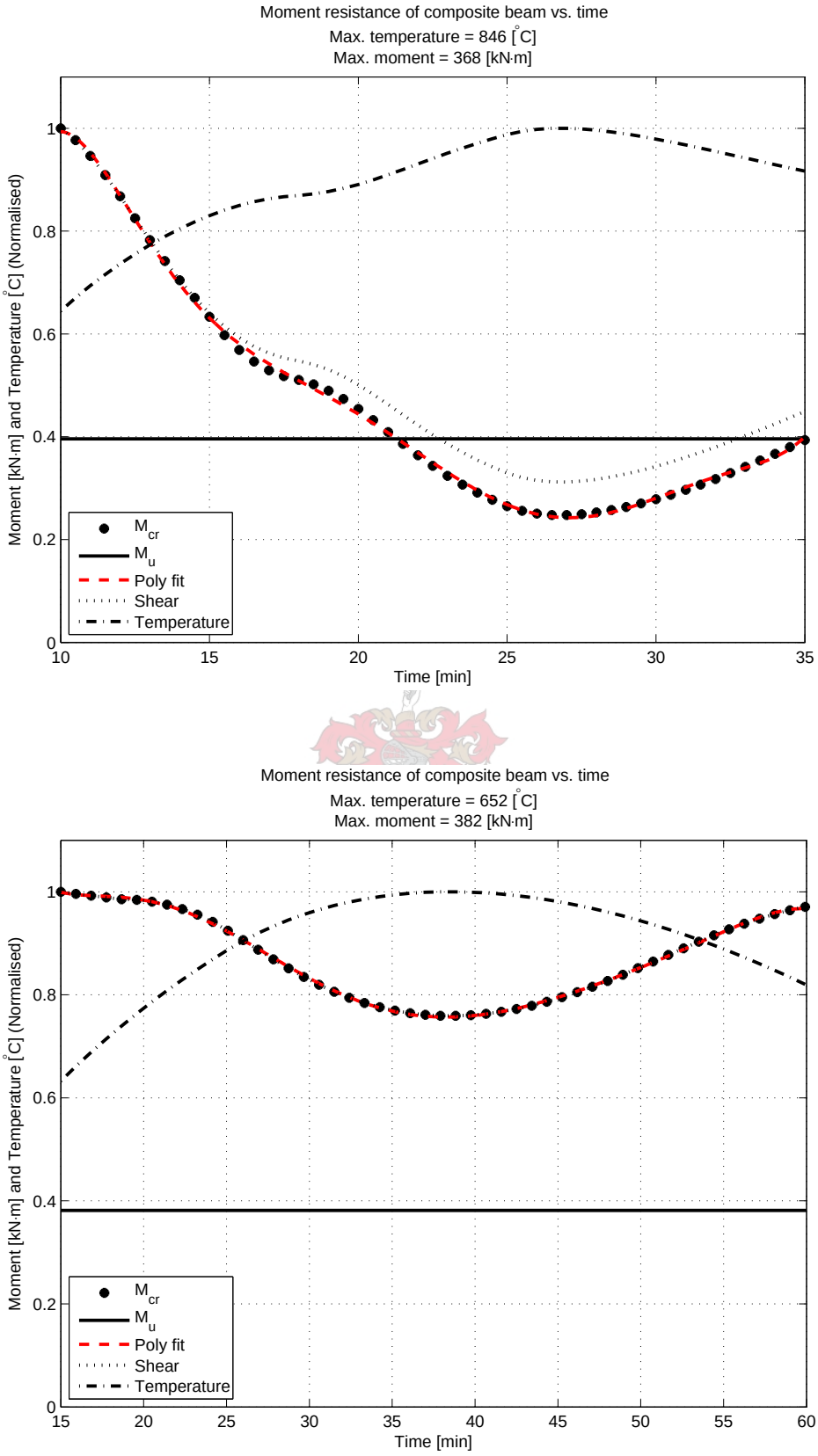


**Figure 3.7:** Loss of moment capacity of a composite beam due to a parametric fire. Top: no fire protection, Bottom: fire protected. Opening factor for the compartment: $O = 0.0723$

## 3.5 Parameter study using numerical methods

### 3.5.1 Normal temperature design ULS and SLS

A parameter study was performed in order to find the appropriate composite beam dimensions with specific regard to the reliability analysis that is shown in chapter 4. In order to perform a sensible study concerning the reliability of a structural component, the component must be close to 100% utilised. If one could design structural elements to be close to 100% utilised for all limit states simultaneously, one could consider this to be an optimal design. This is however highly unlikely and in the particular case of composite beams, this is very difficult to achieve. The deflection of a beam can however be manipulated by pre-camber of the steel section in order to have a beam that is 100% utilised for both the ultimate and serviceability limit states.

The parameter study was implemented numerically using Matlab. In all cases South African Design Codes [1, 10, 9] were used when possible. In scenarios where guidance on fire related issues was required, the Eurocode recommendations were followed. An overview of the main Matlab functions is supplied in appendix B.

The steel sections used in the composite beams are those commonly found in South Africa. The data on these sections were taken from the Southern African Institute of Steel Construction's handbook, [11]. Only "Bond-Dek" profiled steel decking was considered, with a nominal thickness of 1.2 mm. Due to the use of the specific steel decking certain limitations were placed on the possible span of the composite slab and hence the width of the composite beams.



The following parameters were varied in order to influence mainly the deflections of the beams:

- The length of the beam
- The thickness of the concrete slab
- The compressive strength of the concrete
- The amount of shear connection installed between the steel section and the slab
- The effective width of the composite beam
- The assumed limiting deflection of the beam

The deflection is modified for normal temperature design because it is in many cases the limiting design consideration. The objective was to find a beam that satisfies the serviceability limit state, while still being close to 100% utilised for the ultimate limit state. One would then go further and determine the composite beam's fire resistance, when the steel section is protected or unprotected.

Appendix A.1 of this document provides an example of the design calculations, for a typical composite beam. These calculations were numerically implemented in order to produce the

design table A.2 in appendix A.2.

### 3.5.2 Fire temperature design

The temperature at which a particular beam fails can be defined as the critical temperature. This temperature is not dependant on the fire model used but is a characteristic of the composite beam under consideration. The critical temperature can be seen as the resistance of a beam in the temperature domain. The maximum temperature that a beam can reach would also depend on the loading conditions. If a beam is heavily utilised, say 80%, for normal temperature design, the critical temperature would be much lower. Conversely, a higher critical temperature can be reached if the beam is at a low utilisation ratio at normal temperatures.

To illustrate the effect of ventilation conditions and fire load on a composite beam, consider the following: The composite beam with a $I$ 406 $\times$ 178 $\times$ 67 steel section has a critical temperature of approximately 760°C, as determined in section 3.4.6.2. A graph of the maximum steel section temperature of the composite beam vs. fire load and compartment floor area is shown in figure 3.8. To produce the graph, the area of all vertical openings was taken as constant i.e. $A_v = 25$ m$^2$. This assumption of having a constant area of vertical openings could be related to a real life scenario where a compartment has windows on one side only. The compartment floor area can be increased by having a longer compartment but the window area remains constant.

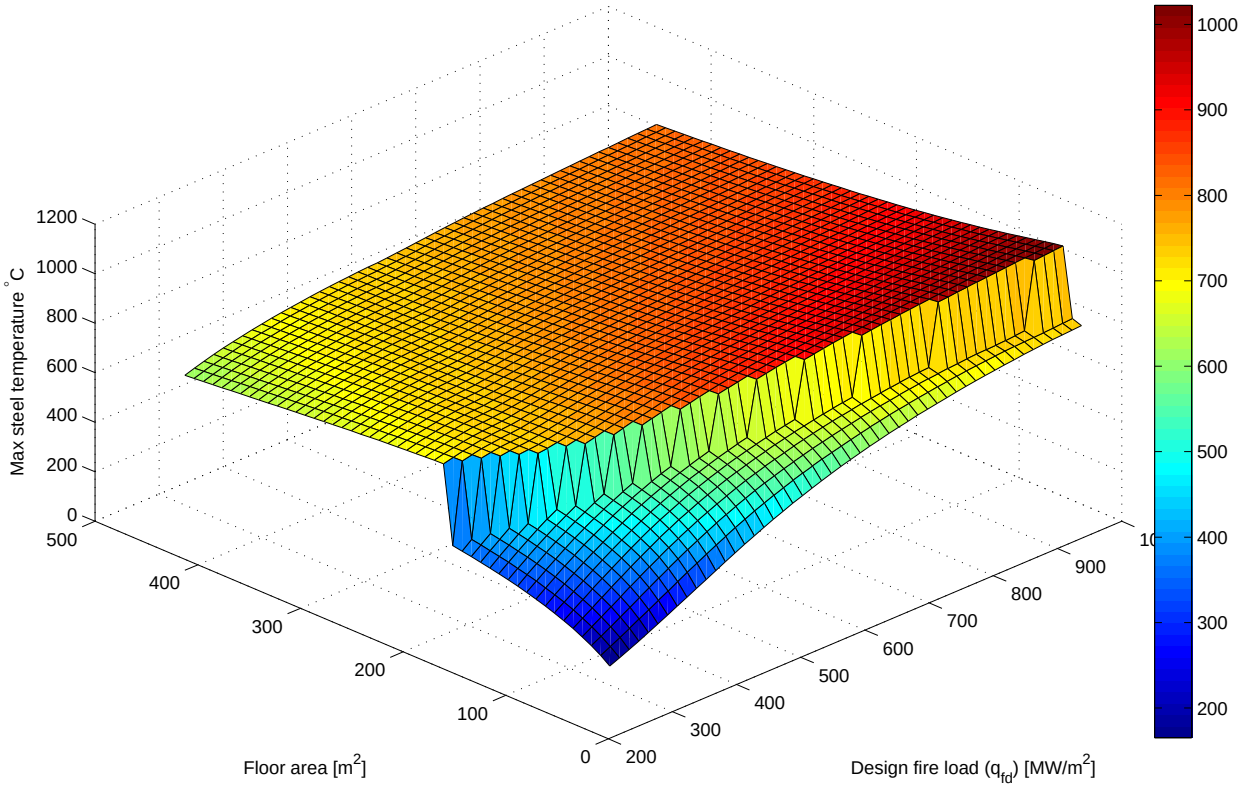


**Figure 3.8:** Effect of compartment floor area and design fire load on the maximum steel temperature of a composite beam with a $I406 \times 178 \times 67$ steel section. Area of vertical openings constant at $A_v = 25$ m$^2$

The plot of maximum steel temperatures is in fact the three dimensional "locus" of the points of maximum temperature, of many parametric fire curves. Figure 2.2 on page 12 is such a plot of various parametric fire curves, obtained by changing the opening factor of the fire compartment. The points of maximum compartment temperature could form one line on the three dimensional surface, as in figure 3.8. The three dimensional plot is not time dependant like a parametric fire curve but still shows the interface between conditions that sustain either fuel or ventilation controlled fires. The pronounced "step" in figure 3.8 is the boundary between fuel controlled and ventilation controlled compartment fires. Refer to figure 3.5 on page 55 for a plot of two fire curves, where this aspect of the parametric fire curves is clearly indicated.

A more realistic ventilation condition might be produced assuming the amount of vertical openings is a function of the floor area. Figure 3.9 is such a plot of maximum steel section temperature vs. fire load and floor area. In this variation of figure 3.8, the vertical openings were taken as 30% of the floor area. This might be more realistic due to the fact that designers would provide more windows and doors for a larger compartment. By assuming that $A_v = 0.3 \cdot A_f$, a constant opening factor is not produced. The opening factor is defined as in equation 3.49 and is still a function of the dimensions of the fire compartment.

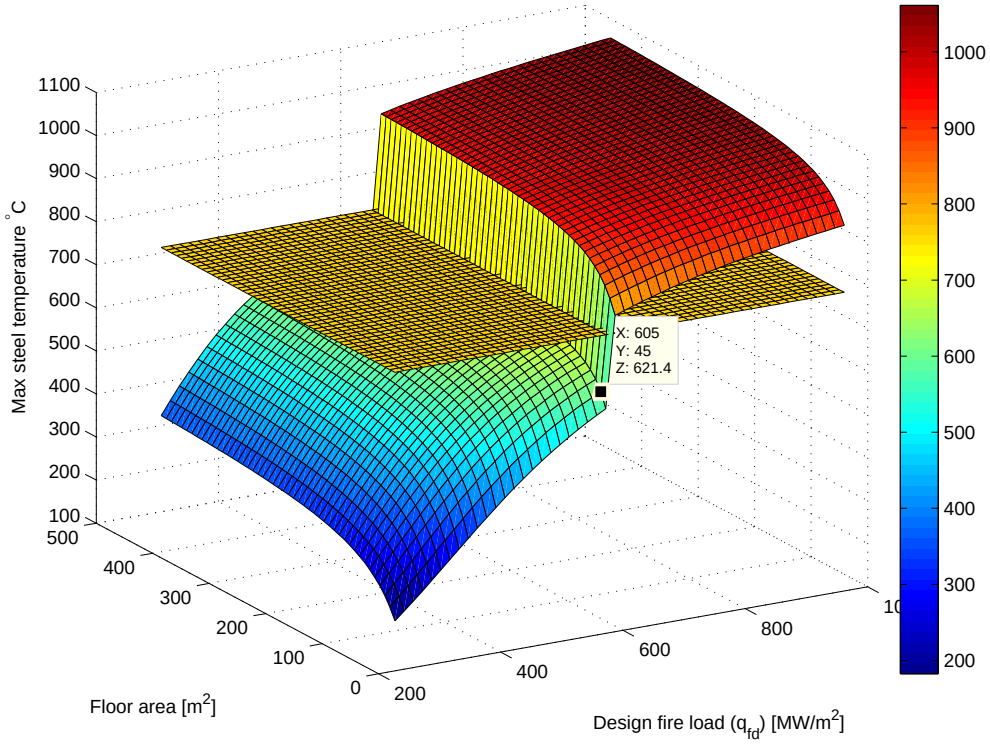


**Figure 3.9:** Effect of compartment floor area and design fire load on the maximum steel temperature of a composite beam with a $I406 \times 178 \times 67$ steel section. Area of vertical openings taken as 30% of the floor area.

$$
\begin{aligned}
O &= \frac{A_v \cdot \sqrt{h_{eq}}}{A_t} \\
&= \frac{0.3 \cdot A_f \cdot \sqrt{h_{eq}}}{2 \cdot A_f + 2 \cdot (w \times h) + 2 \cdot (l \times h)} \\
&= \frac{0.3 \cdot (l \times w) \cdot \sqrt{h_{eq}}}{2 \cdot (l \times w) + 2 \cdot (w \times h) + 2 \cdot (l \times h)}
\end{aligned}
\tag{3.49}
$$

Figure 3.9 shows that the floor area of the fire compartment has a much less significant effect on the maximum steel temperature, due to less variation in the opening factor. It is the fire load that therefore determines whether the fire is fuel or ventilation controlled. Figure 3.8 however shows that it is mostly the change in floor area that forces the transition between fuel and ventilation controlled fires. The horizontal surface in figure 3.9 represents the critical temperature of the beam. Note that for all fire compartment sizes, the beam would be sufficient as long as the design fire load is below 600 MW/m$^2$.

An important conclusion that one can draw from the graphs discussed in this section, is the values of the fire load and the floor area that would allow the designer to use the specified beam for fire design. Figure 3.10 is a reproduction of figure 3.8 but with the resistance/critical tem-

perature superimposed on the graph. All the data points below the horizontal surface indicate design scenarios for which the composite beam with a $I$ 406×178×67 section would be sufficient.

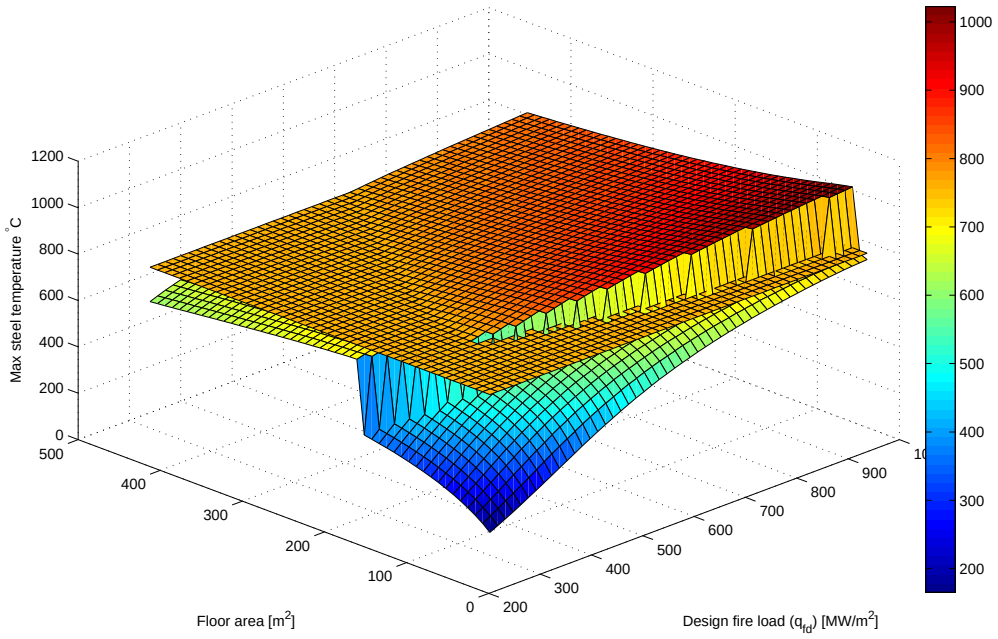


**Figure 3.10:** 3D plot of maximum steel temperatures of a composite beam with a $I406 \times 178 \times 67$ steel section versus fire load and floor area. Horizontal surface indication the resistance of the composite beam.

For this specific case it is interesting to note that fire loads of up to 650 MW/m$^2$ can be used if the floor area of the building exceeds 450 m$^2$. This is due to the small amount of vertical openings (25 m$^2$) compared to the large floor area. The fire is therefore severely ventilation controlled, producing lower temperatures. The fire would however burn significantly longer before complete burnout is reached. For a floor area of 144 m$^2$, the upper bound of the fire load is 395 MW/m$^2$. Floor areas smaller than 45 m$^2$ will always produce steel section temperatures lower than the critical temperature.

It is important to note that a compartment might be situated close to the transition zone, from fuel to ventilation controlled fires. In the case considered here compartments of all occupations (design fire loads), may be either fuel or ventilation controlled if the floor area is in the range: $45 < A_f \leq 260$. To be conservative the engineer should consider that the fire is ventilation controlled, which would produce higher temperatures. However, if the fire is assumed to be fuel controlled figure 3.10 shows that the beam can be used in relatively small compartments with high fire loads.

The parameter study of the influence of ventilation conditions and fire loads, shows that it is possible to use unprotected composite beams in fire compartments of all sizes, depending on

the fire load. The study also shows that it is necessary to test the sensitivity of design fire to the assumed ventilation conditions and fire loads. The parametric fire curves can be used to determine temperatures for a wide range of compartment configurations. The limitations of the curves should however be kept in mind in order to avoid unrealistic fire models. When the limitations of the parametric models are exceeded, one could easily use a one or two zone fire model to predict the fire evolution.

## 3.6 Conclusions for fire design of composite beams

From all that is stated above it follows that there are four main factors that limit the capacity of a composite beam at a given time during a fire. At a certain stage of fire development any one of these factors will be prevalent. The failure modes are:

- Bending failure – loss of steel strength only
- Failure of the shear connectors to transmit the full shear force developed
- Bending failure – Concrete at elevated temperature
- Longitudinal shear failure, if the concrete temperature is elevated

In general composite beams resist fire well. Due to their nature plastic analysis is suitable for their design. Unprotected steel sections are a feasible option for design due to the fact that the capacity of the beam is increased by its connection to the composite slab. Care must be taken when one determines the temperature profile through a composite beam as it reflects strongly in the resistance time that is calculated.



It is clear that due to many factors, it is difficult to determine the exact evolution of loss of strength for a composite beam as a function of time. The designer can however get a good estimate of the resistance of a composite beam at a given time. The methods proposed by the Eurocodes are suitable for basic numerical implementation and hand calculation. This takes a step towards performance based scientific design and a step away from prescription based design.

The maximum temperature that a composite beam can reach during a fire is termed the critical temperature. The critical temperature is a characteristic of the structural element and independent of the fire model used to calculate temperatures in the element. The critical temperature can be used to determine a composite beam's resistance in the temperature domain. If the beam's resistance is greater than the effect $R > E$, the beam is considered safe.

The fire load and the ventilation conditions of the fire compartment are important factors that influence the temperature of the steel section. It is possible to use unprotected composite beams in the fire scenario, for all sizes of fire compartments, depending on these aforementioned conditions.

# Chapter 4

# Reliability based design of composite beams

## 4.1 Introduction to reliability based design

In general terms the verification of a deterministic design, can be done by considering the inequality:

$$R \geq E \tag{4.1}$$

Where $R$ stands for the resistance and $E$ for the load effect or action. If it is the case that the resistance is greater or equal to the effect, the design is considered to be safe. If one considers the resistance and the effect as two independent random variables such as is the case for a Limit State Equation (LSE) of the form $L = R - E$, one can obtain an exact solution for the probability of failure by integration, [37]. In this case the resistance has a general probability density function (PDF) of $\phi_R$ and the load effect a PDF of $\phi_E$. The cumulative distribution functions are denoted $\Phi_R$ and $\Phi_E$ respectively. The probability of failure can then be defined as:

$$p_f = \int_{-\infty}^{\infty} \phi_E(x)\Phi_R(x)dx \tag{4.2}$$

Figure 4.1 is a representation of two such random variables and their relation to each other. It is clear that the relative position of each variable's mean ($\mu_X$) and also their variance ($\sigma_X^2$) would have a impact on the probability of failure. Various numerical simulation procedures exist that can be used to find the probability of failure by means of direct integration of the LSE. These methods are however computationally expensive and time consuming. An alternative approach would be to use a First Order Reliability Method (FORM), which produces good results in most cases.

The method can be implemented using a computer in a few basic steps. The procedure is summarised by Holický [37] as follows:

1. Formulation of the LSE and the random variable ($X$) models.
2. The initial design point ($x^{'}$) is found by satisfying the condition that $G(x^{'}) = 0$, where

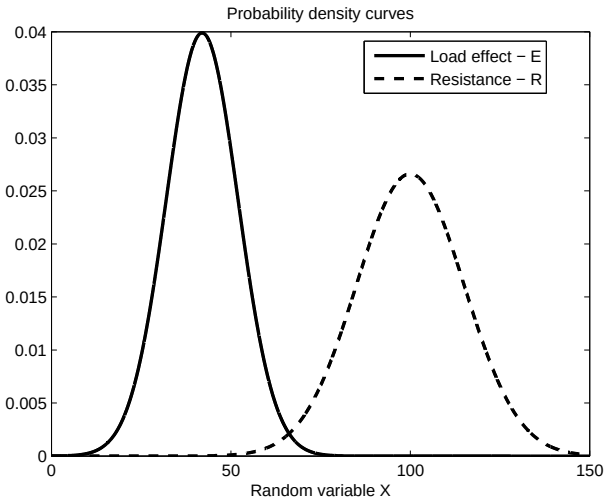


**Figure 4.1:** Two standard normal probability density curves representing load effect and resistance with the overlapping region defining failure probability ($p_f$).

$G(x)$ is the limit state function.

3. If all the random variables are not described by normal distributions, they are transformed to equivalent normal distributions at the design point.

4. All the random variables are standardised by the transformation $u^{'} = \frac{x_i^{'} - \mu_{X_i}^e}{\sigma_{X_i}^e}$. The transformed design point of the standardised random variables are denoted $u^{'}$.

5. The partial derivatives ($D$) of the LSE, with respect to the standardised variables, are calculated at the design point: $D_i = \frac{\partial G}{\partial U_i} = \frac{\partial G}{\partial X_i} \cdot \sigma_{X_i}^e$.

6. The reliability index can now be calculated as: $\beta = \frac{[D]^T[u']}{\sqrt{[D]^T[D]}}$

7. Alpha values or sensitivity factors can be determined from the expression $[\alpha] = \frac{[D]}{\sqrt{[D]^t[D]}}$.

8. The new standardised design point can be determined from: $u_i^{'} = \alpha_i \cdot \beta$.

9. The new standardised variables are transformed back to the original basic variables, using the equation seen in step 4.

10. The steps 1 to 9 are repeated until convergence of the design point or the $\beta$-value are achieved.

The reliability index is defined as:

$$\beta = -\Phi_U^{-1}(p_f) \tag{4.3}$$

where $\Phi_U^{-1}$ is the inverse cumulative distribution function of the standardised normal distribution. The probability of failure can be therefore be defined as:

$$p_f = \Phi_U(-\beta) \tag{4.4}$$

The general form of the LSE: $G = R - E$, for a composite beam, can be found from the conditions for static equilibrium. Therefore in the case where the reliability of the beam in terms of bending moment is checked, the LSE will simply be the difference between the moment resistance and the applied bending moment. The derivation of this limit state equation is shown in section 4.2.3.

The advantage of a reliability based design lies in the use of random variables to represent all variables in the LSE. Due to the nature of engineering problems, most if not all variables are random in nature. The use of reliability based methods provide engineers with a tool to analyse probability of failure and to estimate structural safety in a quantified manner.

The challenge when using FORM methods, is to estimate the important descriptive statistical measures of all the random variables. In some cases this is easily achieved due to the availability of statistical data. Examples of such data are the mechanical properties of construction materials and the own weight of structures. There are however variables that are not so easily defined and which could have a significant influence on the reliability analysis. Such variables might be model uncertainty coefficients, the imposed load on the structure and fire loads in fire compartments.

The sections that follow will describe the assumptions that were made, the development of the LSE's, the choice of random variables and the interpretation of the results of the FORM analysis.

### 4.1.1 Reliability analysis for the fire limit state

Reliability analysis requires rational models or performance functions in order for the analysis to be meaningful. The choice of the fire model can determine how credible a reliability analysis might be. The use of nominal fire models, like the standard temperature time curve, does not allow for the determination of the reliability level of a structural element. Standard temperature time curves are not based on physical fire behaviour and are therefore not a rational design method.

The Eurocode parametric fire curves are an attempt to describe real fire behaviour by a set of analytical equations. A parametric fire model can therefore be used to do a reliability analysis, by which the probability of failure of a structural element can be deduced on a rational basis. The fact that the relative influence of certain factors/parameters (on the reliability of a structure) can be quantified, enables designers to improve the reliability of structures.

The fire limit state is an accidental limit state and therefore a high level of uncertainty exists, involving all aspects leading to failure. Aspects, from the definition of the fire compartment through calculation of temperatures to the consequences of failure, make the problem difficult to define. Structural problems like this are best defined and studied as a system, where one

aspect influences another and correlation between variables can be taken into account. This, in its own right, is however an advanced study to perform which was considered beyond the scope of the thesis.

In the reliability analysis presented here, it is attempted to show the advantages of modern, rational fire engineering principles. The analysis does not take structural interaction or all failure modes of composite construction into account. The following section will describe some assumptions made in order to do a meaningful reliability analysis.

### 4.1.2 Assumptions and methodology

#### 4.1.2.1 Maintained compartmentation during fire

Eurocode 1991-1-2 [3] specifies that the design fire should be applied to one fire compartment at a time unless specified otherwise. If a fire compartment is breached and fire spreads throughout the building the probability of failure can clearly not be predicted unless the whole structure, as a system, is considered.

It is assumed that integrity of the fire compartment is maintained and that insulation is sufficient to prevent fire spread. In the following sections the probability of failure in terms of bending moment is considered. It is therefore assumed that loss of integrity will only take place once failure occurs. It is further assumed that large deflections will not produce a loss of compartment integrity. In order to achieve this, general detailing requirements must be met as described in the document titled: "Fire safe design: A new approach to multi-storey steel framed buildings, [34].



The failure of a structural element during a fire can lead to the loss of compartmentation. It would stand to reason that the probability of failure in case of fire must be smaller than is the case for normal temperature design at the ultimate limit state. For a discussion of the target probability of failure, refer to section 4.4 of this report.

#### 4.1.2.2 The use of a parametric temperature time curve

The limit state equations that are derived for the ultimate and fire limit states are in general only the condition of static equilibrium of the forces in the composite beam section. In the case of the ultimate limit state the beam is analysed at an arbitrary point in time during its design lifetime and all values assigned to the variables are considered as static. This situation changes for the fire limit state. The process that is modelled for the fire limit state is a dynamic situation with respect to the fire duration time. Depending on the configuration of the parametric fire the influence of the fire load on the floor of the compartment could change. The derivation of the LSE's and their use will make this point clear.

Previous sections of this document described how the temperature changes within a fire compartment, based on a chosen fire model. Due to the change in compartment temperature the composite beam undergoes a certain temperature development. One can use the temperature profile within the structural component to determine strength reduction factors for steel and concrete. It can thus be said that the reduction factors ($k$) are dependant on the temperature of the material under consideration, which in turn is dependant on the temperature evolution of the fire compartment.

The strength reduction factors for steel and concrete are experimentally determined. It can be said that the reduction factor for steel yield strength at a specified temperature is very well defined and could be considered as deterministic, in a simplified manner. The aspect that would make such reduction factors clearly random in nature is the assumed temperature of the steel. The temperature of the steel section in a composite beam is very uncertain and one must therefore model the reduction factor as a random variable when performing a FORM analysis. The question however arises of how to describe such variables. What is the mean and what is the standard deviation? In order to find a realistic approximation of the descriptive statistics one must consider how the reduction factors are found.

The Eurocode parametric fire curves are based on a number of variable input parameters. Some parameters that are clearly random variables by nature include: the fire load in the compartment, the ventilation conditions, the material properties of the compartment boundaries etc. In order to find a relation between the compartment temperature and the steel strength reduction factor, one could simplify the problem by only considering the fire load as a random variable. This is justified by referring to Schleich et al. [13]. In a reliability analysis performed by Schleich [13] the limit state function is simplified by considering a specific steel profile and a well defined fire compartment. The only variable that influences compartment temperature, is then the fire load on the floor ($q_{floor}$). The same assumption will be made here.

In section 4.2.3 the limit state equation is developed for the fire limit state. The relation between the fire load and the reduction factor for steel strength is shown in this section.

#### 4.1.2.3 Failure criteria for parametric fires

It has been stated that in order to get meaningful results out of a FORM analysis, one must analyse a structural component that is close to 100% utilised, i.e. a component designed deterministically must be at the point of failure. In the case of fire, failure can be defined as when a component fails before the specified resistance time. This is however only applicable for the standard temperature time curve, due to the fact that failure will always occur for this fire model because the curve has no decay phase.

The parametric fire curves are based on real fire behaviour and therefore have a cooling phase

after a certain point in time. This means that one must design a structural element to survive the total duration of the fire. Consequently it can be said that if failure takes place, it will happen at the time when maximum temperature is reached or before the temperature is reached. In order to find a beam that is 100% utilised in the fire limit state, one must consider a beam with sufficient fire resistance so that it just survives the fire.

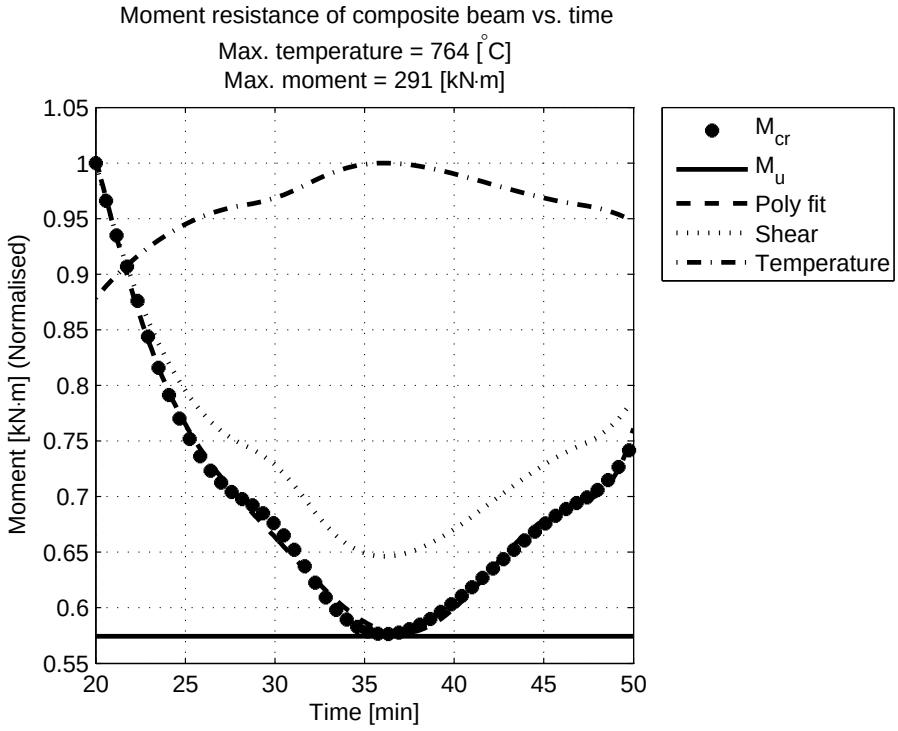


**Figure 4.2:** Composite beam that is 100% utilised using a parametric temperature time curve

Figure 4.2 is a plot of the bending moment resistance of a composite beam versus the time during a parametric fire. The figure serves as an example of a beam that is close to 100% utilised at the fire limit state. Such a beam would be a prime candidate for a reliability analysis.

In terms of a probabilistic approach two things can be done using reliability based methods. One could perform an analysis of a given situation and as output one would get the $\beta$-index of the composite beam. On the other hand the beam can be designed using FORM in order to achieve a target reliability level. In order to achieve the target $\beta$-index, the steel section's properties must be adjusted and fine tuned. Other variables that can be changed are the ventilation conditions and the size of the fire compartment, if the structural engineer could influence these values. For a discussion of the target reliability index refer to section 4.4.

#### 4.1.2.4 Input parameters

The input parameters concerning compartment geometry and lining are chosen in order to obtain design fires, across the spectrum of fuel controlled and ventilation controlled fires. The fire load on the floor is chosen according to the recommended Eurocode values. To change the maximum temperature and the temperature development rates, for a specific fire load, the opening factor and/or the size of the fire compartment must therefore be changed.

The parametric fire temperature at a given point in time is a function of:

$\rho_b$ The density of the enclosure boundary
$c_b$ The specific heat of the enclosure boundary
$\lambda_b$ The thermal conductivity of the enclosure boundary
$A_v$ The total area of all vertical openings
$A_t$ The total surface area of the enclosure (floors,ceiling included)
$h_{eq}$ The weighted average of the opening heights on all walls
$A_f$ The surface area of the floor
$q_{fd}$ The characteristic load fire density on the floor
$t_{lim}$ The limiting value of the time for the growth phase of the fire. Guidance on fire growth rate is given by Eurocode 1991-1-2 Annex E.4 Table E.5, [3]. The fire growth rate can be either slow, medium or fast with $t_{lim}$ correspondingly being 25, 20 or 15 minutes. Also see section 2.2.1 of this document.

Table 4.1 gives a summary of the data used in the various reliability analyses that follow. The data for the characteristics of the compartment boundary were taken from Schleich et al. [13].

**Table 4.1:** Fire compartment input parameters for reliability analysis

| Parameter | Symbol | Value | Unit |
|---|---|---|---|
| Characteristic fire load | $Q_{fk}$ | 511 | [MW/m$^2$] |
| Compartment width | $w$ | 9 | [m] |
| Compartment length | $l$ | 5-55 | [m] |
| Compartment height | $h$ | 4 | [m] |
| Weighted average height of all openings | $h_{eq}$ | 1.5 | [m] |
| Density of the boundary | $\rho_b$ | 2000 | [kg/m$^3$] |
| Specific heat of the boundary | $c_b$ | 1200 | [J/kgK] |
| Thermal conductivity of the boundary | $\lambda_b$ | 1.2 | [W/m/K] |
| Area of all vertical openings | $A_v$ | 25 | [$m^2$] |
| Limiting time the fire growth phase | $t_{lim}$ | $\frac{1}{3}$ | [h] |

In section 4.5.3, the reliability analysis of composite beams in fire, will be discussed. In order to perform the reliability analysis, a composite beam at 100% utilisation is required. The beam with a $I$ 457 $\times$ 191 $\times$ 82 steel section was chosen. In order to get a beam that is exactly 100% utilised, the maximum temperature attained by the beam was influenced by choosing a design fire load that produces steel section temperatures equal to the critical temperature. The ap-

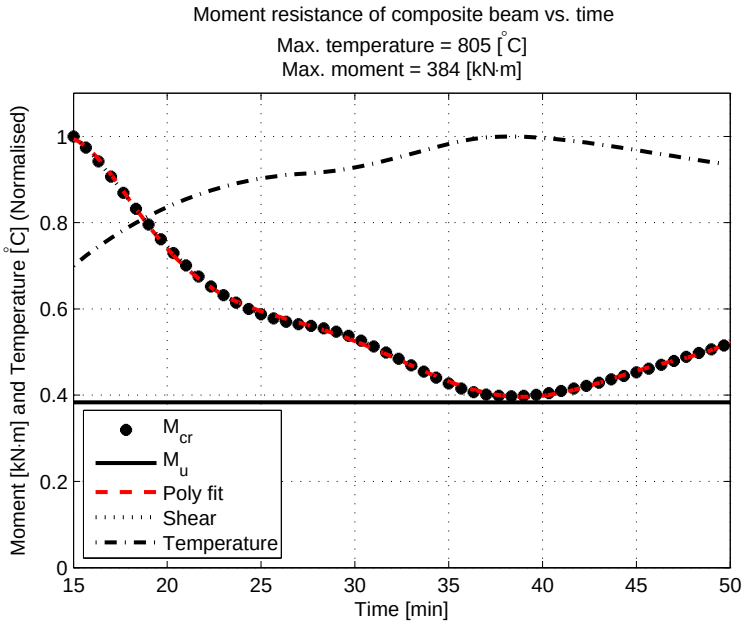


**Figure 4.3:** Composite beam with $I$ 457×191×82 steel section just surviving a fire – Used for reliability analysis. Fire compartment floor area: $A_f = 180$ m$^2$

propriate design fire load was determined to be: $q_{f,d} = 500$ MW/m$^2$. The other characteristics of the fire compartment, are as given in table 4.1 on page 71, with the floor area of the compartment being 180 m$^2$. Refer to figure 4.3 for a plot of beam bending moment capacity as a function of the steel section's temperature.

To compare the results of the deterministic design and the reliability analysis, the characteristic value of the fire load must be derived. From the characteristic value one can derive the mean value of the fire load. The design fire load was previously given in equation (3.48). This equation will be used to derive the characteristic value of the fire load:

$$\begin{aligned} q_{f,d} &= q_{f,k} \cdot m \cdot \delta_{q1} \cdot \delta_{q2} \cdot \delta_n \\ q_{f,k} &= \frac{q_{f,d}}{m \cdot \delta_{q1} \cdot \delta_{q2} \cdot \delta_n} \\ &= \frac{500}{0.8(1.376)(1)(1)} \\ &= 454 \qquad [\text{MW/m}^2] \end{aligned} \tag{4.5}$$

Note that the characteristic fire load does not correspond to a recommended value for a certain fire compartment occupation. The design fire load, from which the characteristic value is derived, is only chosen for purposes of an example. If the design fire load was based on a characteristic value supplied by the Eurocode, other parameters must be manipulated to get a beam that is 100% utilised. In most design scenarios, the steel section's size would be changed in order to increase the sections resistance. In the case of fire design one needs to know the steel section's geometry in order to calculate the massivity factor of the section. It is therefore convenient to use predefined standard steel sections in such calculations.

In the calculation of the characteristic fire load it was assumed that the combustible material consists of mainly cellulosic materials. It was also assumed that no active fire fighting measures are present but safe access routes, a smoke exhaust system and fire fighting devices are available.

If it is assumed that the fire load can be modelled using a Gumbel distribution and that the characteristic value is the 80% fractile of the distribution as recommended in Eurocode 1991-1-2 [3], one can find the mean value of the fire load. In the document by Cajot et al. [17] it is stated that fire load densities obtained from various sources, fit the Gumbel type I distribution well. The coefficient of variation is taken as 0.3. For the equations used in this calculation, the reader is referred to section 4.3.

$$\begin{aligned} \nu &= \frac{\sigma}{\mu} \\ \sigma &= \nu \cdot \mu \end{aligned} \tag{4.6}$$

$$x_p \cong \mu - (0.45 + 0.78 \cdot \ln(-\ln(p))) \cdot \sigma \tag{4.7}$$

By substitution of equation (4.6) into equation (4.7), and rearranging:

$$\begin{aligned} x_p &= \mu - (0.45 + 0.78 \cdot \ln(-\ln(p))) \cdot \nu \cdot \mu \\ x_p &= \mu \left(1 - (0.45 + 0.78 \cdot \ln(-\ln(p))) \cdot \nu\right) \\ \mu &= \frac{x_p}{(1 - (0.45 + 0.78 \cdot \ln(-\ln(p))) \cdot \nu)} \\ &= \frac{454.22}{(1 - (0.45 + 0.78 \cdot \ln(-\ln(0.8))) \cdot 0.3)} \\ &= 374 \qquad [\mathrm{MW/m^2}] \end{aligned} \tag{4.8}$$

The corresponding standard deviation is:

$$\begin{aligned} \sigma &= \nu \cdot \mu \\ &= 0.3 \cdot 374 \\ &= 112.1 \qquad [\mathrm{MW/m^2}] \end{aligned} \tag{4.9}$$

The mean and standard deviation, as well as the compartment characteristics chosen here, will be used in section 4.5.3.1. The comparison of the results obtained by the deterministic design method and the reliability analysis of the same situation, will be made in section 4.5.3.1. This comparison enables one to gain insight into the reliability level obtained using the Eurocode rational fire design method.

## 4.2 Derivation of the Limit State Equations

The design equations for deterministic design are used as an approximation of the real behaviour of composite beams under static loading. The design values used in the analytical deterministic equations, for the variables, are the characteristic values of the basic stochastic variables for loads, material properties and geometry. These characteristic values are multiplied by partial factors for material resistances and loads. Load combination factors ($\psi$-factors) that reduce certain loads when they occur simultaneously at for example the accidental limit states, can also be present. The partial factors are used to calibrate the approximated deterministic method, to a target reliability level.

The Limit State Equation should represent real structural behaviour. This realistic model, combined with stochastic variables, is a much improved method that can be used to determine and improve structural reliability. For the derivation of the LSE's shown in this document, it was assumed that the real behaviour of composite beams is adequately represented by the same analytical expressions used for deterministic design, using statistically defined basic variables. Model uncertainty factors are introduced as basic variables in order to take the simplification and inaccuracy/uncertainty of the mechanical behaviour into account.

### 4.2.1 Ultimate limit state – Bending

The Limit State Equation for the ultimate limit state is developed as follows:

$$\begin{aligned} G &= R - E \\ &= M_{cr} - M_u \\ &= \left(C_r e + C r^{'} e^{'}\right) - M_u \end{aligned} \tag{4.10}$$

In equation (4.10) $C_r$ is the force in the part of the steel profile in compression and $C_r^{'}$ is the force in the part of the concrete slab in compression. $e$ and $e^{'}$ are moment arms of the compressive forces around the working point of the tensile force in the steel profile.

Note that partial shear connection is supplied to transfer the shear force between the steel section and composite concrete slab. The LSE will therefore always be in the form where the steel section is also in compression. As was shown for deterministic design the plastic neutral axis of the composite section might lie within the web of the steel section, the expressions for the distances $e$ and $e^{'}$ will differ if this is the case. The expressions for the compressive forces are as follows:

$$C_r^{'} = 0.68 \cdot b_{eff} \cdot \alpha \cdot t \cdot f_{cu} \tag{4.11}$$

$$\begin{aligned} C_r &= \frac{A_s f_y - C_r^{'}}{2} \\ &= \frac{A_s f_y}{2} - \frac{0.68 \cdot b_{eff} \cdot \alpha \cdot t \cdot f_{cu}}{2} \end{aligned} \tag{4.12}$$

$M_u$ is the ultimate moment that the composite beam must resist. In the case of a simply supported beam the ultimate moment is given in equation (4.13). The permanent and imposed loads are taken as loads in units of [N/m$^2$].

$$\begin{aligned} M_u &= \frac{Wl}{8} \\ &= \frac{(D_{n_i} + L_{n_i})(b)(l)^2}{8} \end{aligned} \tag{4.13}$$

Equation (4.11) together with (4.12) and (4.13), can be substituted into the base form of the LSE and then the expression is as seen in equation (4.14). This equation can be used as a first approximation, to determine the probability of failure of a composite beam in bending. The equation must be developed to include the dimensions $e$ and $e^{'}$ as new dependant random variables. In equation (4.14) $f_y$, $f_{cu}$, $D$, $L$ and $t$ are random variables. See table 4.2 on page 81 for details of all the random variables.

$$G = \zeta_R \cdot [0.5e(A_s f_y - 0.68 b_{eff} \alpha t f_{cu}) + 0.68 b_{eff} \alpha t f_{cu} e^{'}] - \zeta_E \cdot \left[\frac{(D+L)bl^2}{8}\right] \tag{4.14}$$

Consider the following steps to further develop the expression for the LSE: the area of the steel section in compression can be calculated by dividing the steel compression force, by the yield strength of steel. By substitution of the relevant values:

$$\begin{aligned} A_{sc} &= \frac{C_r}{f_y} \\ &= \frac{A_s}{2} - \frac{0.68 b_{eff} \alpha t f_{cu}}{2 f_y} \end{aligned} \tag{4.15}$$

Two cases exist: Firstly where the plastic neutral axis lies within the flange of the steel section and secondly, where the plastic neutral axis lies within the web of the section:

**Case 1 – Plastic Neutral Axis lies within the steel section's flange:** If the area of compression within the steel section lies within the flange of the I-profile, the depth of the compression block from the top of the steel profile can be calculated as follows:

$$\begin{aligned} x &= \frac{A_{sc}}{b_f} \\ &= \frac{A_s}{2b_f} - \frac{0.68 b_{eff} \alpha t f_{cu}}{2 f_y b_f} \end{aligned} \tag{4.16}$$

The distance to the centroid of the area of the steel profile that is in tension, from the bottom

of the steel profile, can consequently be calculated as:

$$\begin{aligned} z &= \frac{[A_s(\frac{h}{2}) - A_{sc}(h - \frac{x}{2})]}{A_s - (b_f)(x)} \\ &= \frac{A_s\left(\frac{h}{2}\right) - \left(\frac{A_s}{2} - \frac{0.68 b_{eff}\alpha t f_{cu}}{2 f_y}\right)\left(h - \frac{1}{2}\left(\frac{A_s}{2b_f} - \frac{0.68 b_{eff}\alpha t f_{cu}}{2 f_y b_f}\right)\right)}{A_s - \frac{A_s}{2} + \frac{0.68 b_{eff}\alpha t f_{cu}}{2 f_y}} \end{aligned} \tag{4.17}$$

From the expressions for $x$ and $z$ given in the equations (4.16) and (4.17), the moment arms $e$ and $e^{'}$ can be obtained. These moment arms are now random variables due to the fact that they are functions of the independent random variables: $f_y$, $f_{cu}$ and $\alpha t$.

$$e = h - z - \frac{x}{2} \tag{4.18}$$

$$e^{'} = h - z + t_{slab} - \frac{\alpha \cdot t}{2} \tag{4.19}$$

**Case 2 – Plastic neutral axis lies within the steel section's web:** if the steel compression area is larger than the area of the steel profile's flange the depth of the compression block, from the top of the steel profile, can be calculated as:

$$x = \left(\frac{A_s}{2t_w}\right) - \left(\frac{0.68 b_{eff}\alpha t f_{cu}}{2 f_y t_w}\right) - \left(\frac{b_f t_f}{t_w}\right) + t_f \tag{4.20}$$

The centroid of the steel compression area, from the bottom of the steel section, is:

$$A_{sc-xx} = \frac{\left(b_f t_f \cdot \left(h - \frac{t_f}{2}\right)\right) + \left((x - t_f) t_w \cdot \left(h - x + \frac{(x - t_f)}{2}\right)\right)}{b_f t_f + (x - t_f) t_w} \tag{4.21}$$

The distance from the bottom of the steel profile to the centroid of the steel area in tension, is as follows:

$$z = \frac{\left(A_s \cdot \left(\frac{h}{2}\right)\right) - (A_{sc} \cdot A_{sc-xx})}{A_s - A_{sc}} \tag{4.22}$$

Finally the analytical expressions for the moment arms $e$ and $e^{'}$ can be found:

$$e = A_{sc-xx} - z \tag{4.23}$$

$$e^{'} = h - z + t_{slab} - \frac{\alpha \cdot t}{2} \tag{4.24}$$

The equation (4.14) can be combined with all other expressions for variables found in either equations (4.18) and (4.19) or (4.23) and (4.24), to formulate the Limit State Equation.

### 4.2.2 The serviceability limit state – Maximum midspan deflection

The limit state equation (LSE) for the serviceability limit state can be derived as seen in equation (4.25). Note that in this case the resistance side of the equation is described by a prescribed maximum deflection.

$$\begin{aligned} G &= R - E \\ &= \frac{L}{300} - \Delta_{tot} \end{aligned} \tag{4.25}$$

The deflections are calculated according to the guidelines given in SANS 10162: Part 1 § 17.3.1, [1]. Also see section 3.3 of this document where the calculation of the deflections is described. The LSE shown here is derived for a unpropped composite beam:

$$\begin{aligned} G &= \zeta_R \left(\frac{L}{300}\right) - \zeta_E \cdot (\Delta_i + \Delta_e + \Delta_{sh} + \Delta_c + \Delta_s) \\ &= \zeta_R \left(\frac{L}{300}\right) \\ &\quad - \zeta_E \cdot \left(\frac{5}{384}\left(\frac{W_1 L^3}{EI} + \frac{(W_2 + W_4)\, L^3}{EI_e} + \frac{0.15 \cdot (W_1 + W_3 + W_4)\, L^3}{EI_e}\right) + 0.85 \cdot \frac{\varepsilon_f A_c L^2 y}{8 n_t I_t}\right) \end{aligned} \tag{4.26}$$

The variables in the LSE are defined as in section 3.3 on page 39 and as follows:

| | |
|---|---|
| $W_1$ | is the weight of the steel beam, steel deck and wet concrete |
| $W_2$ | is the short term part of the imposed load equal to $\frac{1}{2} \cdot Q_{Tot}$ |
| $W_3$ | is the long term part of the imposed load |
| $W_4$ | is the load due to finishes etc. |
| $L$ | is the length of the beam |

For a description of the distributions of all the random variables used for the serviceability limit state, see table 4.3 on page 82.

### 4.2.3 Fire limit state

Again following the procedure as for the ultimate and serviceability limit states, the LSE of a composite beam for the fire limit state can be derived as seen in equation (4.31). Note that the LSE is derived for a steel section that is assumed to be at a uniform temperature and it is also assumed that the steel section is not in compression. This means that the tensile force in the steel section simply is:

$$T = k \cdot f_y \cdot A_s \tag{4.27}$$

Where $k$ is the reduction factor for steel strength at elevated temperatures, $f_y$ the yield strength of steel and $A_s$ the steel section's area. The tensile force in the steel section is balanced by the compressive force in the concrete above the profiled steel sheeting. The thickness of this

compression block is derived as follows:

$$\begin{aligned} T &= 0.68 \cdot h_u \cdot b_{eff} \cdot f_{cu} \\ h_u &= \frac{T}{0.68 \cdot b_{eff} \cdot f_{cu}} \end{aligned} \tag{4.28}$$

The tensile force in the steel profile can however not be greater than the capacity of the shear connectors and the condition that $T <= N \cdot P_{fi,Rd}$ still applies. If the LSE seen in equation (4.31) must apply, the failure mode of the composite beam must not be through shear connector failure.

In the early stages of a fire the shear connectors' capacity is less than the bending capacity of the composite profile. This is due to the reduced amount of shear connection that was installed for normal temperature design. The condition changes as the steel section heats up and loses capacity. The shear connectors are protected by the concrete in the slab and in general the dominant failure mode tends to be the bending capacity of the steel section. The reader is again referred to figure 4.2 on page 70 where the dominant failure mode is clearly indicated.

Another condition that must be met in order for the LSE derived here to apply, is the fact that a part of the steel section must not be in compression. This criteria is met when the depth of the concrete compression block is less than the depth of the concrete above the profiled steel sheet. This condition tends to hold true in most cases due to the fact that the concrete compression block decreases in depth as the fire progresses and the steel section loses strength. In the section on deterministic design for fire it was said that the possibility exists that a part of the concrete compression block could be subject to a strength reduction as well. This situation will not be considered here. A more accurate temperature profile through the concrete is needed in cases where very deep beams are exposed to severely ventilation controlled fires. In such cases where deep concrete compression blocks exist until the late stages of the fire and the time to maximum fire temperature is long, one must consider the use of a finite element heat transfer program to calculate an accurate temperature distribution.

The statistical characteristics of the steel yield strength reduction factor is still unknown at the time of failure. To find the mean and standard deviation of the reduction factor, consider the following: the steel temperature is dependant on the heating of the fire compartment. The temperature of the fire compartment is a function of the fire load, opening factor, compartment geometry and lining materials' characteristics. It is therefore clear that the steel temperature is highly random by nature. In order to simplify the derivation of the LSE one can assume that the temperature is dominated by the variability of the fire load. The compartment characteristics are thus considered as deterministic. The only random variable is then the fire load on the floor of the compartment. A continuous expression for the reduction factor $k$ can be found:

$$k = 0.9674 \cdot \left(1 + e^{\frac{T-482}{39.19}}\right)^{-1./3.833} \tag{4.29}$$

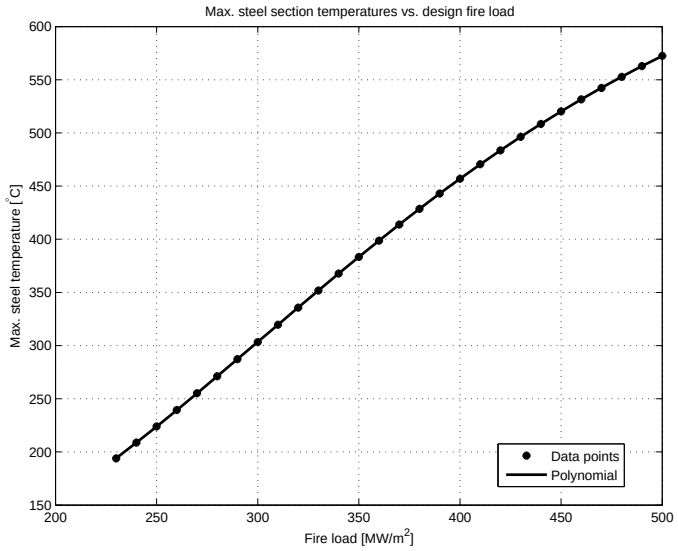


**Figure 4.4:** Maximum steel temperature vs. fire load with fitted polynomial function

where $T$ is the temperature of the steel.

In order to take compartment characteristics into account, when deriving the steel section's temperature, the data points for maximum steel temperature versus fire load can be plotted. The logic behind this stems from the fact that the composite beam would fail before or at the time where maximum temperature is reached. A beam that still (just) has adequate capacity at maximum temperature is considered as an optimal design. Beams that fail before the maximum temperature is reached are not considered.

A continuous function can be fitted to the data, as can be seen in figure 4.4. This function can be substituted into equation (4.29). In many cases a linear function approximates the data well but in some cases a polynomial of higher order is more suitable. The expression for the reduction factor then becomes:

$$k = 0.9674 \cdot \left(1 + e^{\frac{\left(c_1 q_{fd}^{n} + c_2 q_{fd}^{n-1} + \ldots c_n q_{fd} + c_{n+1}\right) - 482}{39.19}}\right)^{-1./3.833} \tag{4.30}$$

Where $c_{ni}$ are polynomial constants.

The LSE can finally be derived in its simplified form:

$$\begin{aligned} G &= R - E \\ &= \xi_R \left[T \cdot (y_F - y_T)\right] - \xi_E \left[\frac{(G+Q)\,(L)^2 \cdot b}{8}\right] \\ &= \xi_R \left[k \cdot f_y \cdot A_s \left(h + t_s + h_c - \frac{h_u}{2} - \frac{h}{2}\right)\right] - \xi_E \left[\frac{(G+Q)\,(L)^2 \cdot b}{8}\right] \\ &= \xi_R \left[k \cdot f_y \cdot A_s \left(\frac{h}{2} + 0.075 + h_c - \frac{k \cdot f_y \cdot A_s}{2 \cdot 0.68 \cdot b_{eff} \cdot f_{cu}}\right)\right] - \xi_E \left[\frac{(G+Q)\,(L)^2 \cdot b}{8}\right] \end{aligned} \tag{4.31}$$

Where:

| | |
|---|---|
| $y_F - y_T$ | The moment arm |
| $\xi_R$ | The model uncertainty coefficient for the resistance |
| $\xi_E$ | The model uncertainty coefficient for load effect |
| $h$ | The height of the steel section |
| $t_s$ | The height of the steel sheeting |
| $h_c$ | The depth of the concrete on top of the steel sheeting |
| $h_u$ | The depth of the concrete compression block |

## 4.3 Random variable models

The choice of random variable models can have a significant influence on the calculation of the reliability index. The designer must be aware of the limitations and use of random variable models. In this study use was made of three distribution types to model the characteristics of the random variables. In tables 4.2, 4.3 and 4.4 in the following sections, it is indicated which variables were assumed to be characterised as Normal, Lognormal or Gumbel distributions. In the tables the following naming convention is used:

N – Normal distribution
LN – Lognormal distribution
GU – Gumbel or Extreme Value Type I distribution

The lecture notes by Holický [37] were used as guideline, when choosing the descriptive distributions of the random variables. For the fire load ($q_{fd}$), the recommendation of Eurocode 1991-1-2 [3] table E.4 was followed. According to the Eurocode, the fire load for office buildings can be characterised by a Gumbel distribution with a mean of 420 MW/m$^2$ and an 80 % fractile characteristic value of 511 MW/m$^2$. From these values one can derive the coefficient of variation as being 0.3. For the mean and standard deviation of the fire load, for structures with occupations other than office buildings, refer to table 3.4 on page 54. For clarity, the characteristics of the Gumbel distribution are provided:

$$\phi_G = e^{-e^{-c(x-x_{mod})}} \qquad ; -\infty < x < \infty \tag{4.32}$$

$$\mu = x_{mod} + \frac{0.577}{c} \tag{4.33}$$

$$c = \frac{\pi\sqrt{6}}{\sigma} \tag{4.34}$$

$$x_p \cong \mu - (0.45 + 0.78 \cdot \ln(-\ln(p))) \cdot \sigma \tag{4.35}$$

$$\sigma = \frac{x_p - \mu}{-(0.45 + 0.78 \cdot \ln(-\ln(p)))} \tag{4.36}$$

Where $\phi_G$ is the probability density function of the Gumbel distribution and $x_p$ is the fractile for a fraction $p$, of the probability density function. In order to do a FORM analysis the mean and standard deviation of all variables must be known.

### 4.3.1 Ultimate limit state

Table 4.2 provides a list of the various random variables that are assumed sufficient to model the composite beam behaviour, for the ultimate limit state. The table gives the mean and standard deviation of each variable and the method by which it is calculated. Note that the calculation of the mean and standard deviation of the variables $f_y$ and $f_{cu}$ is an iterative procedure, due to the fact that the mean is equal to the characteristic value plus two standard deviations and the standard deviation, is a function of the mean.

The information that is given in table 4.2 is as recommended by M. Holický [37] Annex 4: Table 1.

**Table 4.2:** Random variables used in reliability study - Ultimate limit state

| Nr. | $X$ | Description | Distr. type | Caract. value | Mean | | Standard deviation | |
|---|---|---|---|---|---|---|---|---|
| | | | | | Calc. | $\mu_X$ | Calc. | $\sigma_X$ |
| 1 | $f_y$ | Yield strength of steel | LN | 350 | $f_{yk} + 2\sigma$ | 438 MPa | $0.1\mu_X$ | 43.8 MPa |
| 2 | $f_{cu}$ | Concrete compressive strength | LN | 25 | $f_{ck} + 2\sigma$ | 39.1 MPa | $0.18\mu_X$ | 7.03 MPa |
| 3 | $G$ | Permanent load | N | Varies | $G_k$ | | $0.1\mu_X$ | |
| 4 | $Q$ | Imposed load[a] | GU | 3500 | $0.6Q_k$ | 2100 N/m$^2$ | $0.35\mu_X$ | 735 N/m$^2$ |
| 5 | $\zeta_R$ | Model uncertainty (resistance) | LN | – | – | 1.0 | – | 0.15 |
| 6 | $\zeta_E$ | Model uncertainty (effect) | LN | – | – | 1.0 | – | 0.1 |

[a]The mean and standard deviation are according to the values for a 50 year reference period i.e. the long term imposed load

### 4.3.2 Serviceability limit state

Table 4.3 provides a list of the various random variables that are assumed sufficient to model the composite beam behaviour, for the serviceability limit state. It was attempted to highlight the uncertainties of calculating deflections in section 3.3.1, concerning deterministic design. Because of the inherent high uncertainties involved in calculating the deflection of a building component such as the beams, a probabilistic approach seems to make more sense than a purely deterministic approach. However, in the case of a probabilistic approach the question arises of how to accurately model such a condition. In simple terms one must describe the limit state equation as accurately as possible, using the appropriate random variables.

As can be seen in table 4.3, the imposed load was split into a long term and a short term part. This is done in order to calculate the instantaneous deflection due to the short term load. The important factor to note, is that the distribution of long term imposed load differs significantly from the corresponding short term distribution. Both the long term part and short term part are modelled using a extreme value distribution, but the long term imposed load has a 1 in 50 year return period while the short term part has a 1 in 5 year return period.

**Table 4.3:** Random variables used in reliability study - Serviceability limit state

| Nr. | $X$ | Description | Distr. type | Carac. value | Mean | | Standard deviation | |
|---|---|---|---|---|---|---|---|---|
| | | | | | Calc. | $\mu_X$ | C.o.v | $\sigma_X$ |
| 1 | $G_1$ | Permanent load | N | Concrete, steel deck & beam | $G_{1k}$ | | $0.1\mu_X$ | |
| 2 | $G_2$ | Permanent load - fittings etc. | N | 800 N/m$^2$ | $G_{2k}$ | 800 | 0.1 | 80 |
| 3 | $Q_s$ | Short term imposed load | GU | $0.5 \cdot (3500)$ N/m$^2$ | $0.2Q_{sk}$ | 350 | 1.1 | 385 |
| 4 | $Q_l$ | Long term imposed load | GU | $0.5 \cdot (3500)$ N/m$^2$ | $0.6Q_{lk}$ | 1050 | 0.35 | 367.5 |
| 5 | $\zeta_R$ | Model uncertainty (resistance) | LN | – | – | 1.1 | – | 0.1 |
| 6 | $\zeta_E$ | Model uncertainty (effect) | LN | – | – | 1 | – | 0.1 |
| 7 | $\varepsilon_f$ | Free shrinkage strain | N | 400 | $\varepsilon_{fk}$ | 400 | 0.3 | 120 |
| 8 | $\delta_{camber,k}$ [a] | The amount of pre-camber on the beam | N | 0.054 | $\delta_{camber}$ | 0.054 | 0.1 | 0.0054 |

[a] Note that the amount of pre-camber may change as required and is only used in the LSE where specified

### 4.3.3 Fire limit state

Although partitions may be taken as part of the imposed load when designing for the ultimate and serviceability limit states, another approach may be considered when dealing with an accidental limit state. For the deterministic design at an accidental limit state, like the fire limit state, use is made of load reduction factors that reduce the design values of imposed loads on the structure during an accidental situation. This can be justified by considering that

the likelihood of the total imposed load being present when say, a fire develops, is very small. As people evacuate the building when a fire alarm sounds, the imposed load will be considerably less at the time of structural failure. Another example might be that the maximum wind load is highly improbable to occur at the same time as a structural fire. The situation may differ for the type of structure and even the specific location of the component under consideration.

The implication of the above is that the true nature of a load, when doing a reliability analysis, must be considered. In this, a big advantage of reliability based design is found. The use of random variables as input parameters gives the designer the freedom to change the nature of certain loads. When considering partition loads in an office structure, it is clear that the load will not be removed in case of an accidental fire. Although partitions are clearly not permanent loads when considering the ultimate limit state, they can be considered as semi-permanent loads in case of a fire.

For the purposes of this study, the partition loads were considered to be permanent loads that are described by the standard normal distribution, with a higher standard deviation than the own weight of the structure.

**Table 4.4:** Random variables used in reliability study - Fire limit state

| Nr. | X | Description | Distr. | Charac. | Mean | | Standard dev. | |
|---|---|---|---|---|---|---|---|---|
| | | | | value | Calc. | $\mu_X$ | C.o.v. | $\sigma_X$ |
| 1 | $f_y$ | Yield strength of steel | LN | 350 MPa | $f_{yk}+2\sigma$ | 437 | 0.1 | 43.7 |
| 2 | $f_{cu}$ | Concrete compressive strength | LN | 25 MPa | $f_{ck}+2\sigma$ | 39.1 | 0.18 | 7.03 |
| 3 | $G$ | Permanent load | N | Varies | – | 3774 | 0.06 | 226 |
| 4 | $Q$ | Imposed load | GU | 2500 N/m$^2$ | 0.6(2500) | 1500 | 0.35 | 525 |
| 5 | $Q$ | Imposed load (Partitions)[a] | N | 1000 N/m$^2$ | $Q_k$ | 1000 | 0.35 | 350 |
| 6 | $h_c$ | Concrete thickness | N | 65 mm | – | 65 | 0.1 | 6.5 |
| 7 | $\xi_R$ | Model uncertainty (resistance) | LN | – | – | 1.1 | – | 0.11 |
| 8 | $\xi_E$ | Model uncertainty (effect) | LN | – | – | 1.0 | – | 0.1 |
| 9 | $q_{fd}$ | Design fire load | GU | 511 MW/m$^2$ | – | 420 | 0.3 | 126 |

[a]For the fire limit state, this imposed load is included as a permanent load with a significantly higher standard deviation

## 4.4 Target reliability levels

The South African Code of Practice, concerning the general procedures and loadings to be adopted in the design of buildings SABS 0160:1989 §4.5.2 [9], defines the following values for $\beta$-indexes for the ultimate limit state:

- Ductile failure modes, $\beta = 3.0$
- Brittle failure modes, $\beta = 4.0$

- Connection detail between components, $\beta = 4.5$

According to the SABS 0160:1989 [9] it has been shown that a reliability index of $\beta = 3.0$ will be achieved if material strengths with a coefficient of variation of 0.1-0.3 are used. It is also stated that for materials such as reinforced concrete and structural steel, coefficients of variation in the order of 0.1-0.15 would be appropriate and a corresponding improved reliability index of $\beta = 4.0$ can be achieved.

The Eurocode 1990:2001 [2] Annex C6 provides guidance on target values for the reliability index. The Eurocode differentiates reliability targets by dividing structures into consequence classes. An office building would most likely fall in the Eurocode class RC2, which states that there is a medium consequence for loss of human life and that economic, social and environmental consequences are considerable. The reliability targets for a 50 year reference period are then as follows:

- Ultimate limit state, $\beta = 3.8$
- Serviceability limit state, $\beta = 1.5$

M. Holický [37] refers to the ISO 2394:1998 Code [8] when discussing target $\beta$-values. According to ISO 2394:1998 [8], a target value of $\beta = 3.8$ should be used for the ultimate limit state, if the relative cost of safety measures are moderate. It is also suggested that the reliability index should be $\beta = 0$ for reversible serviceability limit states and $\beta = 1.5$ for irreversible serviceability limit states.

A reversible serviceability limit state would correspond to an event that causes no permanent damage, like the instantaneous elastic deflection of a composite beam due to imposed load. If however a deflection leads to cracking of a facade it would constitute an irreversible limit state.

In the case of the fire limit state, it is convenient to consider the Eurocode and ISO type of definition, for target reliability values. Fire has an obvious consequence in terms of damage caused if failure of a structural component should take place. To define the failure mode as ductile or brittle is however not so clear cut. It can be debated that the consequence of failure in case of a fire would be much more severe, than a structural failure at normal temperatures. If a beam fails for the ultimate limit state, in a redundant structure, alternative load paths could restrict damage to be localised. In case of fire, the failure could mean a breach in the fire compartment, whereafter the prediction of the system's probability of failure becomes more complex.

In this study the target reliability for fire will be taken as the Eurocode recommended value for the ultimate limit state. This can be justified by considering that a lower probability of failure is required, due to possible greater consequences in the event of a failure. In terms of the SABS approach of considering whether a failure would be ductile or brittle, the failure of the beam in case of fire could be considered as brittle. A breach in the fire compartment could occur without prior warning due to the fact that the fire incident itself, is the only warning supplied.

Due to this a conservative $\beta$-value can also be justified from a SABS perspective.

Considering all the above, the following values for the reliability index will be used as reference in this document:

- Ultimate limit state (SABS 0160:1989 [9] recommendation), $\beta = 3.0$
- Serviceability limit state (Eurocode 1990:2001 [2] and ISO 2394:1998 [8] recommendation), $\beta = 1.5$
- Fire limit state (Eurocode 1990:2001 [2] recommendation), $\beta = 3.8$

## 4.5 FORM analysis of composite beams

Due to the fact that normal temperature composite beam design is dominated by failure at the serviceability limit state, the assumption is made that the initial deflection of a given beam can be removed by pre-camber of the beam. This technique produces beams that are close to 100% utilised for both the ultimate and serviceability limit states.

It is however very difficult to design a composite beam that satisfies all three limit states while being 100% utilised throughout. For reliability analysis, the same beam can therefore not be analysed for the ULS, SLS and the fire limit state. It should therefore be noted that it is possible to manipulate the deflection of a composite beam in order for the same beam to be analysed for the ultimate and serviceability limit state, although it is not a prerequisite that this must be done. It is however not the intention to calculate the reliability index of a single composite beam for all three limit states, as this would result in meaningless values for the reliability index. In the following sections, beams are chosen for the fact that they are close to 100% utilised for whichever limit state is relevant.

The reliability analysis of the composite beam was done using a purpose written Matlab program. The program has the advantage of being able to change steel section data quickly, in order to compute the reliability index of various composite beams. Another advantage of the Matlab code is the fact that one gains first hand insight into the numerical implementation of the FORM procedure. The set of Matlab functions includes two functions to transform the Lognormal and Gumbel distributions to equivalent Normal distributions. This implies that the program is limited to the use of these three distributions when describing the variables in the LSE.

### 4.5.1 Ultimate limit state

According to the calculations for deterministic design of composite beams, the beam with a $305 \times 102 \times 33$ I-section has a utilisation ratio of 0.97 for the ultimate limit state. This beam was chosen as a representative beam that could be used to do a reliability analysis. The basic

data for the beam is summarised in table 4.5. For a full list of the composite beams with steel sections as listed in the Southern African Institute of Steel Construction's handbook [11], refer to the design table A.2 on page 117 of this document.

**Table 4.5:** Data of representative beam for ultimate and serviceability limit states

| Input parameter | Value | Units |
|---|---|---|
| Steel section designation | $305 \times 102 \times 33$ | [-] |
| Effective width | 2.25 | [m] |
| Length of beam | 9.0 | [m] |
| Percent shear connection | 60 | [%] |
| Thickness of slab | 0.14 | [m] |
| Span between beams | 3.0 | [m] |
| Weight of beam | 107.3 | [N/m$^2$] |
| Weight of deck | 116.7 | [N/m$^2$] |
| Weight of concrete | 2614.3 | [N/m$^2$] |
| Weight of raised floor | 400 | [N/m$^2$] |
| Weight of services | 250 | [N/m$^2$] |
| Weight of ceiling | 150 | [N/m$^2$] |
| Load due to of partitions | 1000 | [N/m$^2$] |
| Imposed load | 2500 | [N/m$^2$] |

The reliability index of the specified beam was calculated as $\beta = 4.85$ and a probability of failure of $p_f = 6.11 \times 10^{-7}$. The influence factors or alpha values can be seen in figure 4.5 on page 87. According to this figure the dominant variable is the imposed load. The reliability index is also sensitive to both of the model uncertainty factors.

Figure 4.6 on page 87 is a three dimensional plot of the surface given by the calculated $\beta$-index. Figure 4.7 is a corresponding x-y axis projection of the surface shown in figure 4.6. The mean and the coefficient of variation of the imposed load are varied in order to show their relative influence on the reliability of the beam. The mean value is plotted as a fraction of the characteristic load.

The plots in figure 4.6 and 4.7 confirm the assumption of using the distribution that describes the point in time value of a long term imposed load[þ]. The recommended value for the mean and standard deviation of short term imposed load with a 5 year return period is: $\mu_X = 0.2Q_k$ and $\sigma_X = 1.1\mu_X$, respectively. From the plot of $\beta$-values, it is shown that the use of the long term imposed load distribution with a mean of $\mu_X = 0.6Q_k$ and standard deviation of $\sigma_X = 0.35\mu_X$, is a more conservative approach as it gives slightly lower $\beta$-values.

[þ] See table 4.2 on page 81 for the distribution characteristics

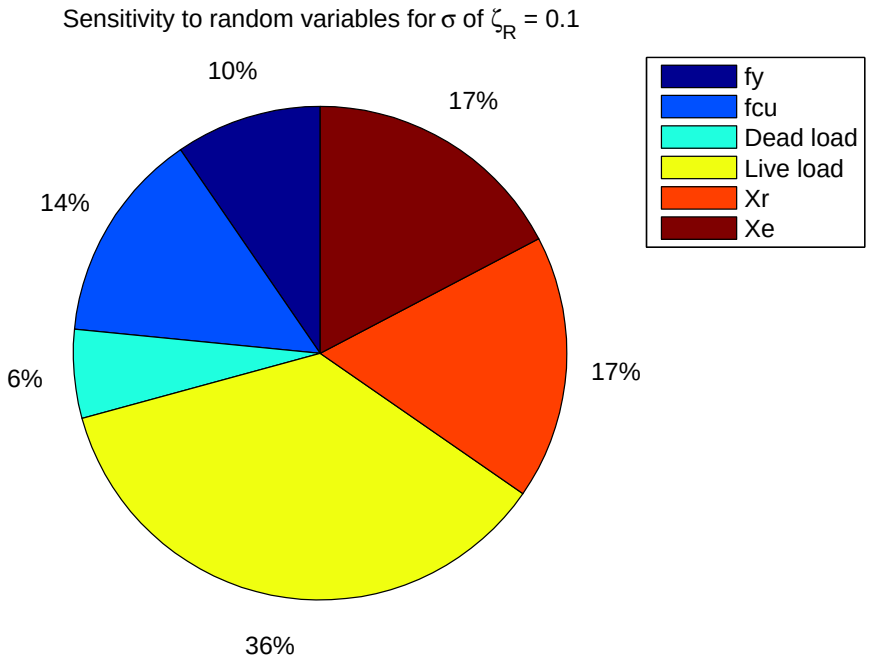


**Figure 4.5:** Relative influence of random variables for the ultimate limit state

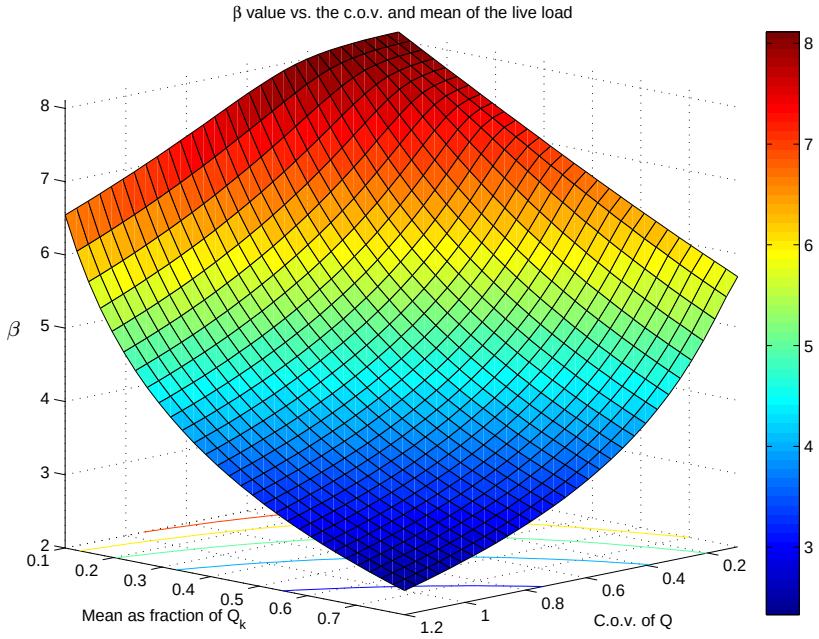


**Figure 4.6:** Change in $\beta$-value as a function of the coefficient of variation and mean of the imposed load at the ultimate limit state

The recommended value for the mean of the model uncertainty coefficient, on the resistance side of the LSE ($\zeta_R$), is between 1 (for bending moment capacity of steel) and 1.25 (for bending moment capacity of concrete), see table 3.9.1 of the JCSS probabilistic modal code, [36]. If the mean value is taken as larger than 1, it is implied that the resistance of analytical models is

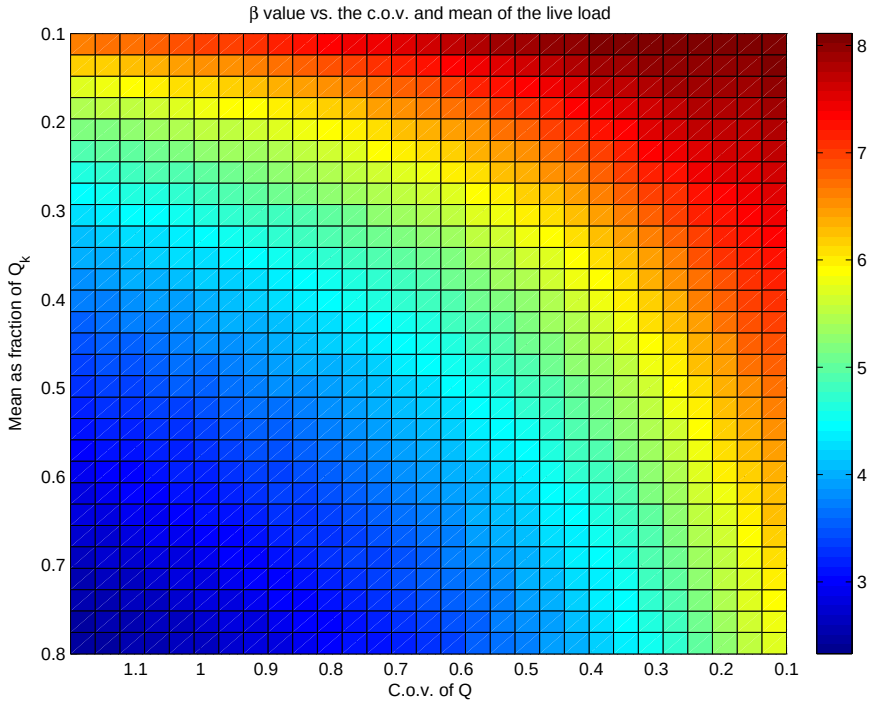


**Figure 4.7:** X-Y axis projection of the surface given by the calculated $\beta$-index shown in figure 4.6

estimated to be conservative. In the study performed it was decided to take the mean of $\zeta_R$ as equal to 1 in order to estimate a conservative reliability index. This is due to the fact that the beam under consideration has a composite section where the bending moment capacity is also related to a shear connection resistance, between the steel section and concrete slab. The amount of actual shear connection is unsure due to construction errors etc. and the conservative approach is therefore justified.

Figure 4.8 on page 89 shows the influence of the standard deviation, of the resistance model uncertainty factor, on the reliability index. It should be noted that even for a high standard deviation of 20%, the $\beta$-index never falls below the target value of 3.0. The $\beta$-index is in all cases higher than even the target index specified by the Eurocode.

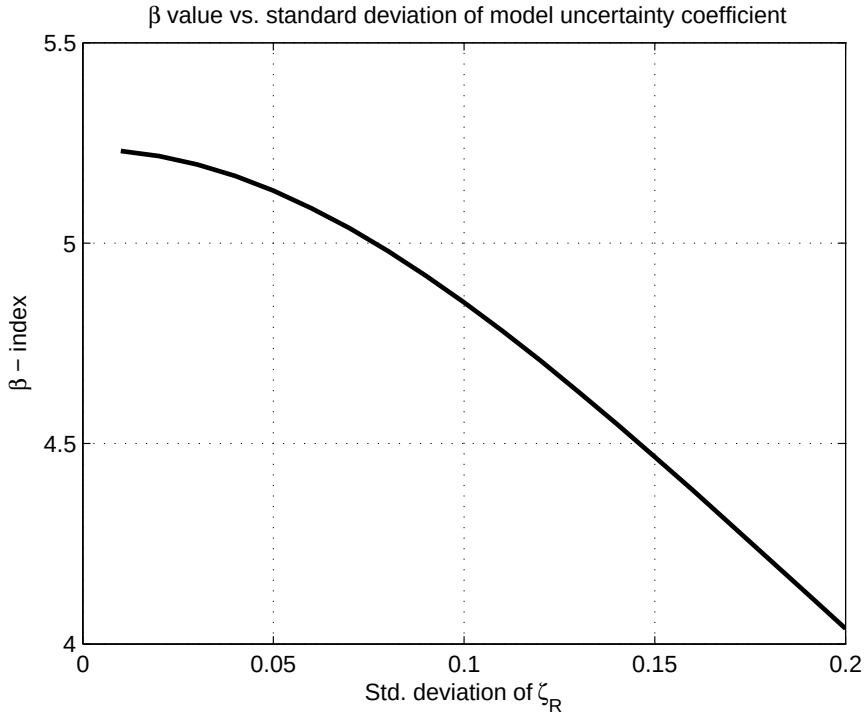


**Figure 4.8:** Change in $\beta$-value as a function of the standard deviation of the model uncertainty factor ($\zeta_R$) for the beam resistance at ultimate limit state

### 4.5.2 Serviceability limit state

The same beam considered for the ultimate limit state is again analysed for the serviceability limit state. The total deflection of the beam for unpropped construction amounts to approximately 84 mm with the initial deflection being 62 mm. The initial deflection is clearly too much and can be reduced by a pre-camber of the steel section. By giving the beam a 54 mm pre-camber the utilisation ratio for the serviceability limit state can be set equal to 1. A pre-camber of 54 mm amounts to a deflection of approximately $\frac{1}{167} \cdot L_{beam}$. This might be considered as an excessive amount of pre-camber due to construction difficulties etc. For purposes of this investigation, it was assumed that the pre-camber is within bounds.

In order to calculate the $\beta$-index of the beam, the short term imposed load was taken as half of the total imposed load. The imposed loads were modelled assuming Gumbel distributions. The short term part was therefore taken as having an extreme value distribution with a return period of 5-years and the long term imposed load with a return period of 50-years.

Figure 4.9 shows the sensitivity factors for the SLS. The reliability index is most sensitive to the value of the short term imposed load. The short term live load plays a role only where instantaneous deflections are concerned and if these deflections do not cause permanent damage, the effects are therefore reversible. The reliability index was calculated as $\beta = 1.71$ and a probability of failure of $p_f = 0.0435$. The beam therefore satisfies the criteria for the serviceability limit state.

If the beam(s) are not pre-cambered, the first beam that satisfies the serviceability limit state has a composite section with a I $406 \times 178 \times 67$ steel section. The $\beta$-index for this beam was calculated as 1.82. The next lighter section with the same depth gives a reliability index of $\beta = 1.21$. If the beams are not pre-cambered, the mass of the section is doubled.

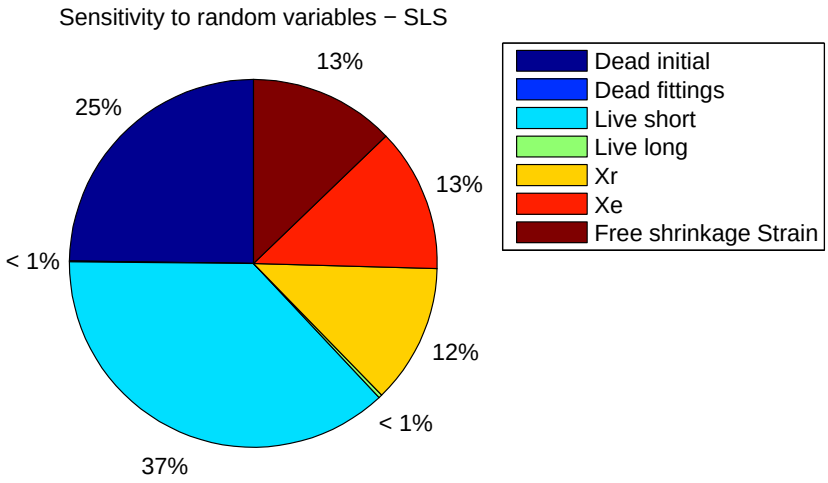


**Figure 4.9:** Relative influence of random variables for the serviceability limit state

### 4.5.3 Fire limit state

The reliability of structural components at the fire limit state must be calculated by considering the total probability of failure. As indicated previously where target reliability levels were discussed, the reliability of structural components in fire must generally be higher than for normal temperatures. Using a rational design method, as was shown, the reliability of composite beams can be improved by considering the nature of the fires they are subjected to and the probability of fire ignition and eventual flashover.

Active fire fighting measures make out an integral part of structural safety in case of a fire. Active fire fighting devices, such as fire extinguishers and sprinkler systems are mainly intended to protect people and to enable them to escape burning structures. A "global fire engineering approach" makes use of the active measures to improve the structure's reliability.

The probability of failure of the active fire fighting measures is very difficult to define and the only way would be by the use of large sets of statistical data. The fact that such probabilities can vary considerably, from country to county and even within certain countries, is a considerable obstacle. Nevertheless, such statistical data are available and can be used to perform reliability analysis and design. With regard to the values used in this document reference is made to the work by Schleich [13]. Schleich references various documents that were not consulted for purposes of this study, the values reported here are however used in order to show

the methodology of such a reliability analysis. Many factors clearly influence the reliability of a certain structural component at the fire limit state and as many sources as possible must be consulted when gathering statistical data on the subject.

In summary, the probability of failure is a function of the following:

- The probability of the structural component failing, $(p_{f,fi})$
- The probability that the fire that causes the structural failure takes place. This probability is a function of several things namely:
  - The probability of ignition, which is determined by compartment floor area and the type of occupancy
  - The probability of failure of the occupants stopping the fire spread before flashover takes place
  - The probability of failure of public safety services stopping the fire and
  - The existence of active fire fighting measures

The risk of fire ignition is a function of the fire compartment size. It stands to reason that a large fire compartment has a greater chance of a fire starting than a small compartment does. For the purposes of this study the probability of getting a fully engulfed fire compartment during the life of the structure, where the design lifetime is taken as 55 years, can be calculated as follows:

$$\begin{aligned} p_{fi,55} &= p_{fi,55}^{ignition} \cdot p_f^{OC} \cdot p_f^{PS} \\ &= \left(10 \times 10^{-6}/[m^2 \cdot year]\right) \cdot (55\ [years]) \cdot (0.4 \cdot 0.1) \\ &= 2.2 \times 10^{-5} \text{ per m}^2 \end{aligned} \tag{4.37}$$

Where:

$p_{fi,55}^{ignition}$ The probability of ignition during the lifetime of the structure
$p_f^{OC}$ $p_f$ of the occupants stopping the fire
$p_f^{PS}$ $p_f$ of the public services stopping the fire

Note that at this stage active fire fighting devices are not taken into account. The improved reliability of the composite beam is calculated by assuming some conditions that will be implicitly present in most office buildings and other public structures. It is assumed that the occupants will try to stop the fire with a certain probability of failure. It is also assumed that the occupants will alert the fire brigade and only then will the fire reach flashover if they fail to extinguish the fire.

The probability of getting a fully engulfed fire compartment during the life of the structure can now be further improved i.e. reduced, by considering various active fire fighting measures. The probability of failure of the active measures for an office building are summarised in table

4.6. The information is taken from the study performed by Schleich [13], see table 9, chapter III.

**Table 4.6:** Active fire fighting measures and their probability of failure for office buildings

| Active fire fighting measure | Probability of failure |
|---|---|
| Sprinkler system | 0.02 |
| One water supply for sprinklers[♭] | 0.5 |
| Two water supplies for sprinklers[♭] | 0.25 |
| Fire detection by smoke | 0.0625 |
| Fire detection by heat | 0.25 |
| On site firemen | 0.02 |
| Off site firemen | 0.1 |
| Automatic transmission of alarm to firemen[♮] | 0.25 |

[♭]On condition that sprinklers are installed
[♮]On condition that a fire fighting service is available

For purposes of an example, a fire compartment is chosen to be 20 m long and 9 m wide with other characteristics as in table 4.1 on 71. Active fire fighting measures are not taken into account. The probability of fire ignition is then calculated by equation (4.37) as:

$$\begin{aligned} p_{fi,55} &= 2.2 \times 10^{-5} \cdot 180 \\ &= 0.00396 \end{aligned} \tag{4.38}$$

This probability corresponds to a reliability index of $\beta = 2.66$. In order to achieve the desired target reliability index of 3.8, the composite beam must have a probability of failure smaller or equal to:

$$\begin{aligned} p_f &\leq \frac{\Phi(-3.8)}{p_{fi,55}} \\ &\leq \frac{7.235 \times 10^{-5}}{0.00396} \\ &\leq 0.01827 \\ \beta_{beam} &\geq 2.1 \end{aligned} \tag{4.39}$$

According to the FORM analysis using input parameters as seen in table 4.4 on page 83 and table 4.1 on page 71, the composite beam with the largest[♮] hot rolled unprotected steel section available in South Africa has a total probability of failure of $2.79 \times 10^{-4}$. This probability of failure corresponds to a reliability index of only $\beta_{total} = 3.45$. The reliability index for the composite beam alone is: $\beta_{beam} = 1.47$. This section is much heavier than is required even for the serviceability limit state if the beams are not pre-cambered.

The plot showing sensitivity factors for the fire limit state is shown in figure 4.10. The fire load

[♮]$533 \times 210 \times 122$ I profile

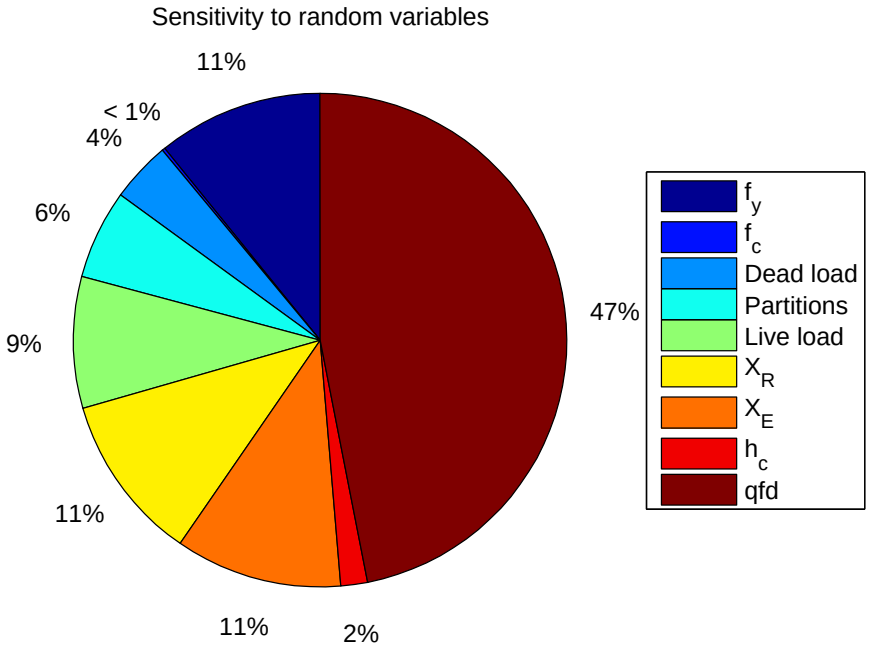


**Figure 4.10:** Relative influence of random variables for the fire limit state

on the floor is clearly the dominant variable in this case. This result supports the finding of similar analyses and the assumption that the fire compartment characteristics can be taken as deterministic, when performing a simplified analysis.

In order to examine the influence of the distribution characteristics of the fire load, figure 4.11 was produced for the composite beam with a $533 \times 210 \times 122$ steel section. The figure shows the influence of the mean and coefficient of variation of the fire load on the reliability index. The "failure surface" or target value is also plotted on the graph. Figure 4.12 shows the projection of the 3D surface seen in figure 4.11, on the X-Z and Y-Z planes respectively. From these projections one can clearly see that the coefficient of variation has a much greater effect on the $\beta$-index than the chosen mean of the fire load. Note that for a coefficient of variation of 0.3, as suggested by the Eurocode, the mean value has no effect on the $\beta$-index.

The 3D plot indicates that unprotected composite beams can not be used in the specified fire compartment, if active fire fighting measures are unavailable. The compartment characteristics may be modified in order for the beam to be satisfactory, the use of such a large section would however be uneconomical. The question arises whether a compartment exists that would enable one to use a smaller unprotected steel section for the composite beam.

Based on the aforementioned example of a beam with a $533 \times 210 \times 122$ I-section, the fire limit state is clearly the dominant limit state concerning the design of composite beams. In order to show that it is possible to use unprotected beams while still adhering to a target reliability level of $\beta = 3.8$, figure 4.13 on page 96 was produced. The figure shows the reliability index

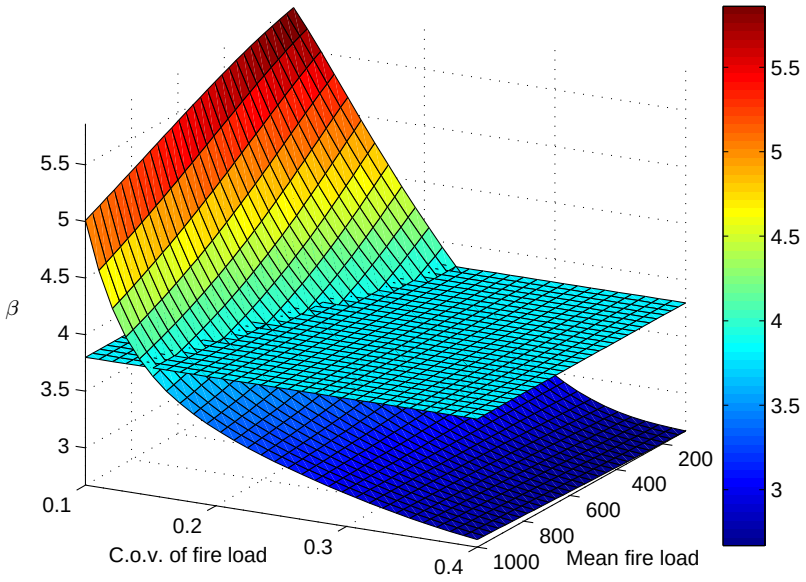


**Figure 4.11:** Change in $\beta$-value as a function of the coefficient of variation and mean of the fire load at the fire limit state. The horizontal plane indicates the target reliability of $\beta = 3.8$

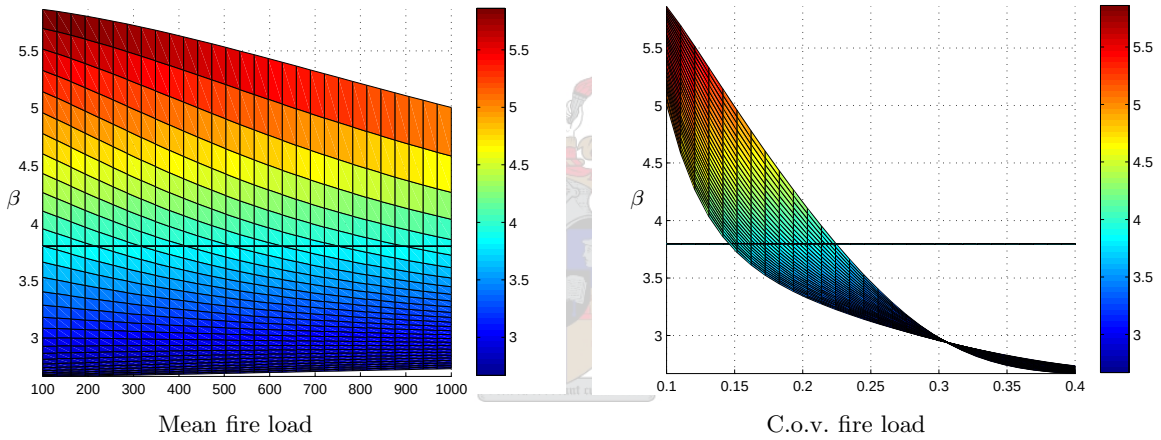


**Figure 4.12:** X-Z and Y-Z plane projections of figure 4.11, indicating sensitivity of $\beta$-value

versus the floor area of the fire compartment and the mean value of the fire load. The area of vertical openings was taken as 30% of the floor area. The coefficient of variation of the fire load was taken as 0.3. The relevant steel section is a $406 \times 178 \times 67$ I-section. This section was also deemed adequate for the ultimate and serviceability limit states.

Figure 4.13 can be compared to figure 3.9 on page 62 where the deterministic design of composite beams were discussed. For the deterministic design, maximum steel section temperatures were plotted as a function of floor area and design fire load. In the case of figure 4.13 the $\beta$-value is plotted as a function of the aforementioned parameters. It should be noted that for fire loads and floor areas where maximum steel temperature were calculated, minimum $\beta$-values are expected. This is verified by the graph figure 4.13.

A major difference between the plot of maximum steel temperature and the $\beta$-value plot, is ab-

sence of the pronounced "step" that indicates fuel and ventilation controlled fires. The absence of this regime is due to an assumption made in order to simplify the numerical implementation of the FORM procedure. Due to the discontinuity in the function of maximum steel section temperature versus fire load, that is used to find the mean and standard deviation of the reduction factor, the FORM procedure fails to converge on a $\beta$-index. In order to solve this problem, it was assumed that the fire is always ventilation controlled. This is a conservative assumption as the higher parametric fire temperatures occurs for this condition. Figure 4.13 should therefore be seen as an approximation.

It was predicted by deterministic design that the unprotected beam with a $406 \times 178 \times 67$ I-section, would be satisfactory for all compartment sizes if the design value of the fire load was below 600 MW/m$^2$. Contrary to this the reliability analysis suggests that the beam will only have sufficient reliability if the floor area of the fire compartment is smaller than approximately 90 m$^2$, for fire loads above 600 MW/m$^2$.

This result can be explained by the differences in steel section temperature, as result of the approximation of the maximum temperature for the reliability analysis. It is however assumed that adequate reliability levels will only be reached for compartments smaller than 120 m$^2$. Figure 4.13 also indicates that for mean fire loads below 530 MW/m$^2$, the $406 \times 178 \times 67$ I-section in compartments up to 140 m$^2$ in floor area, can be used.

Figure 4.11 and figure 4.12 showed that the reliability index is relatively unaffected by the mean value of the fire load, if the coefficient of variation is in the order of 0.3, as was used to produce figure 4.13. This would suggest that it is the ventilation conditions that affect the calculated reliability index the most.

Figures 4.14 and 4.15 were produced to show the influence of the target reliability index, on possible fire compartment configurations for which the chosen composite beam would be reliable. If the $\beta_{target}$-index was chosen as 3.0, the beam can be used in significantly larger fire compartments. Fire compartments with $A_f \leq 140$ m$^2$ can be used for mean fire loads of up to 900 MW/m$^2$.

#### 4.5.3.1 Direct comparison of deterministic design and reliability analysis

In section 4.1.2.4 a specific beam and compartment setup were identified, which can be analysed to obtain its reliability level. The figures seen in the previous section compare the deterministic design of a composite beam with the reliability analysis. Due to some uncertainties concerning steel section temperature, this section is intended to show a direct comparison for only one scenario.

The beam with an $I$ $457 \times 191 \times 82$ steel section was identified for the comparison. The fire

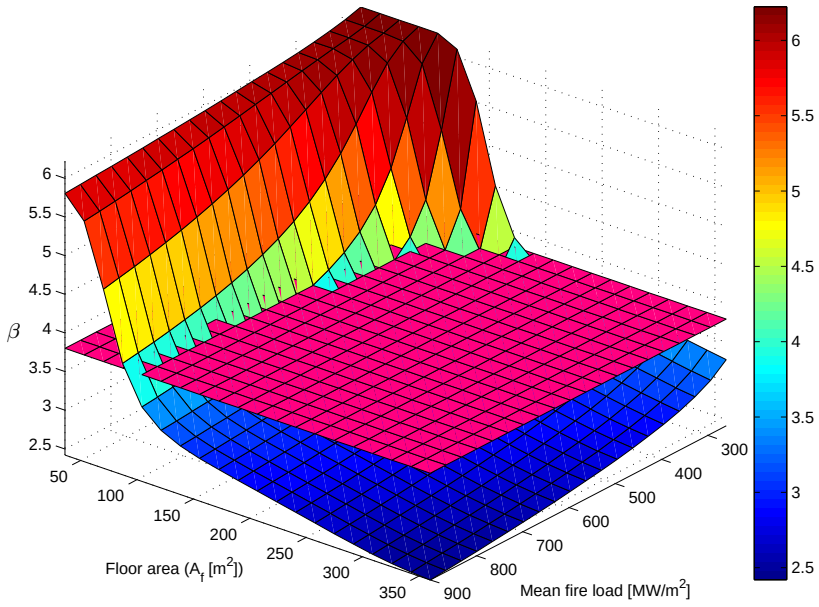


**Figure 4.13:** Influence of fire compartment floor area and mean fire load on the $\beta$-index. Area of vertical openings: $A_v = 0.3 \cdot A_f$. Horizontal plane indicates $\beta_{target} = 3.8$

load was reduced in order to get a beam that just survives the parametric fire. The mean and standard deviation of the design fire, were also derived in section 4.1.2.4. The basic data are as follows:

- The composite beam has an $I$ $457 \times 191 \times 82$ steel section.
- The design fire load, where moment capacity utilisation is $\approx 100\%$, is 500 MW/m$^2$.
- The characteristic 80% fractile fire load, was derived from the design value as being 454 MW/m$^2$.
- The mean of the fire load, using a Gumbel distribution with a coefficient of variation 0.3, was determined to be 374 MW/m$^2$.
- The standard deviation is then 112 MW/m$^2$.
- The compartment floor area: $A_f = 180$ m$^2$.
- All other data is as in table 4.1 on page 71.

A reliability analysis, using the variables with characteristics shown in table 4.4, produces a reliability index of $\beta = 3.39$. This value is lower than the target reliability index, but still higher than the target index for normal temperature design. The corresponding probability of failure is: $p_f = 3.49 \times 10^{-4}$.

On the basis of this limited example, a few questions can be asked: Firstly, is the method for deterministic design of the beam unconservative, due to the low $\beta$-index? Secondly, can the reliability level be improved, by considering possible over-conservative design assumptions?

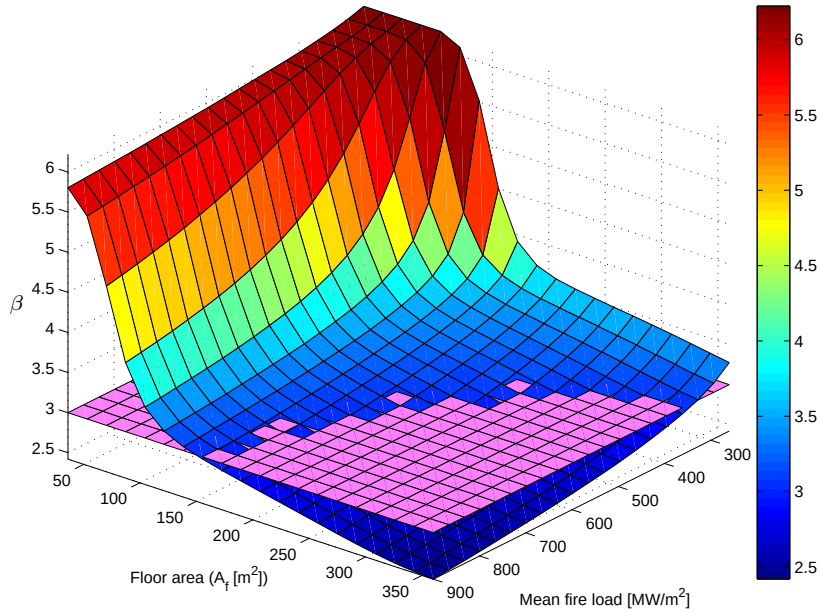


**Figure 4.14:** Reproduction of figure 4.13 with $\beta_{target} = 3.0$

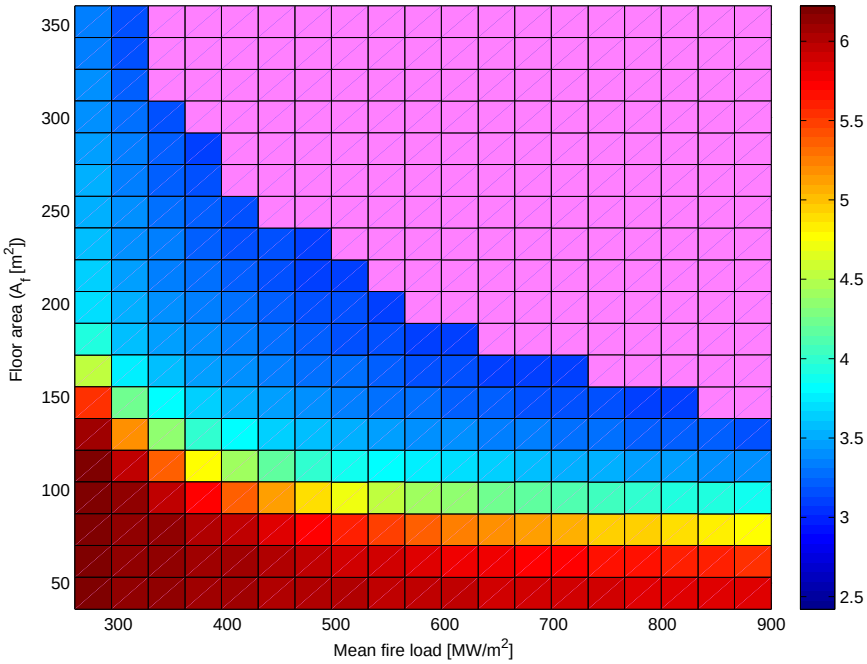


**Figure 4.15:** X-Y plane projection of figure 4.14.

These questions are best answered in a qualitative manner, as the investigation is limited to one design situation. Firstly, one can say that the $\beta$-value is not unreasonably low. It was shown that the $\beta$-index is very sensitive to the assumed temperature of the steel section. This temperature can be influenced by many factors.

Although a target reliability index of 3.8 was assumed for this study, it can be debated whether the target reliability level is too high. The target reliability index was chosen by consideration of consequences of failure. It was also considered that the failure of a fire compartment due to failure of a composite beam could be seen a "brittle failure mode". Based on single element behaviour, these assumptions may hold true. In this case the beams are however part of a highly redundant steel framed structure. Full scale testing has shown that fire compartment breach does not easily occur, even when the secondary beams under consideration lose all capacity. If a lower target reliability index is therefore deemed adequate, the beam under consideration would be sufficient. The "correct" value of $\beta_{target}$ is a complicated issue that can not be answered through the limited study performed here.

Consider the following, with regard to the steel section temperature used to calculate the $\beta$-index. It was assumed that the section is at a uniform temperature in order to simplify the analysis. In reality it might be more accurate to assume different temperatures for the two flanges and the web. The top flange temperature will certainly be lower than the rest of the profile, due to the contact with the composite slab. By assuming that the steel section's average maximum temperature is 7% less than the calculated value, the reliability index changes to: $\beta = 3.84$. For this reliability level the beam would be considered as a satisfactory design.

This example shows clearly that the influence of the maximum steel section temperature plays a significant role in the beam's probability of failure. It is conceivable that there are many other factors that might influence the temperature of the steel section. It has already been pointed out that the size of the fire compartment also has a pronounced effect on the reliability of the beams. Other considerations might be the correct mean and standard deviation values for the model uncertainty coefficients. At this stage the mean of the resistance uncertainty coefficient was taken as 1.1. Depending on the confidence one has in the mechanical response model, these values might also need to be adjusted.

The reliability analysis in general shows that adequate reliability levels can be achieved for certain structural configurations. This statement is made without considering the added benefit of fire protection and active fire fighting measures.

## 4.6 Discussion of the results of the reliability analysis

The various reliability analyses that were performed clearly show the dominant limit state where failure would most likely occur when considering composite beams. Of the three limit states, the fire limit state is dominant when designing unprotected composite beams. This means that pre-camber of the steel section, to satisfy serviceability criteria, would generally not be required if the beams were designed as unprotected, for the fire limit state.

The reliability analyses show that unprotected beams can be used even without the consideration of active fire fighting measures. The results shown in this document generally suggest that unprotected beams are more suited for small fire compartments in buildings with moderate fire loads. The comparison of deterministic design methods and the resulting reliability level of the element suggests that the deterministic designs are slightly unconservative. It was also demonstrated that both the deterministic design and reliability analysis are very sensitive to steel section temperature. The calculated maximum steel section temperatures are in turn very sensitive to the ventilation conditions and design fire loads.

The reliability analysis of composite beams however confirms that the unprotected beams are adequately reliable if conservative design assumptions are made. The role of whole structure behaviour and the use of active fire fighting measures could also greatly improve structural reliability. These aspects are however difficult to quantify. Further investigation into the correct target reliability level for the fire limit state is required.

The appropriate target reliability value is connected with the consequence of structural failure. It is a reality that fires can have devastating consequences. It is however not clear cut, whether the probability of structural failure can be based solely on the probability of single element failures. Whole structure behaviour or in general, system reliability, is the next step when considering structural reliability in case of fire.

# Chapter 5

# Conclusions

## 5.1 The implementation of structural fire engineering principles

Modern Design Codes move away from prescriptive design approaches. Performance based design is considered as an alternative method, by which more economical designs can be achieved. The Eurocodes [3, 7, 6] include sections on the design for fire of structural elements. Computer applications are available that can be used to predict fire development and structural response. These tools enable engineers to make use of rational design methods, in order to implement a performance based design.

Nominal fire curves, like the standard temperature time curve, are conservative models which can still be used to design for fire. The alternative is to design structures in a more scientific way. Parametric fire curves are analytical models that are easily used and which provide scope to make use of physically based thermal actions. Such models can be combined with structural analysis at elevated temperature, ranging from member analysis to entire structures.

In general, the methods provided in the Eurocode [3, 7, 6] only provide guidance on the design of single elements for fire. Single element design is already a significant step towards more economical designs, if it enables one to leave certain elements unprotected against fire. Research however suggests that whole structure behaviour determines the fire resistance of a structure. The robustness of composite structures during fires have been observed and studied. Significant advances in the field of structural fire engineering has been made due to this ongoing research in Europe. Many fire engineering tools are available, which enable engineers to design for fire in a rational manner.

Guidelines such as those produced by the Building Research Establishment in the UK [34, 32], take a step towards enabling designers to consider whole structure behaviour. Advances in computer aided design also provide a means to consider the behaviour of whole structures. These advanced methods can however only be used where a performance based design is accepted.

The consideration of whole structure behaviour is however not justified in many cases. In such

cases it is possible to consider the fire resistance of single structural elements. Structural fire engineers should understand basic structural behaviour due to fire loads. The effects of boundary conditions must be considered when doing single element design. Because simplified calculation models do not explicitly take structural interaction into account, the engineer should be aware of the effects of thermal expansion, thermal gradients and the effect of restraint by the surrounding structure.

It can be concluded that the use of parametric or other natural fire models, is advantageous to the design of composite steel and concrete structures. The incorporation of any active fire fighting measures into the calculation of design fire loads improves the structural safety as well as safety of occupants.

## 5.2 The deterministic design of composite beams for fire

Composite beams have significant capacity at the ultimate limit state. The increased capacity due to the composite action of steel and concrete is not reflected in reduced deflections of the beam. For normal temperature design, composite beams are generally governed by serviceability limitations. This limitation can however by overcome by pre-camber of the composite beam. This technique enables the engineer to use composite beams in structures where the beams must span relatively long distances. Other benefits of composite construction, where profiled steel sheeting is used for floor plates, are speed of construction and reduced labour costs.

If composite beams are designed as unprotected elements for the fire limit state, larger sections are required to survive fires. In general it is therefore the fire limit state which dominates design of composite beams. It can be stated that if unprotected composite beams are designed for fire, sufficient capacity at the ULS and SLS are implied and can only be verified by the designer.

With specific regard to the use of natural fire development models, the following can be concluded: designers should invest effort in the determination of correct and conservative fire compartment characteristics. Ventilation conditions and fire loads can have significant influence on the temperatures of structural elements.

## 5.3 Reliability analysis of composite beams for fire

By using parametric fire curves with variables that can be statistically described, a reliability analysis of a composite beam was performed. The use of nominal fire curves, to determine temperature development, does not support this type of reliability analysis and design. A clear advantage of parametric fire models is therefore in their ability to be used to analyse and improve on the reliability of a structure.

The probability of failure in case of fire is not only related to the reliability of the structural component. Other factors to be considered are the probability of getting a fully engulfed fire compartment during the lifetime of the structure. The reliability of the structure/component can be improved by considering active fire fighting measures. The improved reliability due to active measures is conditional to the maintenance of such active fire fighting measurers.

The advantage of probability based design lies in its ability to predict structural behaviour more accurately. Probability based design can be used to estimate the probability of failure and the associated risk of a failure. The risk analysis of structures for fire is the next logical step in the optimisation of structures for fire.

The reliability analysis of composite beams confirms that unprotected beams can be used even when disregarding the added benefits of active fire fighting measures. The results of the reliability analyses generally suggest that unprotected beams are more suited for small fire compartments in buildings with moderate fire loads. Contrary to this result, the deterministic design procedure suggested that the beams have a wider field of application. This discrepancy is deemed to be caused by inaccuracy in the implementation of the FORM procedure.

It can be concluded that the reliability level of composite beams designed according to South African and Eurocode recommendations are adequate. In cases where reliability indexes are lower than the target value, it can mostly be justified on the basis of over conservative design assumptions and simplified numerical procedures.

# Chapter 6

# Recommendations

The following recommendations can be made:

- The implementation of a rational design approach for fire is recommended. The recommendation is based on its relative ease of implementation, while still being based on sound theory and testing.
- The influence of the temperature profile through structural elements must be accurately determined in order to improve the quality of reliability analysis. Current design aids such as OZone V2.0 enable designers to make use of natural fire models, but the temperature development in structural elements is limited to steel sections. User friendly computer applications must be developed to predict the temperature in composite sections. The finite element method is ideally suited for such applications. The development of such a tool, with fire engineering in mind, is recommended.
- Reliability analysis must be performed for other structural elements, in order to establish a better picture of the performance of various structural elements in fire.
- It is recommended that further investigations are done into the correct target reliability level to be assumed for the fire limit state. The ideal would be to consider the system reliability in order to estimate the probability of progressive collapse in case of a structural failure. Bayesian networks and decision tree analysis could be considered in this regard. The computer application Genie, which is freely available, could be helpful to establish such systems analyses.
- Finally, it is recommended that a comparative study is conducted concerning the cost implications of using modern fire engineering techniques. It should be investigated whether significant cost savings can be expected for the steel industry by designing unprotected steel structures, if possible. All cost aspects should be taken into account including: added weight of steel, speed of erection (especially with regard to structures with composite floors), saving in man hours, the cost of the added design effort etc.

# Bibliography

## 7.1 Codes of Practice and reference documents


[1] Standards South Africa. *The Structural Use of Steel Part1: Limit States Design of Hot–Rolled Steelwork, SANS 10162-1:2005.* SABS, Pretoria, 2005. 33, 34, 36, 38, 39, 40, 41, 42, 59, 77, 111, 113

[2] European Committee for Standardization. *Eurocode – Basis of structural design, prEN 1990.* CEN, Brussels, July 2001. 45, 84, 85

[3] European Committee for Standardization. *Eurocode 1 - Actions on Structures Part 1-2: General Actions - Actions on Structures Exposed to Fires.* CEN, Brussels, January 2002. 8, 10, 12, 13, 45, 51, 52, 53, 54, 68, 71, 73, 80, 100

[4] European Committee for Standardization. *prEN 1994: Design of composite steel and concrete structures, Part 1-1: General rules and rules for buildings.* CEN, Brussels, stage 34 final project team draft edition, January 2002. 45

[5] European Committee for Standardization. *Eurocode 2: Design of concrete structures - Part 1-1: General rules and rules for buildings.* CEN, Brussels, final draft edition, December 2003. 41

[6] European Committee for Standardization. *Eurocode 4 Design of composite steel and concrete structures, Part 1-2: General rules - Structural fire design.* CEN, Brussels, final draft (stage 34) edition, May 2003. 15, 16, 45, 46, 47, 48, 49, 51, 53, 100

[7] European Committee for Standardization. *Eurocode 3: Design of Steel Structures Part 1-2: General Rules - Structural Fire Design.* CEN, Brussels, April 2005. 15, 16, 17, 18, 24, 45, 51, 100

[8] ISO. *General principles on reliability for structures*, 1998. 84, 85

[9] South African Bureau of Standards. *The general procedures and loadings to be adopted in the design of buildings, SABS 0160.* SABS, Pretoria, 1989. 59, 83, 84, 85, 109

[10] The South African Bereau of Standards. *The Structural Use of Concrete Part 1: Design.* SABS, Pretoria, 2.2 edition, March 2000. 41, 59

[11] Southern African Institute of Steel Construction. *Southern African Steel Construction Handbook (Limit States Design).* SAISC, 43 Empire Road Parktown West Johannesburg, fifth edition, 2005. 34, 37, 44, 50, 59, 86, 110, 113, 118

[12] The Council of the South African Bureau of Standards. *Fire Testing of Materials, Components and Elements used in buildings Part II: Fire Resistance Test for Building Elements.* SABS, Pretoria, 1981. 10

[13] J-B. Schleich, M. Holický, A. Arteaga, and L. Rodriguez. *Handbook 5 - Design of buildings for the fire situation*, volume 5 of *Development of skills facilitating implementation of Eurocodes.* Leonardo Da Vinci Pilot Project CZ/02/B/F/PP-134007, Luxembourg, October 2005. 6, 7, 10, 17, 45, 54, 69, 71, 90, 92

## 7.2 Fire engineering principles

[14] A.H. Buchanan. *Structural Design for Fire Safety.* John Wiley & Sons, Ltd, West Sussex PO19 8SQ, England, 2002. 7, 8, 16, 17

[15] J.F. Cadorin, D. Pintea, and J.M. Franssen. The design fire tool OZone V2.0 – theoretical description and validation on experimental fire tests. Technical Report 1st draft, University of Liege, Belguim, June 2001. 24

[16] N.J.K. Cameron. *The Behaviour and Design of Composite Floor Systems in Fire.* PhD thesis, University of Edinburgh, October 2003. 7

[17] L.G. Cojot, M. Haller, and M. Pierre. Part 1: Thermal & mechanical actions. Not published, July 2005. 73

[18] D. Gross. Data sources for parameters used in predictive modelling of fire growth and smoke spread. Technical data NBSIR 85-3223, U.S. Department of commerce National bureau of standards National engineering laboratory Centre for fire reserach, Gaitherburg MD 20899, 1985. 17

[19] W.W. Jones, R.D. Peacock, G.P. Forney, and P.A. Reneke. CFAST - consolidated model of fire growth and smoke transport (version 6). Technical reference guide, National Institute of Standards and technology (NIST) U.S Department of Commerce, December 2005. 14, 23

[20] B. Karlsson and J.G. Quintiere. *Enclosure Fire Dynamics.* Environmental and Energy Engineering series. CRC Press LCC, New York, 2000. 8, 17, 23

[21] B.R. Kirby and L.N. Tomlinson. The temperatures attained by unprotected steelwork in building fires. Published by Corus Research, Development and Technology, 2000. 16

[22] S. Kumar and C.V.S. Kameswara Rao. Fire load in resisdential buildings. *Building and Environment*, 30(2):299–305, 1995. 54

[23] S. Kumar and C.V.S. Kameswara Rao. Fire loads in office buildings. *Journal of Structural Engineering*, 123(3):365–368, March 1997. This is a technical note. 54

[24] S. Lamont. Study of thermal expansion and bowing in a restrained beam. PIT Project Research Report TM3, The University of Edinburgh School of Civil & Environmental Engineering, King's buildings Edinburgh, March 2000. 21

[25] S. Lamont, A.S. Usmani, and M. Gillie. Behaviour of a small composite steel frame structure in a "long cool" and a "short hot" fire. *Fire Safety Journal*, 39:327–357, 2004. 10, 11, 16

[26] J. Milke. Analytical methods to evaluate fire resistance of structural members. *Journal of Structural Engineering*, 125(10):1179–1187, October 1999. 10

[27] A European Joint Research Programme. *The Behaviour of Multi–Storey Steel Framed Buildings in Fire*. British Steel plc, Swinden Technology Centre, Rotherham United Kingdom, 1999. 7, 29

[28] J.M. Rotter, A.M. Sanad, A.S. Usmani, and M. Gillie. Structural performance of redundant structures under local fires. In *Interflam Proceedings*, Edinburgh, 1999. Interflam. 19, 20, 22

[29] A.S. Usmani, D.D. Drysdale, J.M. Rotter, A.M. Sanad, M. Gillie, and S. Lamont. Behaviour of steel framed structures under fire conditions. PIT project main report, The University of Edinburgh School of Civil & Environmental Engineering, King's buildings Edinburgh, June 2000. 15, 19, 22

[30] A.S. Usmani, J.M. Rotter, S. Lamont, A.M. Sanad, and M. Gillie. Fundamental principles of structural behaviour under thermal effects. *Fire Safety Journal*, 36:721–744, March 2001. 7, 16, 19, 21, 22

## 7.3 Composite slabs and beams

[31] C. Bailey. Structural fire design of unprotected steel beams supporting composite floor slabs. In *II International conference on steel construction - II CICOM*, São Paulo Brazil, November 2002. 27, 28, 29

[32] C. Bailey. New fire design method for steel frames with composite floor slabs. FBE report 5, BRE Centre for Structural Engineering, 151 Rosebery Avenue London EC1R4GB, 2003. 3, 7, 27, 100

[33] C.G. Bailey. Efficient arrangement of reinforcement for membrane behaviour of composite floor slabs in fire conditions. *Journal of Constructional Steel Research*, 59:931–949, 2003. 7

[34] G.M. Newman, J.T. Robinson, and C.G. Bailey. *Fire Safe design: A New Approach to Multi–Storey Steel–Framed Buildings*. Fire and Steel Construction. The Steel Construction Institute, Silwood Park Berkshire, 2000. 3, 4, 7, 22, 27, 28, 29, 68, 100

## 7.4 Structural reliability and robustness

[35] L.-G. Cajot, M. Holický, and J.-B. Schleich. Reliability of a steel beam under persistent and fire design situation. In *Safety, Risk and Reliability – Trends in Engineering*, pages 125–130, Malta, March 2001. 18

[36] Joint Committee for Structural Safety. *JCSS probabilistic modal code*. JSSS, Zurich, 12th draft edition, March 2001. 87

[37] M. Holický. *Reliability Analysis for Structural Design*. Klokner institute, Prague, 2005. 65, 80, 81, 84

[38] M.A. Maes, K.E. Fritzsons, and S. Glowienka. Structural robustness in the light of risk and consequence analysis. *Structural Engineering International*, 16(2):101–107, May 2006. 24, 25

[39] U. Starossek. Progressive collapse of structures: Nomenclature and procedures. *Structural Engineering International*, 16(2):113–117, May 2006. 26

[40] D.V. Val and E.G. Val. Robustness of frame structures. *Structural Engineering International*, 16(2):108–112, May 2006. 25, 26

# Appendices

# Appendix A

# Design tables for composite beams - Parameter study

## A.1 Example – Composite beam at normal temperature

The methods proposed in section 3, concerning the deterministic design of composite beams, are best described by an example. The calculations shown here are for a composite beam with a $I$ 406 × 178 × 67 steel section. The data that is not provided in this section can be found in section 3.4.6 and specifically in table 3.3 on page 52.

### A.1.1 Flexural resistance

**Table A.1:** Loads used in design example

| Input parameter | Value | Units |
|---|---|---|
| Steel section designation | $I$ 406 × 178 × 67 | [–] |
| Effective width | 2.25 | [m] |
| Length of beam | 9.0 | [m] |
| Percent shear connection | 0.6 | [%] |
| Thickness of slab | 0.14 | [m] |
| Span between beams | 3.0 | [m] |
| Weight of beam | 219.4 | [N/m$^2$] |
| Weight of deck | 116.7 | [N/m$^2$] |
| Weight of concrete | 2614.4 | [N/m$^2$] |
| Weight of raised floor | 400 | [N/m$^2$] |
| Weight of services | 250 | [N/m$^2$] |
| Weight of ceiling | 150 | [N/m$^2$] |
| Load due to of partitions | 1000 | [N/m$^2$] |
| Imposed load | 2500 | [N/m$^2$] |

The load combinations and partial factors are taken according to SABS 0160 §4.4, [9]. According

to the width to thickness ratios of the steel section, plastic design may be used, as the $I$ 406 × 178 × 67 section is a Class 1 section. The beam is designed as unpropped, fur purposes of the example. Firstly we calculate the ultimate moment for the construction stage before placing of concrete:

$$\begin{aligned} M_u &= \frac{wl^2}{8} \\ &= \frac{(1.2(0.219 + 0.117) + 1.6(0.5))(9^2)(3)}{8} \\ &= 36.55 \text{ kN} \cdot \text{m} \end{aligned} \tag{A.1}$$

where $(w)$ is the load per metre length of the beam.

By providing temporary lateral restraint at mid-span of the steel beam the slenderness ratio is as follows:

$$\frac{L}{r_y} = \frac{4500}{39.9} = 112.8 < 200 \ (\therefore OK) \tag{A.2}$$

According to the design table 5.5 in reference [11] and the calculations performed to generate table A.2, the resistance moment of the steel section is:

$$M_r = 299 \text{ kN·m } (> 37 \text{ kN} \cdot \text{m} \therefore OK) \tag{A.3}$$

Secondly, we calculate the ultimate moment for the construction stage after placing of the wet concrete. The construction live load is increased due to the likelihood of more construction workers and equipment being present:

$$\begin{aligned} M_u &= \frac{Wl}{8} \\ &= \frac{(1.2(2.6 + 0.219 + 0.117) + 1.6(1.0))(9^2)(3) \times 10^3}{8} \\ &= 156 \text{ kN} \cdot \text{m} \end{aligned} \tag{A.4}$$

The steel joist is attached to the steel decking, via the welded shear studs. One can therefore assume that the steel section is laterally supported, along the whole length of the compression flange:

$$\begin{aligned} M_r &= 0.9(Z_{pl})(f_y) \\ &= 0.9(1350 \times 10^{-6})(350 \times 10^6) \\ &= 425 \text{ kN} \cdot \text{m } (> 156 \text{ kN} \cdot \text{m} \therefore OK) \end{aligned} \tag{A.5}$$

The construction of the composite beam has now been completed. The ultimate and serviceability limit states for the composite section must be checked. Note that the load due to movable

partitions, have been included as a imposed load:

$$\begin{aligned} M_u &= \frac{Wl}{8} \\ &= \frac{(1.2(2.6+0.219+0.117+0.4+0.25+0.15)+1.6(2.5+1.0))(9^2)(3)}{8} \\ &= 307 \text{ kN} \cdot \text{m} \end{aligned} \tag{A.6}$$

The corresponding ultimate vertical shear force is:

$$\begin{aligned} V_u &= \frac{W}{2} \\ &= \frac{273}{2} \\ &= 136.4 \text{ kN} \cdot \text{m} \end{aligned} \tag{A.7}$$

The design effective width of the concrete slab is calculated according to SANS 10162:2005 §17.7.1, [1]. The effective width and effective thickness of the slab is:

$$\begin{aligned} b_{eff} &= 2.250 \text{ m} \\ t_{eff} &= 0.140 - 0.075 \\ &= 0.065 \text{ m} \end{aligned} \tag{A.8}$$

The composite beam is designed assuming partial shear connection of 60% $\therefore \alpha = 0.6$ . Therefore a reduced effective thickness must be used, to calculate the concrete compressive force. It is assumed that the steel section is fully utilised, therefore the concrete compressive block is reduced in order to achieve static equilibrium:

$$\begin{aligned} C_r^{'} &= 0.68 \cdot \phi_c \cdot b_{eff} \cdot \alpha \cdot t_{eff} f_{cu} \\ &= 0.68(0.6)(2.25)(0.6)(0.065)(25 \times 10^{-6}) \\ &= 895 \text{ kN} \end{aligned} \tag{A.9}$$

$$\begin{aligned} T_r &= \phi A_s f_y \\ &= (0.9)(8550)(350) \\ &= 2693 \text{ kN} \end{aligned} \tag{A.10}$$

It can be seen that $C_r^{'} < T_r$ and therefore the plastic neutral axis of the section lies within the steel profile. To achieve static equilibrium, a part of the steel section will also be in compression. The reduced effective thickness of the concrete slab, measured from the top of the slab is:

$$\begin{aligned} a &= 0.6 \times 0.065 \\ &= 0.039 \text{ m} \end{aligned} \tag{A.11}$$

The compressive force in the steel section can now be calculated as was shown in section 3.2.2.

$$\begin{aligned} C_r &= \frac{\phi A_s f_y - C_r^{'}}{2} \\ &= \frac{2693 - 895}{2} \\ &= 899 \text{ kN} \end{aligned} \tag{A.12}$$

The area of the steel section that is in compression ($A_{sc}$) is then:

$$\begin{aligned} A_{sc} &= \frac{C_r}{\phi f_y} \\ &= \frac{899 \times 10^3}{0.9(350)} \\ &= 2854 \text{ mm}^2 \end{aligned} \tag{A.13}$$

The physical area of the steel section's flange is 2557 mm$^2$, the composite section's plastic neutral axis lies within the steel section's web. The distance to the plastic neutral axis from the top of the steel section (designated as $x$), is then:

$$\begin{aligned} x &= \frac{A_{sc}}{t_w} - \frac{b_f t_f}{t_w} + t_f \\ &= 48.1 \text{ mm} \end{aligned} \tag{A.14}$$

The centroid of the part of the steel section that is in compression must be calculated. The centroid is calculated from the bottom of the steel profile:

$$\begin{aligned} A_{sc,xx} &= \frac{b_f t_f (h - \frac{t_f}{2}) + t_w (x - t_f)(h - x + \frac{x - t_f}{2})}{b_f t_f + t_w (x - t_f)} \\ &= 399.7 \text{ mm} \end{aligned} \tag{A.15}$$

The distance to the centroid of the steel section tension area (designated as z), is also taken from the bottom of the steel profile:

$$\begin{aligned} z &= \frac{A_s \frac{h}{2} - A_{sc} A_{sc,xx}}{A_s - A_{sc}} \\ &= 107 \text{ mm} \end{aligned} \tag{A.16}$$

The moment arm of the steel compressive force ($C_r$), is designated ($e$). The moment arm of the concrete compressive force ($C_r^{'}$), is designated ($e^{'}$). The moment is taken around the tensile force in the steel section.

$$\begin{aligned} e^{'} &= h - z + t_{slab} - \frac{a}{2} \\ &= 423 \text{ mm} \end{aligned} \tag{A.17}$$

$$\begin{aligned} e &= A_{sc,xx} - z \\ &= 293 \text{ mm} \end{aligned} \tag{A.18}$$

The resistance moment of the composite section can then be calculated:

$$\begin{aligned} M_{cr} &= C_r e + C_r^{'} e^{'} \\ &= 642 \text{ kN} \cdot \text{m } (> M_u = 307 \therefore OK) \end{aligned} \tag{A.19}$$

### A.1.2 Vertical end shear

According to SANS 10162:2005 Table 4 the steel section used in this composite beam can be classified as a Class 1 profile. According to §13.4.1.2 of the aforementioned document the resistance of the composite beam against vertical end shear can be calculated as:

$$\begin{aligned} V_r &= 0.55 \phi_s t_w h f_y \\ &= 624 \text{ kN } (> V_u = 137 \therefore OK) \end{aligned} \tag{A.20}$$

### A.1.3 Number of shear studs

The shear connectors that will be used are 19 mm headed studs. According to table 9.3 of reference [11], such studs have a shear resistance of 58.4 kN when used in pairs. The force that the shear connection must resist is 895 kN. This is the lesser of the compression force in the concrete slab and the tension force in the steel section, according to §17.9.5 of SANS 10162:2004, [1]. Thus, the number of studs between points of maximum and zero bending moment are:

$$\begin{aligned} N &= \frac{895}{58.4} \\ &= 15.3 \therefore 16 \text{ studs} \end{aligned} \tag{A.21}$$

The spacing of studs is then:

$$\text{Spacing} = \frac{4500}{8} = 563 \text{ mm} \tag{A.22}$$

The centre to centre spacing of the ribs of a "Bond-dek" profiled sheet is 452 mm, which is less than the required spacing. Therefore the shear studs must be installed in pairs in every rib of the steel sheeting. The actual number of studs that will be installed can be used for fire resistance calculations. The actual number is then $4500/452 = 9.96$ studs multiplied by two studs per rib thus: $N = 20$ studs between critical sections.

### A.1.4 Longitudinal shear

The concrete is subject to a shear force equal to the total longitudinal compressive forces, minus the concrete and steel reinforcement compressive forces in the area above the steel I-profile's

flange. The concrete force is given by $0.68\phi_c A_c f_{cu}$ and the longitudinal reinforcement force by, $\phi_r A_{rl} f_{yr}$. Thus:

$$\begin{aligned} V_u &= \sum q_r - 0.68\phi_c A_c f_{cu} - \phi_r A_{rl} f_{yr} \\ &= 824 \text{ kN} \end{aligned} \tag{A.23}$$

$V_u$ is the combined shear force on the two longitudinal shear planes and $A_{rl}$ is the area of longitudinal reinforcement within the area $A_c$. The length of each shear plane is the distance along the beam between points of maximum and minimum bending moment.

The factored resistance of the concrete shear planes can be calculated by equations **??** and **??** and is the lesser of the two values obtained. In this case $V_r = 1148$ kN which is bigger than the ultimate longitudinal shear force. In this calculation the area of longitudinal reinforcement was conservatively neglected. The minimum transverse reinforcement is according to SANS 10162 §17.5.4.2 is:

$$\begin{aligned} A_{rt} &\geq 0.001(65)(4500) \\ &\geq 293 \text{ mm}^2 \end{aligned} \tag{A.24}$$

$$\begin{aligned} V_r &= 0.8(0.85)(293)(2)(450)(10^{-3}) + 2.76(0.6)(65)(4500)(2)(10^{-3}) \\ &= 1148 \text{ kN} \\ &\text{or} \\ V_r &= 0.4(0.6)(25)(65)(4500)(2) \\ &= 3510 \text{ kN} \end{aligned} \tag{A.25}$$

Therefore the resistance against longitudinal shear is sufficient. Note that the calculated value for the area of transverse reinforcement was used. In practice one would use a larger value for the area due to the fact that reinforcement bar only comes in standard sizes. The calculation is therefore conservative.

### A.1.5 Deflections

The effective moment of inertia is calculated to accommodate partial shear connection and interfacial slip effects:

$$\begin{aligned} I_e &= I_s + 0.85(p^{0.25})(I_t - I_s) \\ &= 243 \times 10^{-6} + 0.85(0.6^{0.25})(825 \times 10^{-6} - 243 \times 10^{-6}) \\ &= 678 \times 10^{-6} \qquad [\text{m}^4] \end{aligned} \tag{A.26}$$

The various components of deflection are calculated for a unpropped steel section:

$$\begin{aligned}\Delta_i &= \frac{5}{384} \cdot \frac{WL^3}{EI} \\ &= \frac{5}{384} \cdot \frac{1.1(2950)(9)(3)(9^3)}{(200 \times 10^9)(243 \times 10^{-6})} \\ &= 17.1 \text{ mm}\end{aligned} \tag{A.27}$$

The deflection due to short term imposed load, assuming that half of the imposed load is considered as being short term load, is then:

$$\begin{aligned}\Delta_{sh} &= \frac{5}{384} \cdot \frac{WL^3}{EI_e} \\ &= \frac{5}{384} \cdot \frac{1750(9)(3)(9^3)}{(200 \times 10^9)(678 \times 10^{-6})} \\ &= 3.3 \text{ mm}\end{aligned} \tag{A.28}$$

The creep deflection is calculated by increasing the short term deflection (elastic deflection), due to long term loads by 15%. Thus the deflection due to all loads minus the initial deflection of the steel section will be calculated. Note that in the first square bracket of equation A.29, the elastic deflection due to all long term loads is calculated. In the second square bracket the elastic deflection (using the effective moment of inertia ($I_e$)), due to the weight of the steel beam, concrete slab and steel sheeting, is subtracted from the total elastic deflection. This must be done so that the initial deflection due to the unpropped construction, is not counted twice.

$$\begin{aligned}\Delta_c &= 1.15 \cdot \left[\frac{5}{384} \cdot \frac{(0.5 \cdot (W_{live} + W_{partitions}) + 1.1 \cdot (W_{finishes})) \cdot L^3}{E_s I_e}\right] \\ &\quad + 0.15 \cdot \left[\frac{5}{384} \cdot \frac{1.1 \cdot W_{initial} \cdot L^3}{E_s I_e}\right] \\ &= 1.15 \cdot \left[\frac{5}{384} \cdot \frac{(0.5 \cdot (1750) + 1.1 \cdot (800)) \cdot 9^3}{(200 \times 10^9)(678 \times 10^{-6})}\right] \\ &\quad + 0.15 \cdot \left[\frac{5}{384} \cdot \frac{1.1 \cdot 2950 \cdot 9^3}{(200 \times 10^9)(678 \times 10^{-6})}\right] \\ &= 1.1 \text{ mm}\end{aligned} \tag{A.29}$$

Lastly the shrinkage deflection is calculated:

$$\begin{aligned}\Delta_s &= 0.85 \cdot \frac{\varepsilon_f A_c L^2 y}{8 n I_t} \\ &= \frac{(400 \times 10^{-6})(0.1462)(9^2)(0.0968)}{8(7.69)(825 \times 10^{-6})} \\ &= 7.7 \text{ mm}\end{aligned} \tag{A.30}$$

The total deflection of the beam is approximately:

$$\begin{aligned}\Delta_{tot} &= \Delta_i + \Delta_{sh} + \Delta_c + \Delta_s \\ &= 17.1 + 3.3 + 1.1 + 7.7 \\ &\approx 29.2 \text{ mm}\end{aligned} \tag{A.31}$$

## A.2 Design tables

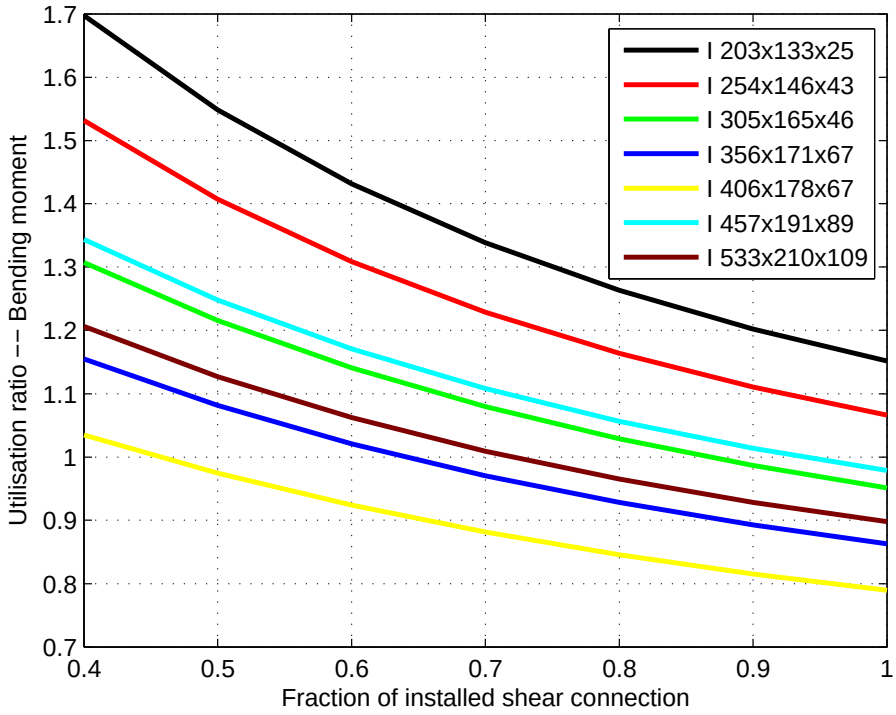


**Figure A.1:** Utilisation ratio of bending moment capacity, for various composite beams, versus the amount of installed shear connection

Figure A.1 shows the influence of the percentage shear connection that is supplied, on the utilisation ratio of some composite beams. The graph shows that for typical sections, the moment capacity decreases with only 20-30% when the installed shear connection is changed from 100% to 60%. This illustrates that significant benefit is not derived from full shear connection between the steel section and the composite slab. It is therefore less costly to install partial shear connection.

**Table A.2:** Composite beam data – Designed according to SANS. Data: $L = 9$ m, $b_{eff} = 2.25$ m, $t_{slab} = 140$ mm, 60% shear connection, simply supported beam, limiting deflection: $D_{Lim} = \frac{L}{300} = 30$ mm, free shrinkage strain: $\varepsilon_f = 400\mu$, imposed load = 2.5 kN/m$^2$, unpropped construction used.

| A | B | C | D | E | F | G | H | I | J | K | L | M | N | O | P | Q | R | S | T | U | V | W |
|---|---|---|---|---|---|---|---|---|---|---|---|---|---|---|---|---|---|---|---|---|---|---|
| | | Construction stage 1 | | | | Construction stage 2 | | | Composite stage | | | | | Deflections | | | | | | | | |
| | Joist desig. | $L_e$ | $M_{r1}$ | $M_{u1}$ | $\frac{M_{u1}}{M_{r1}}$ | $M_{r2}$ | $M_{u2}$ | $\frac{M_{u2}}{M_{r2}}$ | $M_{cr}$ | $M_u$ | $\frac{M_u}{M_{cr}}$ | $V_r$ | $\frac{V_u}{V_r}$ | $I$ | $I_e$ | $I_t$ | $\Delta_1$ | $\Delta_2$ | $\Delta_3$ | $\Delta_4$ | $\Delta_T$ | $\frac{\Delta_{Tot}}{\Delta_{Lim}}$ |
| | | [m] | $[kN \cdot m]$ | | | $[kN \cdot m]$ | | | $[kN \cdot m]$ | | | $[kN]$ | | $[mm^4]$ | | | $[mm]$ | | | | | |
| 1 | I203x133x25 | 4.50 | 43 | 32 | 0.73 | 82 | 151 | 1.85 | 211 | 302 | 1.43 | 201 | 0.67 | 23.5 | 118.6 | 150.6 | 169 | 19 | 6 | 13 | 207 | 6.90 |
| 2 | I203x133x30 | 4.50 | 59 | 32 | 0.54 | 99 | 152 | 1.54 | 231 | 302 | 1.31 | 229 | 0.59 | 28.9 | 139.3 | 176.5 | 138 | 16 | 5 | 13 | 172 | 5.75 |
| 3 | I254x146x31 | 4.50 | 68 | 32 | 0.47 | 124 | 152 | 1.22 | 265 | 303 | 1.14 | 261 | 0.51 | 44.3 | 183.5 | 230.3 | 90 | 12 | 4 | 11 | 118 | 3.93 |
| 4 | I254x146x37 | 4.50 | 96 | 33 | 0.34 | 153 | 153 | 1.00 | 297 | 303 | 1.02 | 279 | 0.48 | 55.5 | 217.9 | 272.6 | 72 | 10 | 3 | 11 | 97 | 3.25 |
| 5 | I254x146x43 | 4.50 | 122 | 34 | 0.28 | 179 | 153 | 0.86 | 329 | 304 | 0.92 | 324 | 0.42 | 65.5 | 250.2 | 312.4 | 62 | 9 | 3 | 11 | 85 | 2.83 |
| 6 | I305x102x25 | 3.00 | 45 | 32 | 0.70 | 106 | 151 | 1.43 | 258 | 302 | 1.17 | 307 | 0.44 | 43.6 | 184.2 | 231.5 | 91 | 12 | 4 | 10 | 117 | 3.92 |
| 7 | I305x102x28 | 3.00 | 62 | 32 | 0.51 | 129 | 152 | 1.18 | 284 | 302 | 1.06 | 326 | 0.41 | 54.4 | 216.2 | 270.7 | 73 | 10 | 3 | 10 | 97 | 3.24 |
| 8 | I305x102x33 | 3.00 | 81 | 32 | 0.40 | 152 | 152 | 1.00 | 312 | 303 | 0.97 | 358 | 0.38 | 65.0 | 248.5 | 310.2 | 62 | 9 | 3 | 10 | 84 | 2.79 |
| 9 | I305x165x40 | 4.50 | 129 | 33 | 0.26 | 197 | 153 | 0.78 | 352 | 304 | 0.86 | 321 | 0.42 | 85.5 | 294.8 | 365.3 | 47 | 8 | 3 | 10 | 67 | 2.24 |
| 10 | I305x165x46 | 4.50 | 157 | 34 | 0.22 | 227 | 154 | 0.68 | 388 | 304 | 0.78 | 356 | 0.38 | 99.3 | 333.3 | 412.0 | 41 | 7 | 2 | 10 | 60 | 1.99 |
| 11 | I305x165x54 | 4.50 | 194 | 35 | 0.18 | 266 | 155 | 0.58 | 434 | 305 | 0.70 | 415 | 0.33 | 117.0 | 381.6 | 470.8 | 35 | 6 | 2 | 10 | 53 | 1.75 |
| 12 | I356x171x45 | 4.50 | 150 | 34 | 0.23 | 243 | 154 | 0.63 | 420 | 304 | 0.72 | 421 | 0.32 | 121.0 | 389.7 | 480.1 | 34 | 6 | 2 | 9 | 50 | 1.67 |
| 13 | I356x171x51 | 4.50 | 188 | 35 | 0.18 | 282 | 154 | 0.55 | 464 | 305 | 0.66 | 450 | 0.30 | 142.0 | 440.6 | 541.2 | 29 | 5 | 2 | 9 | 44 | 1.48 |
| 14 | I356x171x57 | 4.50 | 221 | 35 | 0.16 | 318 | 155 | 0.49 | 507 | 306 | 0.60 | 497 | 0.27 | 161.0 | 488.0 | 598.1 | 26 | 5 | 2 | 9 | 40 | 1.34 |
| 15 | I356x171x67 | 4.50 | 282 | 37 | 0.13 | 381 | 156 | 0.41 | 583 | 307 | 0.53 | 574 | 0.24 | 195.0 | 569.8 | 696.0 | 21 | 4 | 1 | 8 | 35 | 1.17 |
| 16 | I406x140x39 | 4.50 | 87 | 33 | 0.38 | 226 | 153 | 0.68 | 413 | 303 | 0.73 | 434 | 0.31 | 124.0 | 403.1 | 497.0 | 32 | 6 | 2 | 8 | 48 | 1.61 |
| 17 | I406x140x46 | 4.50 | 122 | 34 | 0.28 | 280 | 154 | 0.55 | 477 | 304 | 0.64 | 481 | 0.28 | 157.0 | 482.9 | 592.6 | 26 | 5 | 2 | 8 | 40 | 1.34 |
| 18 | I406x178x54 | 4.50 | 212 | 35 | 0.16 | 331 | 155 | 0.47 | 535 | 305 | 0.57 | 530 | 0.26 | 187.0 | 551.6 | 674.4 | 22 | 4 | 1 | 8 | 35 | 1.18 |
| 19 | I406x178x60 | 4.50 | 257 | 36 | 0.14 | 378 | 155 | 0.41 | 584 | 306 | 0.52 | 549 | 0.25 | 215.0 | 612.5 | 746.3 | 19 | 4 | 1 | 8 | 32 | 1.06 |
| 20 | I406x178x67 | 4.50 | 299 | 37 | 0.12 | 425 | 156 | 0.37 | 642 | 307 | 0.48 | 624 | 0.22 | 243.0 | 678.0 | 824.5 | 17 | 3 | 1 | 8 | 29 | 0.97 |
| 21 | I406x178x74 | 4.50 | 347 | 37 | 0.11 | 476 | 157 | 0.33 | 701 | 308 | 0.44 | 694 | 0.20 | 274.0 | 746.9 | 906.2 | 15 | 3 | 1 | 8 | 27 | 0.90 |
| 22 | I457x191x67 | 4.50 | 326 | 37 | 0.11 | 463 | 156 | 0.34 | 698 | 307 | 0.44 | 668 | 0.20 | 294.0 | 792.1 | 959.8 | 14 | 3 | 1 | 7 | 25 | 0.83 |
| 23 | I457x191x74 | 4.50 | 380 | 37 | 0.10 | 523 | 157 | 0.30 | 763 | 308 | 0.40 | 721 | 0.19 | 334.0 | 874.7 | 1056.8 | 13 | 3 | 1 | 7 | 23 | 0.76 |
| 24 | I457x191x82 | 4.50 | 431 | 38 | 0.09 | 576 | 158 | 0.27 | 827 | 309 | 0.37 | 789 | 0.17 | 371.0 | 952.8 | 1148.6 | 11 | 2 | 1 | 7 | 21 | 0.71 |
| 25 | I457x191x89 | 4.50 | 487 | 39 | 0.08 | 636 | 159 | 0.25 | 888 | 309 | 0.35 | 851 | 0.16 | 411.0 | 1029.8 | 1238.2 | 10 | 2 | 1 | 7 | 20 | 0.67 |
| 26 | I457x191x98 | 4.50 | 553 | 40 | 0.07 | 702 | 160 | 0.23 | 962 | 311 | 0.32 | 924 | 0.15 | 458.0 | 1120.2 | 1343.2 | 9 | 2 | 1 | 7 | 19 | 0.62 |
| 27 | I533x210x82 | 4.50 | 485 | 38 | 0.08 | 649 | 158 | 0.24 | 923 | 309 | 0.33 | 879 | 0.16 | 475.0 | 1179.0 | 1416.0 | 9 | 2 | 1 | 6 | 18 | 0.59 |
| 28 | I533x210x92 | 9.00 | 215 | 40 | 0.18 | 747 | 159 | 0.21 | 1025 | 310 | 0.30 | 942 | 0.15 | 553.0 | 1320.1 | 1578.4 | 8 | 2 | 1 | 6 | 16 | 0.53 |
| 29 | I533x210x101 | 9.00 | 257 | 41 | 0.16 | 825 | 160 | 0.19 | 1109 | 311 | 0.28 | 1014 | 0.14 | 616.0 | 1433.2 | 1708.4 | 7 | 2 | 1 | 6 | 15 | 0.50 |
| 30 | I533x210x109 | 9.00 | 292 | 42 | 0.14 | 891 | 161 | 0.18 | 1180 | 312 | 0.26 | 1084 | 0.13 | 668.0 | 1527.9 | 1817.4 | 7 | 1 | 1 | 6 | 14 | 0.47 |
| 31 | I533x210x122 | 9.00 | 362 | 43 | 0.12 | 1008 | 163 | 0.16 | 1305 | 313 | 0.24 | 1208 | 0.12 | 762.0 | 1691.7 | 2004.8 | 6 | 1 | 0 | 6 | 13 | 0.44 |

# Appendix B

# Description of numerical methods employed by the student

Matlab was used to do the numerical implementation of the design of composite beams. Various Matlab functions are used to implement the design of composite beams for the following scenarios:

- Normal temperature design
- Fire temperature design
- Reliability analysis:
  - Ultimate limit state
  - Serviceability limit state
  - Accidental limit state – Fire



The sections that follow, describe the interdependency of the functions, a description of each M-file and the main input that is requested from the user.

## B.1 Design – Normal temperatures

**Table B.1:** Matlab functions used for normal temperature design

| Normal temperature design | | | |
|---|---|---|---|
| Parent function | Children | Children | Children |
| Norm_temp_design.m | beamname.m<br>userdata.m | beamdata.m | |

At execution, the function `Norm_temp_design.m` calls `beamname.m` in order to produce a list of standard steel sections, as one can find in the "Southern African Steel Construction Handbook", [11]. The user is prompted to specify the steel section that will be used in the composite beam.

Steel sections 1–31 can be specified. If the number of the steel section is specified as 1000, calculations are performed for all the sections.

After input of the beam's desired steel section, the user is prompted to specify whether the composite beam is propped during construction, or left un-propped. The choice of steel section, is passed to the function `userdata.m`. `userdata.m` calls the function `beamdata.m`, that contains the relevant data of the steel section. The function `userdata.m`, can be edited in order to change the amount of shear connection that is supplied, the concrete slab thickness, the length of the beam and the centerline distance between beams i.e the sheeting span.

The function, among other things, calculates moment resistances and deflections, for the specified composite beam(s). The output of the function looks as follows:

```
For deflection purposes: Are the beams propped?
Yes = 1, No = 2
Answer: 2
The beam is designed as UNPROPPED
Steel compression zone is NOT IN FLANGE
OK - Resistance bigger than the effect
Class 1 profile
********************** Input parameters ************************
Input =
Effective width (Construction) = 2.25       [m]
                Length of beam = 9          [m]
      Percent shear connection = 0.6        [%]
             Thickness of slab = 0.14       [m]
            Span between beams = 3          [m]
                  Load of beam = 219.417    [N/m^2]
                  Load of deck = 116.739    [N/m^2]
              Load of concrete = 2614.365   [N/m^2]
          Load of raised_floor = 400        [N/m^2]
              Load of services = 250        [N/m^2]
               Load of ceiling = 150        [N/m^2]
            Load of partitions = 1000       [N/m^2]
                  Imposed load = 2500       [N/m^2]
   Imposed construction load 1 = 500        [N/m^2]
   Imposed construction load 2 = 1000       [N/m^2]
******************** Tabulation of results *********************
Output =
         Steel section designation = 20: I 406x178x67  [--]
  Resistance moment construction 1 = 298.5618          [kN.m]
    Ultimate moment construction 1 = 36.5529           [kN.m]
  Utilisation ratio construction 1 = 0.12243           [--]
  Resistance moment construction 2 = 425.25            [kN.m]
    Ultimate moment construction 2 = 156.1465          [kN.m]
  Utilisation ratio construction 2 = 0.36719           [--]
```

```
   Steel section moment of inertia = 243              [10^6 mm^4]
     Transformed moment of inertia = 824.5413         [10^6 mm^4]
       Effective moment of inertia = 678.0481         [10^6 mm^4]
                Initial deflection = 17.1153          [mm]
            Short term deflection = 3.3073            [mm]
                 Creep deflection = 1.1318            [mm]
              Shrinkage deflection = 7.6874           [mm]
          Total midspan deflection = 29.2419          [mm]
              Allowable deflection = 30               [mm]
  Utilisation ratio for deflection = 0.97473          [--]
Resistance moment composite action = 641.7979         [kN.m]
  Ultimate moment composite action = 306.8065         [kN.m]
Utilisation ratio composite action = 0.47804          [--]
```

## B.2 Design – Fire temperatures

**Table B.2:** Matlab functions used for fire temperature design

| Fire temperature design | | | |
|---|---|---|---|
| Parent function | Children | Children | Children |
| fire_resist.m | beamname.m<br>userdata.m<br>loads.m<br>steel_carac.m<br>temperature.m<br>parametric_temp.m<br>steeltemp.m<br>kfac.m | beamdata.m | |

The fire resistance calculation, is done using the main function `fire_resist.m`. As is the case for normal temperature design, the user is prompted to choose the steel section of the composite beam. The user input is passed to `userdata.m` which calls `beamdata.m`. The user is also prompted to specify the following:

- The use of fire protection materials or not.
- The use of the standard temperature time curve or the parametric fire curve.
- The number of shear studs per critical length of the beam. This is the number that was installed according to the normal temperature design.
- The start time of the analysis in minutes. This start time can be specified as 0. In order to get a good polynomial fit, on the data points, it is however convenient to specify a different start time. this becomes apparent with first use of the program.

- The end time of the analysis, in minutes, must also be specified. The specification of an end time that is too long might lead to a known instability in the code. A error message is displayed:

```
??? Error using ==> fire_resist
    Loss of concrete strength, this mode of failure not supported
```

  If this is the case, one must be manually re-run the function. The error message is due to the fact that the parametric fire reached an advanced stage where the concrete also loses strength. The calculation of when this situation would occur is based on a conservative estimate, due to heating according to the standard temperature time curve. If the moment resistance of the section is required at such a stage of the fire, it would be wise to determine a more accurate temperature profile in the composite beam.

- If the use of a parametric fire curve was specified, the user is lastly prompted to input the design fire load on the floor of the fire compartment, the units is $[MW/m^2]$.

After the function executes, the plot of fire moment resistance versus time is produced as output. A example of such output would be figures 3.6 and 3.7 on pages 57 and 58, respectively. At this stage, one can refine/change the output by specifying that the function should run again. Any of the original input data can be changed or re-used. It is not necessary to re-enter the input values by hand if one wishes to use the previous values, as the program will use previous input, when one specifies none.

A polynomial function is fitted to the data points plotted in the output figure. This is done in order to find the failure time, in a computationally inexpensive manner. When one is satisfied with the composite beam's behaviour during the fire, one can exit the loop in the program. As final output the failure time of the beam is shown in the Matlab command window.

The other functions called by `fire_resist.m`, are briefly described as follows: `loads.m`, calculates the permanent loads and imposed loads, according to the input specified in the function `userdata.m`. `steel_carac.m`, returns the specific heat of steel as a function of the steel temperature. For a plot of this temperature dependant material property, refer to figure 2.4 on page 17. The functions `temperature.m` and `parametric_temp.m`, calculate the fire compartment temperature as a function of time for the standard temperature time curve and the parametric temperature curve, respectively. The parametric temperature calculation is done according to the compartment characteristics specified in `userdata.m`. The function `steeltemp.m`, calculates the steel section's temperature, for either a protected section or a unprotected section. Lastly, the function `kfac.m`, returns the steel yield strength reduction factor, for a given steel temperature.

## B.3 Reliability analysis

**Table B.3:** Matlab functions used to do reliability analyses

| Reliability – Fire Limit State | | | |
|---|---|---|---|
| Parent function | Children | Children | Children |
| reliability.m | beamname.m | | |
| | userdata.m | beamdata.m | |
| | polyfind.m | steel_carac.m | |
| | | parametric_temp.m | |
| | | steeltemp.m | |
| | loads.m | | |
| | plotLSE.m | | |
| | lsezero.m | lse.m | beamprops.m |
| | log2norm.m | | |
| | ex2norm.m | | |
| | reduced.m | | |
| | parder.m | lse.m | |
| | original.m | | |
| | kfac.m | | |

The reliability analysis for the ultimate, serviceability and fire limit states are all performed using the FORM procedure. Table B.3 show the Matlab functions, used to implement a reliability analysis, for the fire limit state. Table B.3 show the functions that `reliability.m` call to execute the FORM procedure. As in the implementation for normal and fire temperature design, the user specifies the steel section of the composite beam that is used. The user can also change the data contained in the function `userdata.m`, to influence the reliability level of the composite beam.

In the case of the reliability analysis for the fire limit state, the function `polyfind.m` is used to find a polynomial, that fits a range of maximum steel temperatures. This procedure was described in section 4.2.3 of this document. The polynomial found by the function `polyfind.m` gets passed on to the function `lse.m`. By use of this polynomial, the reduction factor for steel yield strength can be calculated as a function of the mean value of the fire load.

The functions: `lsezero.m, log2norm.m, ex2norm.m, reduced.m, parder.m` and `original.m`, are used to implement the First Order Reliability Method as described in the beginning of chapter 4.